

AN INVESTIGATION INTO THERMAL AND OPTICAL PERFORMANCE OF A MULTI-PURPOSE LED AUTOMOTIVE EXTERIOR LIGHTING SYSTEMS

A Thesis

by

Ferina Saati Khosroshahi

Submitted to the

**Graduate School of Sciences and Engineering in Partial Fulfillment of the
Requirements for the Degree of**

Master of Science

in the

Department of Mechanical Engineering

Özyeğin University

December 2015

Copyright © 2015 by Ferina Saati Khosroshahi

AN INVESTIGATION INTO THERMAL AND OPTICAL PERFORMANCE OF A MULTI-PURPOSE LED AUTOMOTIVE EXTERIOR LIGHTING SYSTEMS

Approved by:

Assoc. Prof. Dr. Mehmet Arik, Advisor
Department of Mechanical
Engineering
Özyeğin University

Assoc. Prof. Dr. GökseninYaralıoğlu,
Department of Electrical and Electronics
Engineering
Özyeğin University

Prof. Dr. İsmail Ekmekçi
Applied Science Faculty
Istanbul Ticaret University

Özyeğin University

Date Approved: December 2015

To my passionate family and my friends who care

ABSTRACT

Vehicle lighting is important for both security and comfort. In addition, external lighting standards need to be reliable and are subject to international norms for the prevention of accidents. For this reason, automobile manufacturers pay extra attention and effort to apply the highest standards, and develop highly reliable products. While incandescent and sodium-based lighting systems are currently used in conventional vehicles, their lifetime and efficiencies (i.e. lumens/Watt) are very low compared to LEDs (Light Emitting Diodes). Furthermore, given that vehicles are mobile systems - in contrast to stationary systems - a higher premium is placed on having energy sources which are optimized for mass, cost and power so new technologies are needed. LED-based lighting for automobile applications is a rather new concept for lighting technology. Due to the fact that conventional lighting systems cannot perform better than LEDs for quality, lifetime, efficiency and the volume, novel LED lighting products have to be developed and offered. For this reason, during the last decade LED-based technologies have been investigated intensively, resulting in an exponential growth in the number of reports and publications. This project undertook research on a novel 3-function (i.e. stop, signal and position) LED lighting technology. The research took into account challenges such as having a driver circuit with an LED light engine, as well as operation in a very harsh environment (high temperature and high frequency vibrations). It was on the basis that thermal management and alternative novel thermal technologies for reducing weight and increasing performance are investigated. In this project, a new LED-based stop light was investigated and a prototype lamps were developed, which is producing 90 lumens. LED junction temperature was kept below 100 °C. During the project, thermal management with conventional cooling solutions was developed using analytical and numerical models and were validated with experimental studies. Possible advance cooling schemes to abate local hot spots at the LED and driver electronics sides are explored via computational models and validated with prototype tests.

Keywords: LED automotive lighting, Heat transfer, Electronics packaging, System integration, Low weight thermal design

ÖZET

Araç aydınlatması güvenlik ve konfor açısından önemlidir. Buna ek olarak, dış aydınlatma standartları kazaların önlenmesi için uluslararası normlara tabi ve güvenilir olmalıdırlar. Bu nedenle, otomobil üreticileri yüksek standartları uygulayabilmek için ekstra dikkat ve çaba harcayarak, son derece güvenilir ürünler geliştirirler. Akkor ve sodyum bazlı aydınlatma sistemleri şu anda geleneksel araçlarda kullanılırken, bunların ömrü ve verimliliği (lumens / Watt) LED (Işık Yayan Diyot) ile karşılaştırıldığında oldukça düşüktür. Araçların sabit sistemlerin tersine hareketli sistemler olmaları kütle maliyet ve güç açısından optimize edilmiş daha yüksek kaliteli enerji kaynaklarına sahip olmalarını gerektirir. Otomobil uygulamaları için LED bazlı aydınlatma teknolojisi oldukça yeni bir kavramdır. Geleneksel aydınlatma sistemlerinin kalite, kullanım ömrü, ve kapladığı hacim açısından LEDler kadar performans sağlayamaması LED aydınlatma ürünlerinin daha çok geliştirilip farklı alanlarda kullanımlarının önerilmesine yol açtı. Bu sebeple son on yıldır LED temelli teknolojilerin, yoğunlukla incelenmeleri rapor ve yayınlarda eksponensiyel bir artışa neden olmuştur. Bu projede 3-fonksiyonlu (stop, sinyal ve pozisyon) yeni LED aydınlatma sistemi araştırılmıştır. Bu araştırmada LED ışık motoruyla birlikte seçilen sürücü devresinin kullanımından ya da yüksek sıcaklık ve yüksek frekanslı titreşimler gibi ortam şartlarındaki aşırılıklardan gelen zorluklar hesaba katılmıştır. Bu araştırma ısı yönetimine ve performansın artırılıp kütlelenin azaltılabileceği alternatif yeni termal teknolojilerin araştırılmasına dayanmaktadır. Projede, yeni bir LED tabanlı fren lambası incelenmiş ve 90 lümen üreten prototipler geliştirilmiştir. LED pn birleşme sıcaklığı 100°C altında tutularak LEDler 60°C ortam sıcaklığında çalışabilecek hale getirildi. Proje süresince, geleneksel soğutma çözümleri ile ısı yönetimi analitik ve sayısal modeller kullanılarak geliştirildi ve sonuçlar deneysel çalışmalarla doğrulanmıştır.

Anahtar Kelimeler: LED otomotiv aydınlatma, ısı transferi, Elektronik paketleme, Sistem entegrasyonu, düşük ağırlıklı termal tasarım

ACKNOWLEDGEMENTS

This work would not have come to fruition were it not for the support of a number of people. First and foremost, I would like to gratefully acknowledge the trust and support lent me by Prof. Mehmet Arık. His acceptance of my request for undertaking re- search under his supervision has meant a lot to me. I thank him for the time he has generously provided, in answering my questions and providing help throughout the period of research. It has been a privilege for me to work with him, and I hope the results obtained from the various aspects of this research can go some way towards repaying his trust. Experimental work comprised an important part of this research. I would like to thank ARTgroup members in Energy Technologies Laboratory, Özyeğin University, whose role cannot be overstated. I acknowledge Prof. Celal Sami Tüfekçi for his guidance, and Mr. Ulas Yıldırım, especially for their time and effort in the experimental stage. The support of Farba Co., Bursa in building one of the experimental setups is greatly appreciated. I was lucky in being able to rely on the engineering help of Mr Ersel Tursucular, FARBA R & D manager, along with Mr Ibrahim Özdil and Mr Merih Öztürk during my research. I would also like to mention the role of Mr Thamer Salem who was a great help in the final stage of this research, as well as Mr Ehsan Abbasi who provided assistance in proofreading the thesis. This research was sponsored by the Turkish Ministry of Science, Industry and Technology through the “Sanayi Tezleri Programı”(San-Tez Program). Last but certainly not least, I would like to thank my family. On many fronts, I am what I am through their mere presence. My husband, Hamid, who patiently tolerated my long absence and did not hesitate to help me in all aspects; my mother, Fahimeh and my father, Gholamreza, my husband’s family as well as my two sisters, Elmira and Kiana have provided unrelenting support and words are inadequate in my appreciation of them. I dedicate this work to them, and I hope it can be accepted as a small token of my gratitude for all that they have sacrificed for me.

LIST OF TABLES

- 1.* Comparison of energy and fuel consumption [10]..5
- 2.* Selected studies about thermal issues and possible solutions..12
- 3.* Typical convective heat transfer coefficient values [18]..15
- 4.* Different board concepts from FR4 to special IMS [1]..27
- 5.* Different board concepts from FR4 to special IMS..30
- 6.* Project Packages..37
- 7.* Performance metrics of prototypes..42
- 8.* Package thermal resistances obtained from numerical and analytical models..47
- 9.* Properties of elements in LED package..49
- 10.* Initial conditions of FE model..52
- 11.* Conductivities of the components which lead to the thermal resistance reported in the package data sheet..54
- 12.* Power rate and heat dissipation for each function..64
- 13.* Function modes of the system..76
- 14.* Experimental vs CFD results of the FR4 prototype..80
- 15.* Verification of IR data by thermocouple readings..81
- A-1.* The three functions and their details..100

LIST OF FIGURES

- 1.** Images of LEDs in automotive lighting applications (interior and exterior) [30]..8
 - 2.** A burnt LED system (dark points clear inside LED) [2]..9
 - 3.** Characterizing heat transfer in an electronic package..16
- 4.** Variation of thermal resistance with equivalent heat transfer coefficient [3]..17
 - 5.** A system for LED cooling in automotive headlamp [3]..18
 - 6.** Heat sink temperature contours..19
 - 7.** The LED multi-chip module [4]..20
 - 8.** Distribution of resistances in a typical car lamp system [4]..22
 - 9.** Novel cooling system of LED headlight [5]..23
 - 10.** Effect of air velocity on junction temperature and h[5]..23
- 11.** Assembly of IMS (a) Cup of aluminum nitride with wire-bonded LED (b) circuit (c) dielectric (d) substrate aluminum [6]..24
 - 12.** Temperature versus pin length and width [6]..25
- 13.** Dual Thermal Interface Measurement of the LED package using two types of boards (D: Standard Cu-IMS, E: Special Design of Cu-IMS) [1]..28
 - 14.** Attachment of silicon die to a two-layer substrate and via array [7]..28
 - 15.** A sample model of high-conductive material embedded inside the board..32
- 16.** Farba LED backlight in an IETT city bus (image taken by author in streets of Istanbul)..39
 - 17.** The design concept in exploded view..40
 - 18.** The package under microscope; various methods, different angles..43
 - 19.** Data sheet provided by the LED company [Osram] ..44
- 20.** Leadframe in its most simplified geometry as given in the data sheet [Osram]..45
 - 21.** A sample thermal resistance network..46
 - 22.** Analytical model (suggested) results..47
 - 23.** Geometry of the LED package on board and mesh elements..48
 - 24.** Temperature contours of anode and cathode with thermal resistances..50
 - 25.** Chip, adhesive and printed circuit board temperature contours..50
- 26.** Basic comparison between Aluminum vs FR4 PCB constant heat flux is applied as thermal boundary condition on the area between; A: chip, B: die attach, C: Silicone encapsulant, D: Lead frame, E: Moulding compound, F: Solders, G: Solder pads, H: PCB..51

27. Maximum temperature versus the number of elements in MAPDL model showing mesh-independency..52
28. Two cases of single package numerical model analyzes with different boundary conditions..53
 29. Temperature contours in (a) chip and (b) solders (scales are different)..55
 30. Sensitivity of a single packages thermal resistance to die attach conductivity..56
 31. Sensitivity of a single packages thermal resistance to plastic conductivity..57
 32. Sensitivity of single packages thermal resistance to leadframe conductivity..57
33. Sensitivity of a single packages thermal resistance to silicone encapsulant conductivity..58
 34. Sensitivity of a single packages thermal resistance to board conductivity..59
 35. Sensitivity of a single packages thermal resistance to solder conductivity..60
 36. Effect of components conductivity on junction temperature sensitivity..61
 37. Geometry created in Solidworks CAD..62
38. Geometry of Board inside its plastic enclosure along with initial temperature contours..63
 39. First numerical results of CFD modeling..63
40. Multi-functional LED backlight board with thermal vias, (a) front layout, (b) Back layout..65
41. A sample thermal resistance network for the automotive lighting system board in free-space..66
 42. Basic parameters and settings of Icepak model..67
 43. Mesh sensitivity plot for Icepak model..68
44. The temperature contour in post processing of the lamp model, (a-1) board conductivity 0.2W/mK, electronics side, (a-2) board conductivity, 0.2W/mK, LEDs side, (b-1) board conductivity 0.8W/mK, electronics side, (b-2) board conductivity 0.8W/mK, LEDs side, (c-1) board conductivity 2.5W/mK, electronics side, (c-2) board conductivity 2.5W/mK, LEDs side, (d-1) board conductivity 160W/mK, electronics side, (d-2) board conductivity 160W/mK, LEDs side, (e-1) board conductivity 1000W/mK, electronics side and (e-2) board conductivity 1000W/mK, LEDs side..70
45. Basic comparison between the max. Temp. in different board materials..71
 46. Initial modeling with heat pipes..72
 47. Mesh independence plot..72
 48. Experimental Setup Parts: IR camera test..74
 49. Experimental Setup Parts: Integrated Sphere test..75
 50. Reaching steady-state by temperature sensors..76
 51. IR images..77
 52. A painted version of the board..78
53. Temperature contours comparison for the Electronics Side for (a) FR4 vs. (b) thermal clad Board..81

- 54.** LEDs side of temperature distribution in (a) thermal clad prototype and (b) FR4 prototype..82
- 55.** Experimental Setup: Heat Pipe..83
- 56.** Cartridge Heaters..84
- 57.** Thermocouple placement and the heat pipe test set..85
- 58.** Estimation of pore diameter using a high-resolution microscopic system..86
- 59.** Simulation of a heat pipe equivalent in CFD model (left) and IR thermal image of the actual measurement setup (right)..87
- 60.** (a) Embedded heat pipes in a polymer (left) and an aluminum board (right) along with their (b) temperature distribution by IR camera..88
- 61.** Temperature gradient of 2K obtained when manufacturing conditions are not optimum in a Teflon plane, (a) IR image and (b) contours extracted with MATLAB for a similar case..89
- 62.** Aluminum-based substrate with a single heat pipe at the same heat removal condition; (a) IR image and (b) temperature contours extracted with MATLAB (right)..89
- 63.** Comparison between a heat-pipe embedded in a plate using IR image (right); Line 1 representing a heat pipe embedded in board and Line 2 a simple heater on a simple board (no heat pipe)..90
- 64.** Comparison of results with literature (Loh et al. [29])..91
- 65.** Using line function to determine the maximum temperature difference on thermal clad board (line that is drawn on thermal image on right side gives temperature plot on the left side: temperature versus X-position on the line)..93
- 66.** Embedded highly conductive plate analogous to heat pipe in the model, cross sections from different views..94
- 67.** Temperature contour of the automotive lighting system when two short super-high-conductive bars are placed on the board surface, acting as heat pipes..95
- 68.** Temperature distribution of several high-conductive plates embedded in board; (a) components: LEDs and electronics components, plates, (b) board and plastic enclosure around it..96
- A-1.** Reaching steady-state by optical output..100
- A-2.** Board technology [Bergquist]..101
- A-3.** Board technology efficiency in terms of heat transfer [Bergquist]..102
- B-1.** A heat pipe [22]..103
- B-2.** Shape of the liquid-vapor interface [22]..104

NOMENCLATURE

LPWLumens per Watt
SMTSurface Mount Technology
SSLSolid State Lighting
JBJunction to base (board)
COB Chip-on-board
DBC direct bond copper
$q_{x,cond}$rate of heat flow in the x-direction
A_c area of the cross-section
dT / dxgradient of temperature in the x-direction
k_x thermal conductivity
q_{conv} rate of heat flow due to convection
A_ssurface area of the heat flow
T_s temperature of the surface
T_{inf} temperature of the coolant
hheat transfer coefficient
ϵsurface emissivity
T_s surface temperature
T_∞ temperature of the surroundings
R_{jc}junction-to-case resistance
R_{ja} junction-to-ambient resistance
T_cLead temperature (temperature on the slug for LED)
$R_{th,jc}$ Thermal resistance of junction to case
T_j Chip junction temperature
P Heat power
T_c Case temperature

CONTENTS

CHAPTER I: INTRODUCTION.....	3
1.1 LEDs in Automotive Lighting Systems.....	4
CHAPTER II: THERMAL MANAGEMENT IN AUTOMOTIVE LED LIGHTING; A REVIEW	13
2.1 Heat Transfer Modes in Electronics Cooling	13
2.1.1 Conduction.....	13
2.1.2 (Natural or Forced) Convection.....	14
2.1.3 Radiation.....	14
2.1.4 Heat Transfer Modes in Electronics Packaging	14
2.3 Literature Review.....	17
2.4 Advanced Cooling Strategies for Power Electronics Packaging	31
2.4.1 Heat Spreading Technologies	31
2.4.2 Heat Pipe.....	32
2.4.3 Thermal Enhancement in PCB Technologies	33
2.4.4 Embedding a Heat Spreader in a Circuit Board	34
2.4.5 Thermal interface materials (TIMs).....	35
2.4.6 Novel Substrate Technologies	35
CHAPTER III: ANALYTICAL AND NUMERICAL INVESTIGATIONS.....	36
3.1 A General Overview of the Project Work Packages	36
3.2 Thermal Design Requirements and Concept Development.....	40

3.3 Single Package Analysis	42
3.3.1 Slicing an LED Package.....	43
3.3.2 Analytical Study.....	45
3.3.3 Numerical Study.....	47
3.4 System Level Analysis	61
3.4.1 Analytical Study.....	65
3.4.2 Numerical Study.....	66
3.5 Developing Other Concepts for the Prototype	71
CHAPTER IV: EXPERIMENTAL ANALYSIS	73
4.1 Measurement System	73
4.2 Experimental Testing Procedure.....	75
4.2.1 Validation of Computational Results; Board Testing.....	77
4.3 Experimental Testing Procedures: Heat Pipe.....	83
4.4 Deviation and Uncertainty Analysis	92
CHAPTER V: LOCAL ENHANCED CONDUCTION MODELS	93
CHAPTER VI: CONCLUSIONS.....	97
APPENDIX A: OPTICAL AND ELECTRONIC CONCEPT DEVELOPMENTS ...	99
APPENDIX B: HEAT PIPE DETAILS.....	103
REFERENCES	105
VITA.....	108

CHAPTER I

INTRODUCTION

Owing to the importance of lighting as a key role in transportation systems, there is significant potential for new technologies to enhance the lighting performance. Light emitting diode (LED), as a candidate for efficient systems of lighting is based on solid state lighting (SSL). Today, high power LEDs have brought several benefits into the automotive lighting industry. They are increasingly being utilized in all functions of low beam, high beam, cornering light, daytime running lights and turn indicator in head and rear lamp modules. Light color of an LED headlight system is typically 5500 K which is close to that of daylight. The driver's eyes perceive higher contrast and therefore are put under less strain. In the vehicle lighting industry, the most common in terms of usage is the halogen technology which has been there for decades. The wide usage is primarily due to the fact that it is mostly available and is low in costs. Halogen has the largest share in global automotive lighting market revenue which is then followed by Xenon and LED for interior and exterior use in transportation systems. However, the main disadvantage of halogens in automotive lighting is the fact that they use a lot of energy and require extra maintenance. A halogen light bulb often burns up due to the evaporation of the tungsten in the filament, leaving the filament and eventually reaching the glass and causing the lamp to reach the end of its lifetime. Xenon head and tail lights, despite lasting longer than halogen lamps, having higher efficiency and providing better visibility, create significant glare and as such, have the potential to create critical problems in traffic. Xenon lamp costs are also very high and

the materials used in them are often harmful. LEDs, on the other hand, consume low amounts of energy and come in small sizes and are therefore subject to innovative designs for various shapes. Power conservation means cost saving, higher efficiency, and overall, different vehicles being better in power distribution. Radiated energy or the heat emitted by LED is rather negligible in comparison with incandescent bulbs which is a help in reduction of lamp's and optics reflector's depth and hence, there is no need for higher temperature and plastic materials (higher heat glass transition temperature) which are usually more costly. The initial high production costs of LEDs in automotive lighting are rapidly decreasing with the increase in usage and decrease of single package costs. LEDs are very advantageous in creating opportunities for using the space available when installing the headlamps and therefore, provide unique variety in styling and freedom for the production of brand characteristic. They are bright and fast enough when it comes to response time. LED taillight technology is improving rapidly and it is expected that with increase in response reaction rapidness, the stopping distance will be significantly shorter as well. LEDs also have an extremely high lifetime, with the potential of lasting more than a vehicles lifetime and their application contributes to avoiding CO₂ emission and reducing fuel consumption.

1.1 LEDs in Automotive Lighting Systems

LEDs are much more efficient than conventional bulbs. In order to encourage progress and efficiency in automotive lighting systems, a great amount of research is undertaken through the past few decades on the automotive lighting types and efficiency and reliability. LEDs in automotive lighting give higher efficacy (light produced over energy consumed) than halogen lamps. Reduced power consumption is equal to less fuel consumption and therefore less CO₂ emission from each vehicle with LED lighting.

Average annual fuel cost must be calculated according to an average mid-sized car based on almost half of highway and half of city driving for 15,000 miles each year and current fuel prices. The average annual fuel cost for a mid-sized car is therefore \$2,150 for regular gasoline (for fuel price of \$3.24 /gallon) [8]. Considering the relative fuel consumption of an average car's lighting system to be almost 5 percent on average conditions (since lighting fuel consumption depends on air resistance and air velocity, also to the usage of daytime running light) [9]. The amount of saving for a typical lifetime of a mid-sized car may seem ignorable, but considering the sum of greenhouse gas emissions of such amount of gasoline saving which is more than one metric ton of Carbon Dioxide Equivalent per car, we conclude that LED lamp is the most environment-friendly lamp which can be used in automotive lighting [10]. Table 1 depicts the comparison of energy and fuel consumption and thereafter, CO₂ emission for LED daytime running light and conventional light on.

Table 1. Comparison of energy and fuel consumption [10]

	Daytime running light with LED	Conventional light-on
Energy consumption	2*7 W	300 W
Fuel consumption	0.014 l/100 km	0.3 l/100 km
CO ₂ emission vehicle	0.36 gCO ₂ /km	7.86 gCO ₂ /km

Since 1960s, headlights did not go through a major change until high intensity discharge headlights (so-called HIDs) were invented almost two decades ago. Technology of headlight did not change after the halogen headlight in 1962 which quickly became an essential part of cars throughout Europe. US cars, however, were operating with non-halogen lighting until 1978. Next, systems using HID technology (also known as Xenon headlights) were first used by BMW in 1991. In 2008, the first LED headlights were

installed on Lexus LS by factory for 600h hybrid low-beam and side lighting, with the turn-signal and high-beam lighting using traditional technology. LED is still not common in general automotive lighting (other than high-end technologies) but many automotive lighting producers already adopted LED for DRL, turn signals and brake lights. The advent of LED headlamps depended a great deal on the ability of LED technology to produce the necessary lumens or brightness for use in the automotive industry. In order to properly light the way, a vehicle demands 800lumens. Due to aggressive research and development, LED lamps were produced by 2009 with an output of 100 to 200 LPW. Once these mega bright LED lamps became available, car-makers still had to overcome the cost of technology. Lexus was the first to offer them in their prestige vehicles in 2007 and 2008, followed by Cadillac in 2009. Soon, the cost of LED lighting dropped over 100 percent from \$ 5 to \$ 1 per bulb. This accelerated the use of LED headlamps, and several hybrid and electric vehicles, such as the Toyota Prius and Nissan Leaf offered LED headlamps as standard features [11]. As previously mentioned, LEDs are being used more and more for headlights and hence, innovations are created in safety of cars. Central high mounted stop lamps (CHMSL) are among the pioneers in LED application since developing a 5mm package for Japanese market before the twentieth century had come to an end. LEDs were applied to every function including: tail light, turn indicator, fog light, back up light and brake. In 2005, mass production of LED rear lamps started with brake, turn and position [12]. As an example, Audi's styling signature was LED DRLs for a while, which created a huge motivation for other automotive lighting companies to go for LEDs. Automotive companies have since been working on safety and better adaptation of LED usage. In one of the recent related shows, a Matrix LED lighting was introduced which divides LEDs into a number of different segments, allowing the LEDs to be dimmed, lets them to work in conjunction with lenses and reflectors and allows them to be activated and deactivated

independently. LEDs in their new arrangements also make it possible to react accordingly, adjusting light with the environmental conditions automatically. This reduces the driver's need for interference and lets him focus fully on the driving. When LEDs are used for automotive lighting (exterior), the alternator of vehicle requires less energy and thus, the load in engine is reduced and vehicle's total efficiency is increased. Companies like Audi, BMW, Mercedes-Benz and Opel are vigorously active in developing smart lighting systems. One good example could be BMW, even developing laser headlamps, which are not superheated beams designed to the VWs and Fiats, but white lighting that can be precisely modulated and, hardly uses any energy [13].

LEDs are so-called semiconductor devices which are converters of electricity to light. LEDs are known as SSL devices since light emission occurs through a solid block of semiconductor material —and not through vacuum and gas tube, which is how traditional fluorescent and incandescent light emission works. Figure 1 shows examples of LEDs in automotive applications. Similar to all p-n junction diodes, LED's performance and reliability significantly depends on its junction temperature as all diodes which have p-n junction. The results of a failure, particularly one of electrical are usually important. It is often easy to see exactly which part has failed. It is harder to reconstruct the circumstances that led to the failure in the first place, but necessary for the root cause to be found.



Figure 1. Images of LEDs in automotive lighting applications (interior and exterior) [30]

Figure 2 shows a typical burning due to one component on a PCB. Moreover, light output of LED is reduced by increase in junction temperature and therefore, causes LED to have a short lifetime. Hence, in order to keep the junction temperature lower than its maximum, a thorough thermal design is quite critical.

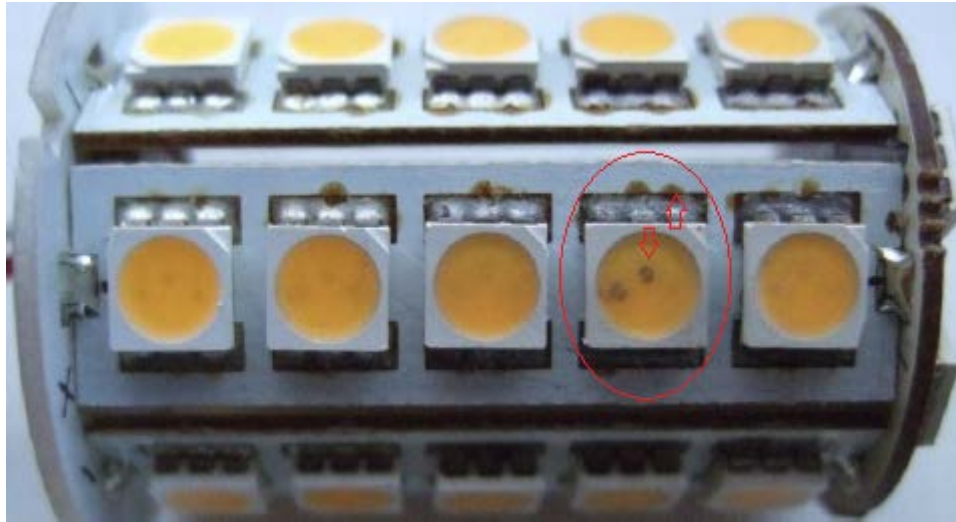


Figure 2. A burnt LED system (dark points clear inside LED, shown by red arrows) [2]

Generally, junction temperature limit for most LEDs that are connected via SMT is a temperature in 100- 125°C range. Recently though, some high power (HP) LEDs have been introduced with maximum junction temperature of 160°C but still, 100 °C is the safest margin to maintain the best efficiency. Thermal conduction is the primary heat removal mode inside an LED package from the die to the substrate or heat sink and then to the ambient or outside environment (means of heat transfer are briefly discussed in next chapter). Conduction is usually very efficient for heat removal which is why the heat flow path should always be kept as short as possible. This also means a lower thermal resistance (conductivity) which eventually leads to higher Efficiency becomes significantly more important when it comes to high heat flux (in some cases even higher than the sun) which is usually the case in HPLEDs. Automotive exterior lighting is also using high-power LEDs in front and rear lightings, either pure LEDs or combined with other lighting methods. The combined functional lamp is also one of the cases for which utmost care must be taken for eliminating any safety or junction issues which is even more critical in harsh environments [14].

In the instance of headlights, motion of vehicle can be taken advantage for enhanced cooling capability. In such a case, forced convection occurs in vehicle's motion which can reportedly keep the LED junction temperature below upper limits [5]. Metal core PCBs (despite their high costs) are often used in related studies. Cooling capacity is reported as improved when insulated metal substrate and ceramic and direct bonded copper ceramic substrates are used. While all the mentioned methods work well when used in automotive industry, they are not sufficient when it comes to high costs. As a high-cost solution, pyrolytic graphite heat sinks and heat spreaders can also be a novel solution. According to a comparative study [16], corruptions and failures might occur as a result of moisture entering into housings and enclosures which could damage the circuit boards permanently. Consequently, LEDs will dim and burn out eventually. In such an event, replacement might be the one and only solution. Although early failure is sometimes supported for a replacement from by guarantee of the company, the LED assemblies are usually made of complicated circuit boards and there are models for which the design does not allow any repair (since they come in sealed-units). In case the car is new, since new LEDs would be an extra expense which is unnecessarily added while repairing could be an option. Although cost effectiveness makes the manufacturers decide about which of the options to choose. According to the model of a new lighting system, the cost might be more than \$100 while repairing is potentially lower in cost. However, as repairing mostly requires replacement of the LED strip itself, it is usually easier than fixing each LED package on the strip [17].

Although different studies have been done on automotive LED thermal investigations, only a few have provided any thermal details; therefore, a comparative discussion was done. A brief history of automotive lighting industry is given and an entry to the research is introduced. Table 2 provides a literature survey of selected thermal publications in LED automotive lighting technology. The studies have taken quite

different approaches and kept the possibilities wide open for further research. As comes in Table 2, the general result of publications in the field reveals that when comparison between air cooling and liquid cooling in active and passive modes is done, desired junction temperature range is achieved using active liquid cooling (refer to Lin et al. [4]) and heat pipe is the most efficient option since it does not require an extra input power. However, heat pipe as a semi-passive liquid cooling method is a rather unexplored field when it comes to LED boards and automotive lighting and is only mentioned in two of the studies and reported as unfeasible in one of them ([6]) due to high costs of flexible HPs. The other study of heat pipes' thermal performance in automotive lighting ([4]) has started the basic experimental measurements of a simple heat-pipe-based setup. The current study has further improved the heat pipe thermal efficiency in an LED board, suggesting a novel design with high performance.

Having introduced the subject under study in chapter 1 (The Introduction), chapter 2 of the thesis in hand goes through a deeper review of all related articles in the thermal performance of automotive lighting industry (exterior). Thereafter, thermal challenges and obstacles in LED automotive lighting is discussed while going into details of thermal management in power electronics packaging using advanced cooling strategies including advanced thermal spreaders, PCB technologies, embedding heat pipes into boards and finally, thermal interface materials. Chapter 3 explains analytical and numerical investigations along with the milestones achieved, starting with a single LED package study and progressing into a complex lighting system of a vehicle, focusing on a specific design of a prototype developed initially in Farba Co., Bursa, Turkey. Following the theory and simulations, experimental setup details and measurement settings are described in chapter 4, validating the CFD results of chapter 3 with the results. Three different setups are introduced using the infrared camera (for thermal measurements), the integrated sphere (for optical measurements) and the heat pipe

setup (for performance measurements) and results are discussed. The idea of locally enhancing the conduction in LED boards is given in chapter 5 using the experimental achievements and Icepak models and explaining the core idea of the thesis in hand. To put it in a nutshell, chapter 6 summarizes the conclusions, followed by appendixes in chapter 7 for concept development studies of the three LED board prototypes studied and a quick description of how a heat pipe functions. The thesis ends with a list of references used and a vita of the author.

Table 2. Selected studies about thermal issues and possible solutions

	Lin et al. [4]	Lai et al. [6]	Jang et al. [5]	Chen et al. [3]
Ambient tem. (C)	20	30	15,25, 35	85
Cooling method	Air/liq.	Air/liq.	Air	Air
Active or passive	Passive/active	Passive	Active	-
Junction tem. (C)	110/60	200/105	30	150
Type of board	DBC	IMS	-	DBC
Total heat power	-	40.5	30	-
JB thermal resistance (K/W)	-	2	-	1.3
Novelty	Heat pipe	Novel materials	Air gap	-

CHAPTER II

THERMAL MANAGEMENT IN AUTOMOTIVE LED LIGHTING; A REVIEW

In this chapter, a review is undertaken on heat transfer modes in electronics packaging and LEDs for automotive lighting. Thereafter, a literature review is presented, so as to provide a detailed survey of the scholarly work in this field following the introduction to automotive lighting which was discussed in the previous chapter.

2.1 Heat Transfer Modes in Electronics Cooling

An electronics packaging is designed according to heat transferred via conduction, convection and radiation from sources to the surrounding environment. These modes are described in the following sections.

2.1.1 Conduction

When energy is transferred in a medium from a region of higher temperature to a region of lower temperature, conduction occurs. For an arbitrary direction, heat flow rate is proportional to area (cross-sectional) and temperature gradient in the same direction. The mathematical expression called Fourier's law comes as in Equation (1):

$$q_{x,\text{cond}} = -k_{(x,T)} A_c dT/dx \quad (1)$$

2.1.2 (Natural or Forced) Convection

Convection occurs when heat is transferred in a fluid according to random motion and bulk motion of particles combined together. Mathematical expression for the phenomenon is known as Newton's law of cooling, Equation (2).

$$q_{\text{conv}} = h A_s (T_s - T_{\text{inf}}) \quad (2)$$

2.1.3 Radiation

When heat is transferred due to difference between emission and absorption of electromagnetic waves by matter, radiation has occurred. A surface at a uniform temperature which is exchanging radiation with its surroundings, net heat flow rate is mathematically expressed by Equation (3).

$$q_{\text{rad}} = \epsilon \sigma A_s (T_s^4 - T_{\infty}^4) \quad (3)$$

2.1.4 Heat Transfer Modes in Electronics Packaging

Generally, conduction plays the most important role in transferring the heat produced in electronic elements to the cooler ambient. In some cases, radiation can be negligible and thus, conduction and convection modes are considered as the only means of heat transfer. Convection can either be active, passive and liquid or gas. In the literature survey part, various modes of cooling and their application in automotive lighting is explained. In an overall heat transfer state though, all the three equations (1), (2) and (3) are combined. As will be described later on, radiation usually plays the least important role and in such a case, equations (1) and (2) are used only and shown in the Figure 2, conduction heat transfer from chip occurs inside the package body and afterwards to heat sink. Convection heat transfer then removes heat from the system to the environment.

Table 3. Typical convective heat transfer coefficient values [18]

Convection heat transfer mechanism	$h_{min}(W/m^2.K)$	$h_{max}(W/m^2.K)$
Gas nat. conv.	2	25
Liquid nat. conv.	50	1000
gas forced conv.	25	250
Liquid forced conv.	100	20000
Condensation/ Boiling	2500	100000

There are a couple of parameters which are characterizing the transfer of heat in electronics packaging. These mainly include resistance from junction point to case R_{jc} , along with resistance from junction to ambient R_{ja} . First one could be defined as temperature difference between chip (or die as source of heat) and the casing (average package temperature) divided by the heat transferred by conduction heat transfer between two points. Thermal resistance between junction point and ambient, on the other hand refers to conduction heat transfer between the chip and ambient. Figure 3 illustrates a case where chip and package layers are cooled by means of a heat sink and resistances are drawn. Interface resistances must as well be taken into account when calculating the total thermal resistance, given their high impact on the result.

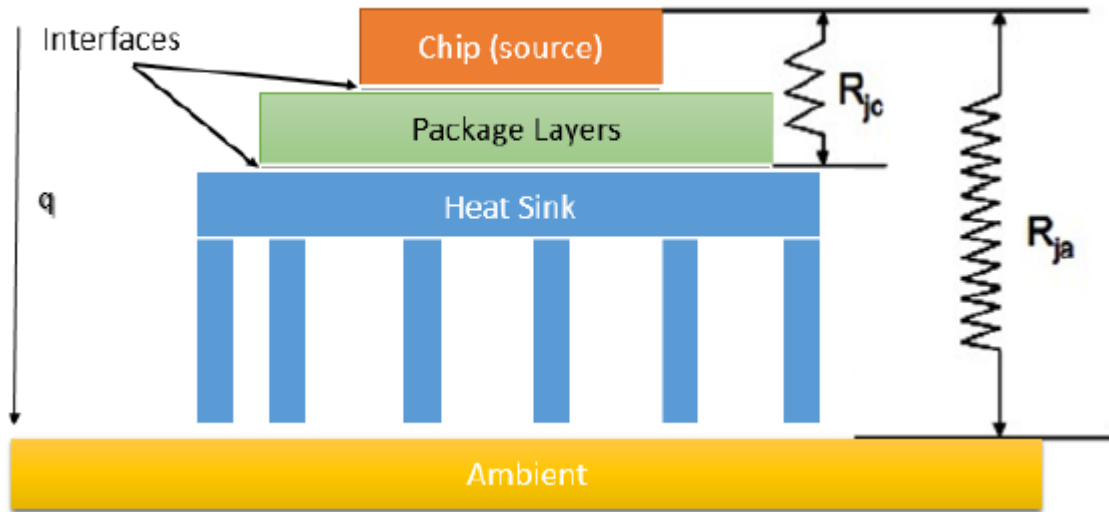


Figure 3. Characterizing heat transfer in an electronic package

In order to evaluate a system's thermal design, junction temperature must be calculated and measured. Common measurement methods are either direct or indirect. In the indirect method, case temperature is measured (T_c). Afterwards, an extrapolation is done using thermal resistance of junction to case ($R_{th,jc}$) which is found in the data sheet provided by the manufacturer of LED. The indirect case is mathematically described with equation (4).

$$T_j = P R_{th,jc} + T_c \quad (4)$$

Measuring junction temperature in the direct method is done experimentally where a very low current is applied through an LED ($< 100A$) in which junction voltage V_j is measured while it changes according to ambient temperature. The resultant linear plot of T_j vs. V_j is used to determine the junction temperature in the actual current.

2.3 Literature Review

Today, the high pace of change in packaging technology is significantly caused by electronics and the way they are used in each and every aspect of life including: transportation, communication, education, entertainment, agriculture, environmental controls, health care, research and defense. According to a study by Bottoms et al [31], diversity, cost effectiveness (cheapness) and higher performances are possible only when significant changes and developments occur in package design, materials and the procedure.

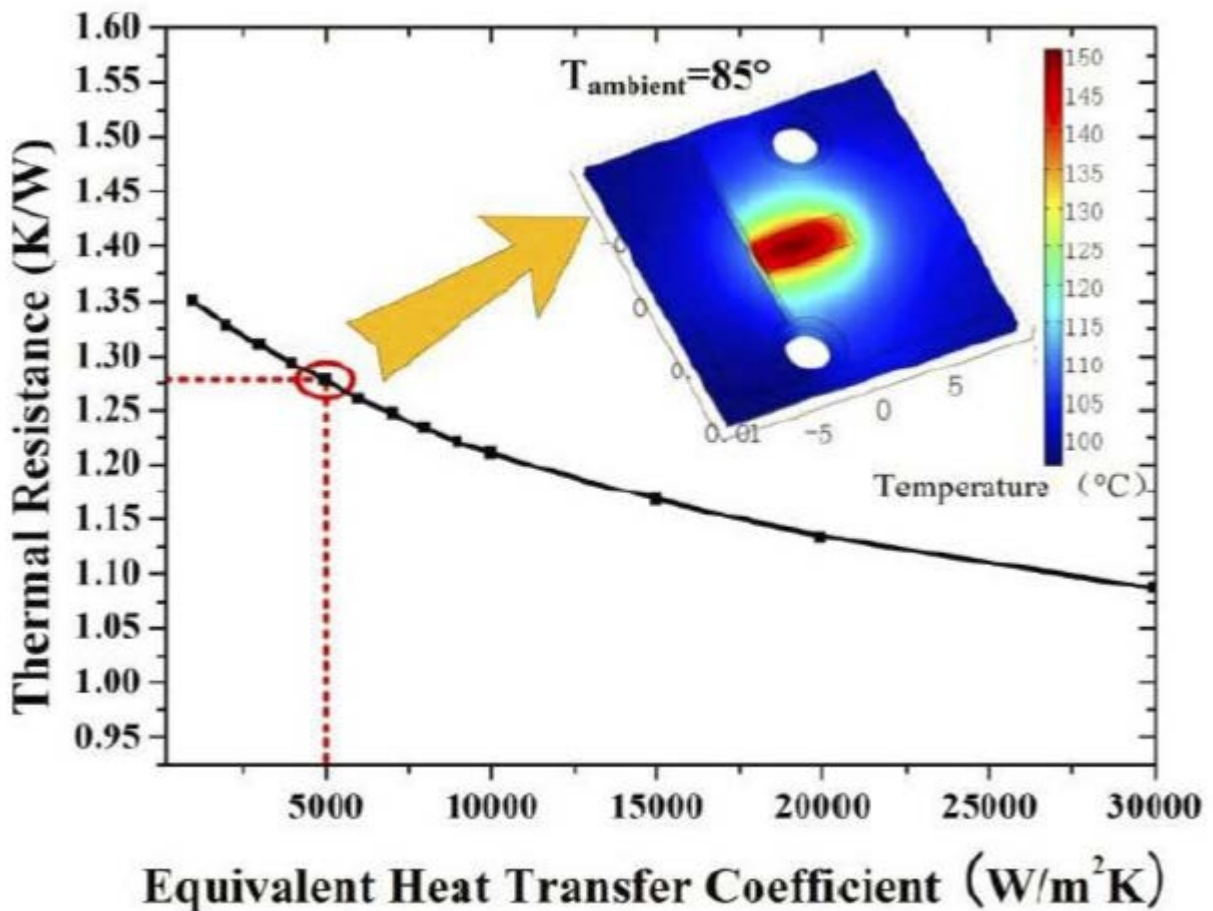


Figure 4. Variation of thermal resistance with equivalent heat transfer coefficient [3]

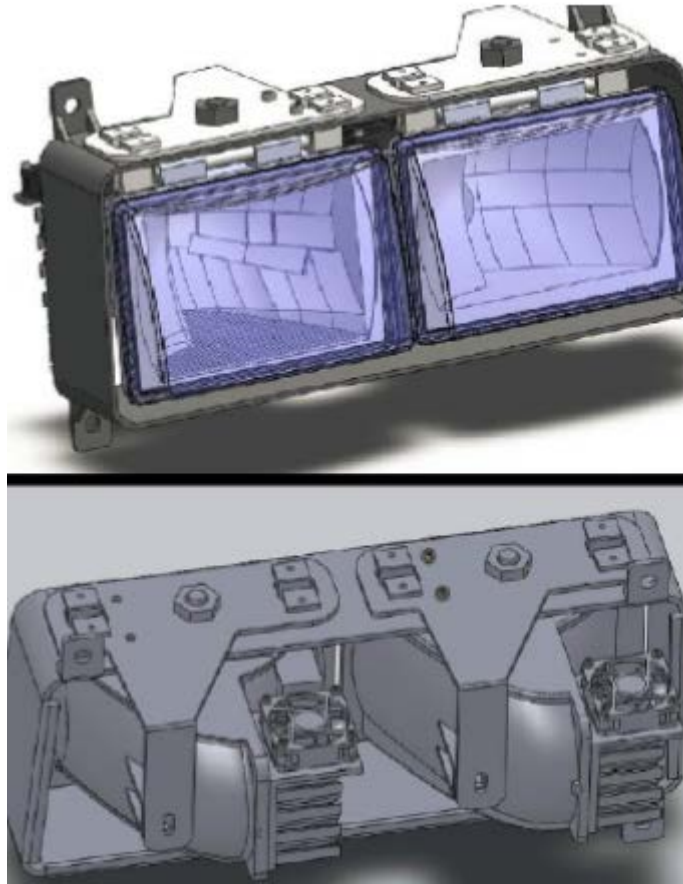


Figure 5. A system for LED cooling in automotive headlamp [3]

Chen et al. [3] studied chip-on-board (COB) technology in which a direct bond copper (DBC) board is used for automotive lighting by in which optimization of copper and ceramic's thicknesses is done in order to achieve the lowest thermal resistance possible. Figure 4 shows heat transfer coefficients (calculated as equal HTC) at the lower area of the package. Heat distribution is obtained when EHTC is $5000\text{W}/\text{m}^2\cdot\text{K}$ and environmental temperature is 85°C . Thermal resistance is less than $1\text{ K}/\text{W}$ in the simulation results when EHTC is large enough. In Chen et al.'s study, investigation of optical issues has taken precedence and limited research is done on the thermal management aspect of the system. Without any prior comparison between various cooling methods, active air cooling is chosen. For this, heat sink design is done and

optimization on size and structure along with fan is considered as shown in Figure 5. The simulated heat distribution is shown in Figure 6 (software used is not mentioned). The junction temperature is not measured, but estimated to be less than 150°C when ambient temperature is 85°C. It is reported that this ambient temperature is necessary due to the fact that headlamp is close to the engine compartment. It is claimed that the measurements are to be taken during further research.

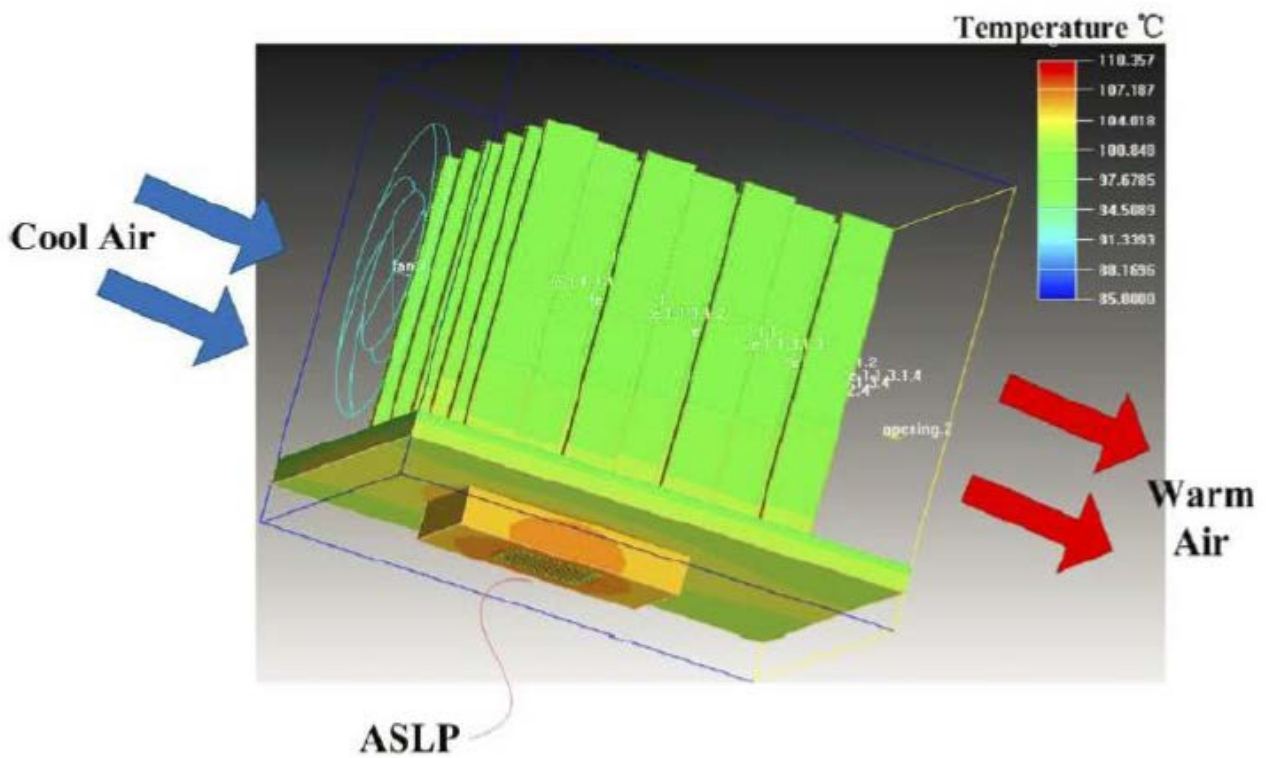


Figure 6. Heat sink temperature contours

Lin et al. [4] created a module composed of LED chips, DBC ceramic substrate, copper block with a through-hole in which heat pipe is utilized with fins. The module is designed as a multi-chip packaging for headlights and takes advantage of relative air flow during motion of the vehicle resulting in forced convection keeping the junction temperature of LED chips below 60°C. As Moore one of founders of Intel Corporation

predicted, with both increasing heat generation and heat flux, pure metal heat sinks are getting close to the limits of their ability of heat dissipation, which relies only on conduction and convection. Therefore, active cooling methods employing external energy are needed, such as air cooling, water cooling, thermoelectric cooling, and a variety of combined methods. The method used for measuring junction temperature was forward voltage method; in this method, the following process was followed. For the calibration measurement, Lin et al. [4] placed an LED sample in the temperature-controlled chamber of the analyzer. A small forward current (less than 5mA) drove the sample to ensure that the junction temperature was equal to the chamber temperature. It was then heated to different temperatures, and corresponding forward voltages of the chips were measured. Thereafter, V_f versus T_j relationship was fitted by an equation:

$$V_f = A + B T_j \quad (5)$$

where both A and B are fitting coefficients. After the calibration measurement, a DC forward current of 350mA was applied to the module to make all the LED chips work regularly. The forward voltage of the module was recorded during the experiments. Using the previously fitted equation, the junction temperature was obtained. The complete module is shown in Figure 7.



Figure 7. The LED multi-chip module [4]

Lin et al.'s experiment is compared with ANSYS model in terms of structural parameters. The major influencing factors on thermal performance of systems is discussed and optimization is done. Both natural and forced air convection are tested. With four 1W LEDs, natural convection took the junction temperature up to 110°C in 1500 seconds. Forced convection, on the other hand, took the temperature to not more than 60°C and reaching equilibrium required less time to achieve. Resistances are discussed and plotted as shown in Figure 8 and it is seen that convection and contact resistances significantly influence the thermal performance of the module. Chips could be controlled within different ranges by setting different threshold value of the system. Thus the junction temperature could be under 60°C. Since contact resistance is the second highest resistance, Lin et al. studied in further detail by comparing simulation data and experimental results at different temperatures. If possible, they concluded that it is better to cast heat pipe and fins into a component so that contact resistance is eliminated. The third highest thermal resistance is reported to be for LED which depends on the material of its substrate and the fourth is DBC layer which is dependent on its thickness only. Jang et al. [5] designed an arrangement of 30 LEDs of 1W for headlight. Their study uses a novel cooling system by putting two inlets for air in front of the automobiles as shown in Figure 9. In the design, heat is removed through a rear outlet by air at high temperature.

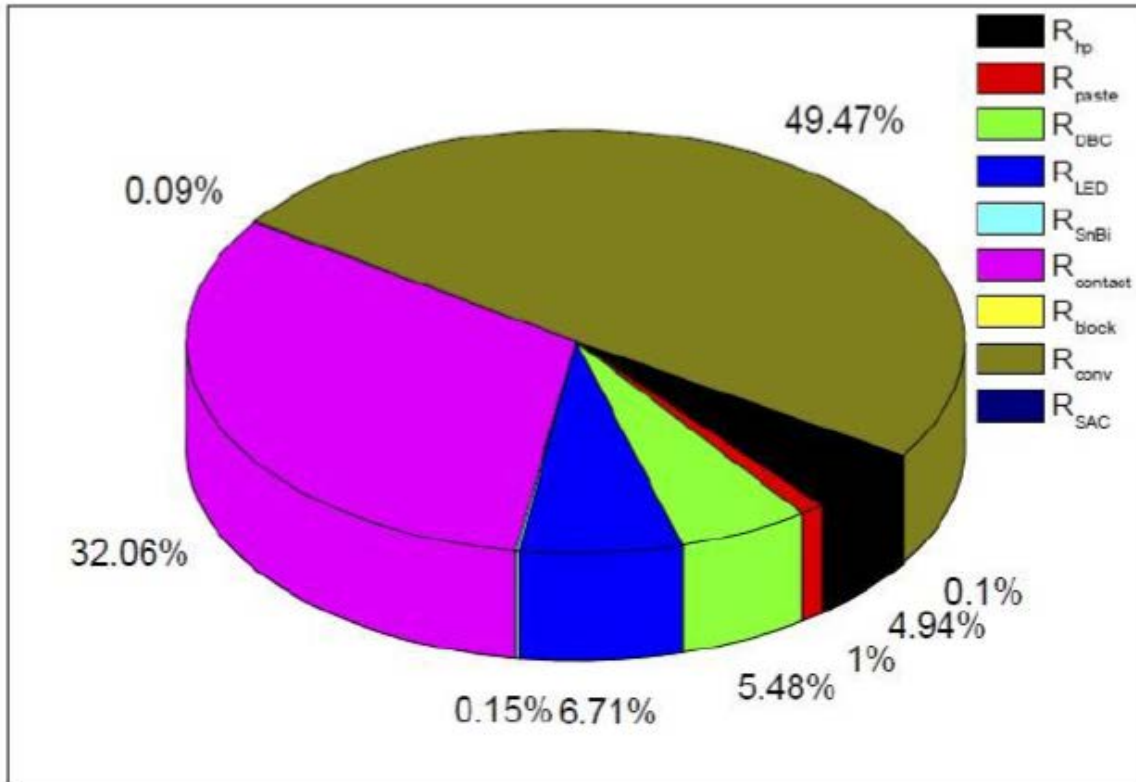


Figure 8. Distribution of resistance in a typical car lamp system [4]

Jang et al. studied the effect of fins by modeling and simulation using FLOTHERM software. The size of fin used in the model is the same as size of LED package in the design (1cm^2). The heat transfer coefficient increases from very low to $83\text{ W/m}^2\text{K}$ as the air velocity increases from stationary to 120 km/h . Three different ambient temperatures of 15 , 25 and 35°C are applied. The junction temperature decreased significantly by use of both fins and air velocity and results are plotted accordingly (Figure 10). Jang et al.'s study in author's opinion will not be practical when it comes to commercial use and ease of design Due to the car speed usually being between 0 to 120km/h , velocity of air passing over the LED headlamp was considered in exact same range for velocity in this study and for system of air-cooling system with no fins, when environmental temperature is 25°C . The heat produced caused JT to increase increased by more than 10°C . When there is 50W of heat production, the maximum JT did not

yet rise higher than 50°C, which on its own is a proof for air cooling as a sufficient system for LED automotive lighting system.

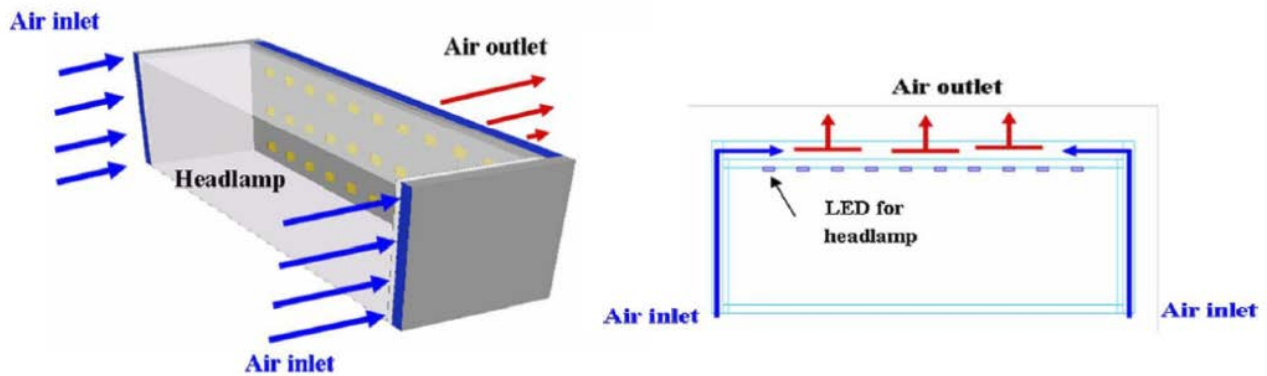


Figure 9. Novel cooling system of LED headlight [5]

In another study, Lai et al. [6] designed a low-beam headlamp system with luminous flux of 1000lm where each LED had an average output of 40lm/W. Unpackaged chip was used as bright LED of Cree XBright 900 with 900 μm^2 area. The chip generates light from 460 to 470nm and emits blue color. Lai et al. expect that each LED is generating 2.7W heat under appropriate conditions.

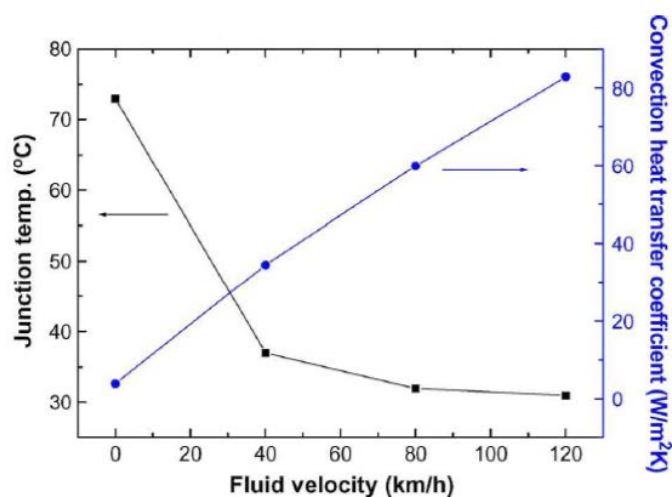


Figure 10. Effect of air velocity on junction temperature and h [5]

LEDs are mounted on boards of Lai et al.'s system with overall production of 40.5W. LEDs are individually packaged using a layer of phosphorus coating on top. Aluminum nitride with 200W/mK conductivity is chosen for ceramic as both a thermal path and an electrical insulation. Then, the package is mounted on an IMS as shown in Figure 11.

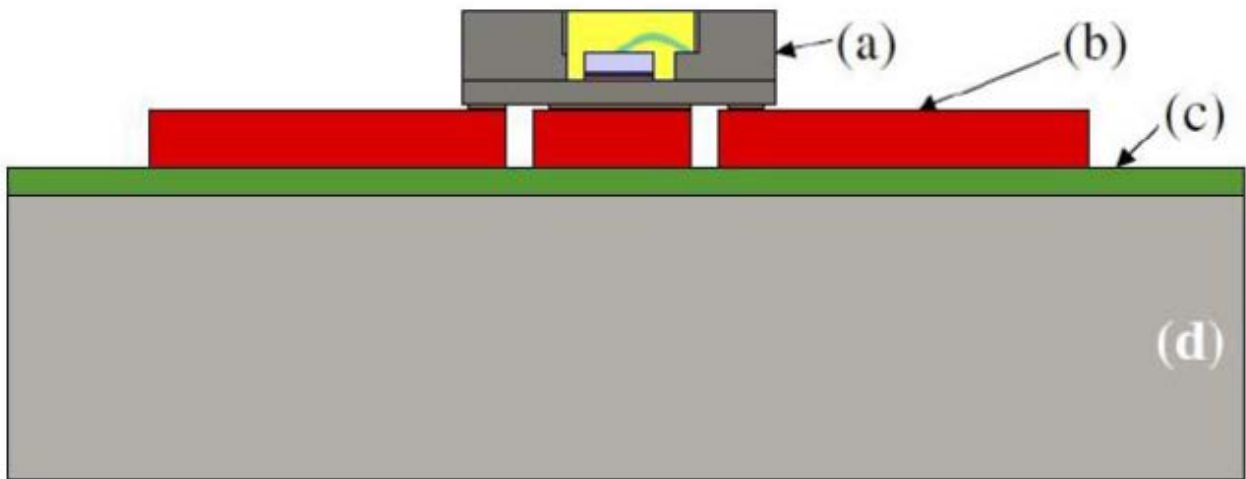


Figure 11. Assembly of IMS; (a) Cup of Aluminum nitride with wire bonded LED, (b) circuit, (c) dielectric, (d) substrate Aluminum [6]

Lai et al. investigated the inside of an insulated metal substrate (IMS) and how there is a foil of copper as circuit layer bonded with metal base (aluminum) plate and a thin dielectric layer. The IMS is studied by using different combination of materials and thickness; it is then optimized, with the only problem remaining being its manufacturability. Four cooling approaches are discussed by Lai et al.: (1) Passive air cooling approach in which heat sink (or any other passive heat spreader) is placed on the insulated metal substrate board with direct touching. Heat spreader size is limited which can be due to space constraints. Junction temperature increases to more than 200°C. (2) Active air cooling: Also not a feasible method, given that space limitations

in the enclosure necessitate numerous high flow fans. Therefore, liquid cooling is chosen. (3) Passive liquid cooling can be applied in two different ways: {3-a} Passive closed-loop or indirect cooling: water can be used. Lai et al.'s simulations confirm this method to be feasible; however, buoyancy forces require that the heat exchanger be positioned above the source of heat but in the design of headlight a heat exchanger must be placed below modules of LED; {3-b} Heat pipe as a heat spreader: in this approach, a loop heat pipe system is used by Lai et al. in order to improve heat transfer from substrate to heat exchangers. Each individual LED board in the automotive applications needs to be mechanically adjustable so that light beams are properly aligned and thus, heat pipe must be flexible (in order to be bended). Accordingly, such unit may become high in cost and therefore, inefficient. As engineering and cost consideration are the most significant when it comes to mass production, this method is usually unfeasible.

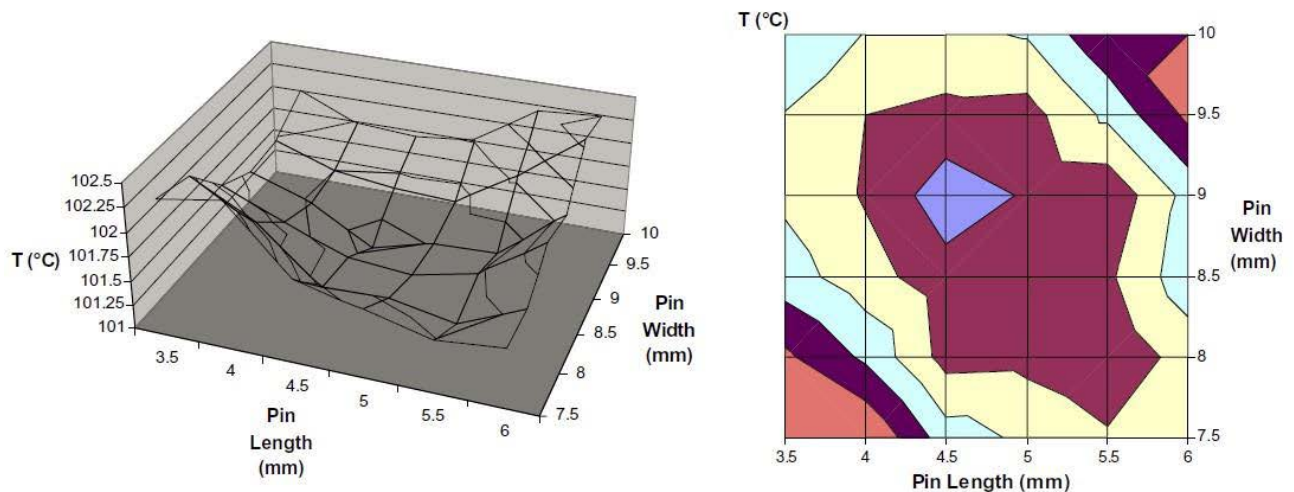


Figure 12. Temperature versus pin length and width [6]

(4) In active liquid cooling approach there is a pump and several cold plates which are connected thermally to sources of heat and the reservoir (liquid) and heat exchanger. One heat exchanger is usually shared by high-beam function and low-beam function, in which case a heat sink has a base that is liquid-cooled. Water with additives is used and the pump only uses cold liquid. Several configurations are considered by Lai et al. Placement of heat sink is horizontal and therefore the design is with pins rather than fins. Optimization of the heat sink with several parameters is done by an iterative procedure with heat sink base thickness (t), heat sink height (H), pin length (l), width (w), N_x (pin numbers in direction of X) and N_y (pin numbers in direction of Y). Optimised heat sink is derived by simulation, and the results are shown in Figure 12. To summarize, heat sink dimensions for the current application are optimized like this (dimensions in mm): $t = 5$, $H > 30$, $h > 25$, $l = 4.5$, $w = 9$, $N_x = 8$, $N_y = 7$ where design margins are (for $< 1^\circ\text{C}$ increase in JT): $3.5 < l < 6$ and $5 < w < 10$ and $35 < N_x < 45$ and $N_y > 7$. Ambient temperature is assumed to be 30°C . It is claimed that as bright white LEDs develop, the required power driving a certain light output decreases constantly. Thus, dissipation of heat decreases as well. With reduction of power requirements for a system which means lower heat dissipation, the solution to problem of heating may be simplified to passive air cooling alone [6]. However, Elger et al. [1] mention that in an LED automotive headlight with compact board, high accuracies between primary optics part and LEDs are needed. This fact brings up the challenge of PCB tolerances and the need for a tolerance analysis. Ambient temperature is 22°C in this study. Power of 18W is applied on a small PCB and maximum allowed junction temperature is 150°C , and it is claimed that the board material and the solder connection limit the operating temperature of the system but not the junction temperature.

Table 4. Different board concepts from FR4 to special IMS [1]

Design description	FR4 Tg150, filled and capped via	FR4 Tg150, copper insert	Al-IMS, standard	Cu-IMS, standard	Special Cu-IMS 1	Special Cu-IMS 2
Board thickness [mm]	1.5	0.9	1.5	1.5	1.5	1.5
Copper trace thickness	0.75	0.7	0.75	0.75	0.35	0.75
Dielectric thickness	nm	nm	100 μm	75 μm	nm	nm
Dielectric thermal conductivity	nm	nm	4 W/mK	1.3 W/mK	nm	nm
Specific design information	Copper filling 10% around thermal pad	nm	nm	nm	nm	nm

Today, IMS is mainly made by Al (merely sometimes with Cu) and is an alternative for FR4 boards in LED automotive lighting industry. Ceramic boards are expensive and are rarely used. In the platform used in Elger et al.'s study [1], solutions with copper IMS are used. These cause R_{th} of the board to drop roughly by 1K/W. Various concepts for the board are investigated: these start from the FR4 standard boards to special IMS (as seen in Table 4). Thermal resistance is measured by a T3ster system here. Figure 13 shows large reduction in thermal resistance (the R_{th} is reduced by 3K/W) which happens by applying a thermal contact with core. Finite element simulations are performed for evaluating what close packaging does in terms of thermal impact on the LEDs. It is concluded that a flame retardant board that has thermal vias will be a sufficient one for multi-cavity reflector whereas packages with one single LED have large distance when they are mounted.

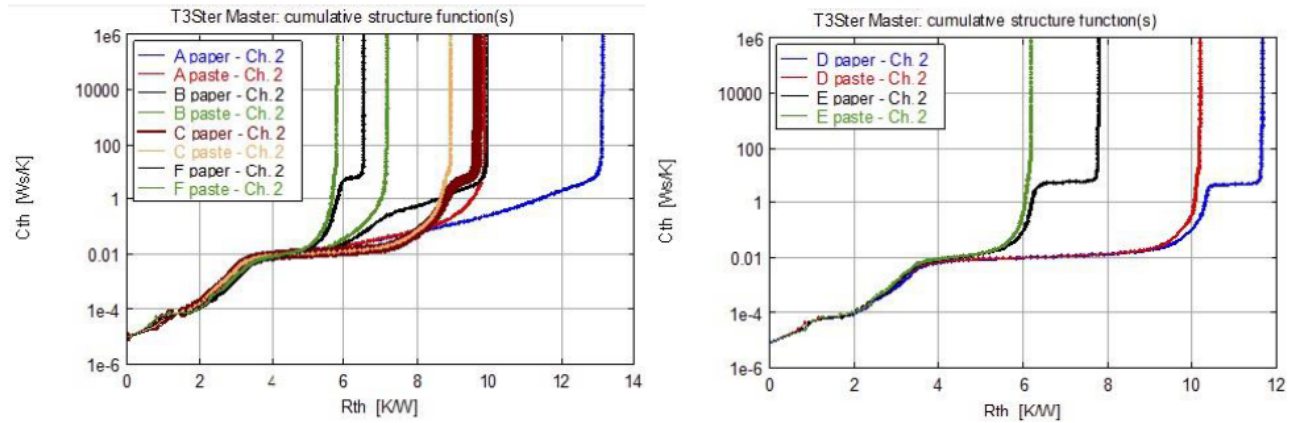


Figure 13. Dual Thermal Interface Measurement of the LED package using two types of boards (D: Standard Cu-IMS, E: Special Design of Cu-IMS) [1]

As a suggestion, Guenin [7] designed a special board solution for a different case in which several LED packages are mounted close to each other onto a board (vias are fabricated for creating interconnection, both electrical and thermal, between different layers of metal; vias are mostly hollow cylinders made of copper and have thin layers on inner surface of holes that are drilled through laminated dielectric and metal layers, as shown in Figure 14. Vias provide electrical path between dielectric layers and are also enhancers of heat flow along the thermal path. Therefore, it is generally termed as “thermal via”).

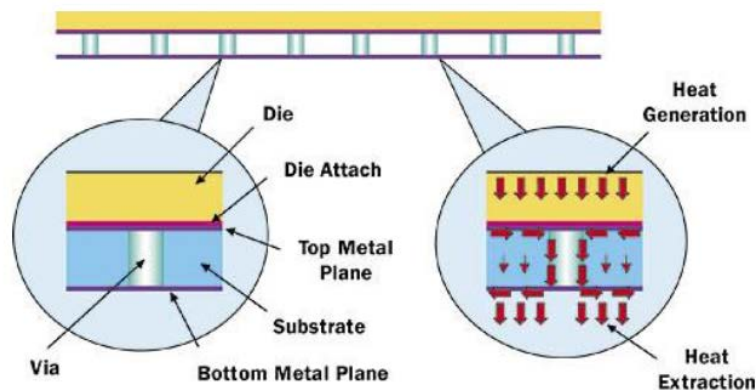


Figure 14. Attachment of silicon die to a two-layer substrate and its via array [7]

Guenin's special board solution acts as a means of reduction in operating temperature of solder joint in the range of 10 to 20 °C. Controlled high end soldering technology is also mentioned as a necessity to reach higher reliability and to be able to function in higher temperatures. It is also shown (using simulations) that for a single LED, junction to heat sink thermal resistance decreases from 9.3K/W to 7.8K/W for standard metal-core board to 5.0K/W for the special design (i.e., 46% decrease in resistance). Although different studies have been done on automotive LED thermal investigations, seven of them provided details of thermal design; therefore, comparative discussion is done in Table 5 in which studies have taken quite different approaches and therefore kept the possibilities open for further research. Heat pipe as a (semi-)liquid cooling method is a rather unexplored field which is only mentioned in two of the studies and reported as unfeasible in one of them; the other has started the study but the design can be further improved and a different design can be suggested which gives better thermal performance, and thus will have higher potential of being implemented.

Table 5. Different board concepts from FR4 to special IMS

Ambient T °C	85	20	15, 25, 35	30	25	nm*	50
JT limit °C	Nm	nm	nm	125	150	nm	100, 125
JT in passive air cooling °C	Nm	110	30	200	nm	nm	nm
JT, active air cooling °C	150	nm	nm	nm	nm	nm	nm
JT, passive liq. cooling °C	Nm	nm	nm	not suitable	nm	nm	nm
JT in active liq. cooling °C	60(135 no fan)	nm	plate	150 pump, cold	nm	nm	nm
Type of board	DBC	DBC Ceramic	nm	Optimized IMS	Cu IMS	nm	nm
Total heat power (W)	Nm	nm	30	40.5	nm	35	3.3
Power per LED (W)	Nm	1	1	2.7	nm	5	3.3
Thermal resistance of junction to board (K/W)	1.3	nm	nm	2	5	nm	nm
Equivalent heat transfer of cooling (W/m ² k)	nm	nm	nm	nm	nm	nm	nm
Technology Type	Conv.**	Heat pipe	Airgap w/wo fins	packaging	Cu IMS		Electric Conv.

(*nm: not mentioned, ** Conv is an abbreviation for conventional).

2.4 Advanced Cooling Strategies for Power Electronics Packaging

The cooling technologies utilized as means of removing the produced heat from electronics packaging are reviews in this section. According to author's investigations, current cooling technologies have a range consisting heat sinks (natural convection heat spreaders) to forced convection, jet impingement coolers, thermoelectrics, heat pipes, direct immersion, vapor space condensers, phase change materials, submerged condensers and microchannels. Evolution of the electronics has been reviewed for finding the cooling techniques' historical background and is presented by Bergles et al [20]. Extensive nature of this field creates the need for an in-depth review of each technique of electronics cooling but it is beyond the scope of this study to discuss them all. However, Bergles et al. also provide an overview of the techniques which are the most used and most common and of those that are promising for automotive lighting systems with heat pipes as good examples.

2.4.1 Heat Spreading Technologies

Different heat spreaders are used in electronics packaging. In order to dissipate the heat, the spreaders are used in die/chip level so that heat is removed from junction point to the package and board, and then out to the environment. Heat removal could either be done directly to the ambient or by means of a heat spreader in between. Heat pipes embedded in an aluminum or copper base heat sink can significantly improve heat removal. Spreaders are placed inside the electronic enclosures so that heat transfer from discrete components to the walls of enclosure happens in the best manner. The material used for a heat spreader may either be aluminum, copper or copper-tungsten/moly which all have thermal conductivities less than 400W/mK. There are also composite

spreaders used which might either be of ceramic, or carbon composites ($< 1,200\text{W/mK}$). Advanced heat spreader technologies also include high conductivity plates ($500 - 5,000\text{W/mK}$), vapor chambers ($> 5,000\text{W/mK}$), and oscillating flow heat spreaders (up to $120,000\text{W/mK}$). In some of the applications such as semi-conductorm the integrated circuit needs to have an electrical isolation and high thermal conduction, therefore dielectric heat spreaders are made with nonmetallic materials could be ideal (as used as a layer in printed circuit boards) [21]. An example of a high-conductive plate embedded inside prototype board can be seen in Figure 15.

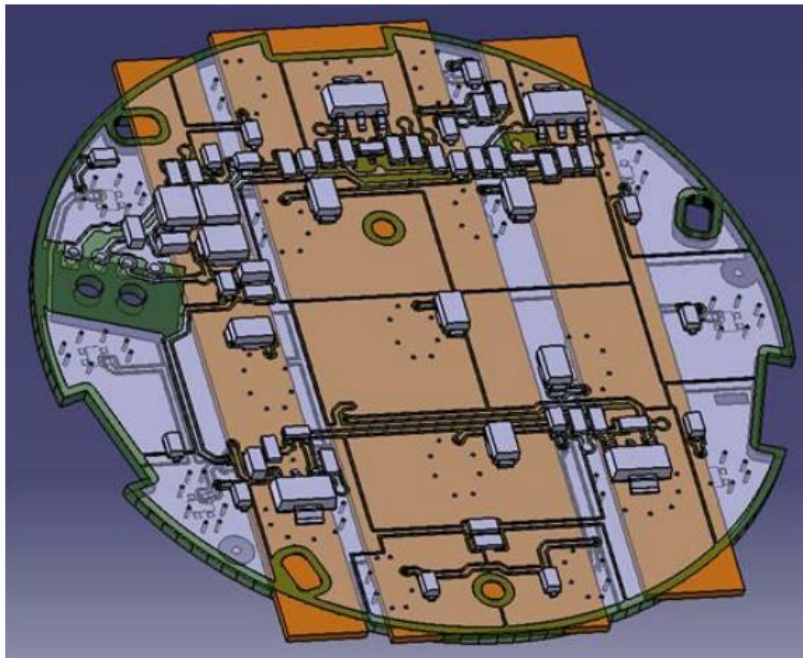


Figure 15. A sample model of high-conductive material embedded inside the board (simulation by Farba Co.)

2.4.2 Heat Pipe

Heat pipe, as a heat transfer system has become one of the best options for efficiency in electronics cooling today [22]. Among advantages of a heat pipe in electronics

packaging is that a heat pipe can remove huge amounts of heat compared with conventional methods. This means large quantities of heat is transported from a small area of cross section in large distances (as heat pipe length can be large). One of the important advantages of a heat pipe is that it inserts no extra power to the system and therefore, not like active cooling methods, there is no additional heat added by using them for cooling. Moreover, due to their small size and the fact that they can be designed to be in various shapes and sizes, the overall process is much easier for both manufacturers and designers. Moreover, a heat pipe makes the system compatible to control heat rates of heat transfer with small temperature gradient (end to end) at different levels of temperature [23]. Thermal performance is improved by heat pipes in a silent and passive manner and in the meantime the size of other heat spreaders is decreased and the electronics packaging becomes more reliable. Furthermore, flexibility of package design is also improved since heat sinks can be placed farther away at the end of heat pipe. Heat pipe can be have a direct attachment on the surface of PCB which increases performance effectively by reducing the need of interfaces [24]. Due to high potential of heat pipes, several studies has been done on heat pipes in recent decades. Analyses are by computational, theoretical and experimental simulations and setups which have shown significant progress for heat pipes various applications.

2.4.3 Thermal Enhancement in PCB Technologies

Printed circuit boards in modern electronics packaging is being designed by complicated methods. Nowadays in the package design interconnections play an important role where thermal behavior and overall size are even more focused upon

than electrical and cost requirements. Therefore, one of the most important areas of study is the geometry and material of layers inside a PCBs. Several production methods have been development since the first PCB was invented by Dr Eisner in 1940s. These different types are still used without significant change in today's technology but are mostly inefficient in thermal aspect. There are certain trends influencing the most on PCB production procedure and technology. These include computer technology requiring high frequency boards and circuits with better components which means even higher heat flux and extremely high heat removal needed. Also, products which are using digital parts and by that reduce the total cost of the conventionally expensive tools and parts are now in need of proper cooling with low costs. Overall, the fact that all electronic and digital products tend to be smaller and thinner in size day by day while becoming high in both functionality and density necessitate the PCBs evolution in order to keep up the pace of electronics technology world [25].

2.4.4 Embedding a Heat Spreader in a Circuit Board

Recently, the idea of a low resistance heat spreader as heat pipe embedded inside a printed circuit board has started to be studied (e.g. by Pounds et al. [26]) in which aluminum as the most common material is selected for base in metal core printed circuit boards. Copper is mostly used for solder when heat pipes are to be placed and fixed in an MCPCB which by all means increases the heat transfer through the substrate even more. Modern heat pipes are smaller in size and can remove very high powers and since they are usually placed on the source, it would perhaps be the best choice to embed one of them in case design parameters allow thermal engineers to do so.

2.4.5 Thermal interface materials (TIMs)

In order to fill the gap between main surfaces of the sources and other components close to the source, thermal interface materials must be used. The materials eliminate the air gap between touching surfaces which is thermally inefficient considering the high thermal resistance of air. These materials are nowadays easily available and ready to use with a range of thermal conductivities of various polymers. Applying them in interfaces significantly affects the performance with improving heat transfer in contact areas. In other words, higher contact conductivity means lower resistance and efficient heat dissipation along with electric insulation and other important mechanical properties.

2.4.6 Novel Substrate Technologies

According to MCPCB substrate technology, different systems are available for a substrate design process. Among these the most important three methods include one layer, two-layer and ultra-thin substrate system. One-layer design has a lower routing area than the multi-layer type and the advantage of ultra-thin type is the fact that it is flexible and can be bended. Appendix A gives a brief description of the substrate technology used in one of our prototypes (thermal clad board).

CHAPTER III

ANALYTICAL AND NUMERICAL INVESTIGATIONS

This chapter demonstrates analytical and numerical analyses, beginning with a general overview of the overall project work packages, and thereafter, introducing the concept of the lamp under study. In our studies EES is used for analytical modeling and ANSYS/ Icepak is used in numerical investigations.

3.1 A General Overview of the Project Work Packages

The purpose of the project was developing an advanced LED lighting system such that the concurrent effort expended on prototyping would allow novel results to be obtained. The system is an electronics and LED driver circuit which ought to fit in a limited area (footprint area), and aims to become a standard system to be used in various types of small and large vehicles. The project plan is composed of seven work packages as shown in Table 6. During the first one, thermal design requirements were completed and literature survey was accomplished by reading all the patents and papers related to thermal modeling of automotive lighting. In the next work package, concept development was worked on and the thermal studies of single LED package was done with modeling the LED (after hours of reverse-engineering to about the internal specifics) and continuing to the system level study. For modeling, ANSYS program was used; especially Mechanical APDL finite element analysis. After the completion

of software modeling studies, manufacturability and thermal design efficiency have also been studied to develop the most suitable material combination inside an LED in terms of conductivity. Besides, analytical modeling (resistance network) was also performed in EES program, so that the LED packages is increased beyond the target thermal parameters.

Table 6. Project Packages

No.	Package name
1	Determination of the thermal design requirements
2	Modeling/ concept development studies
3	Determination of the thermal performance studies
4	Prototype development and production
5	Preparation of advanced technology performance heat map
6	Experimental validation studies
7	Concluding temperature contours of the prototypes and comparison

The second work package included improving the system design concept and optimally removing the heat generated in the model created according to the system. When operated for single-chip-modeling, ANSYS Mechanical APDL was used but for the multi-chip system modeling, ANSYS ICEPAK program was used. In ICEPAK, the idealized version of the prototype was modeled so that we could get a general idea developed. Using this model, three-dimensional temperature distribution and the heat generated in the light engine was found and local hot spots on the double-sided printed circuit board and also inside with and without its enclosure were investigated. In the third work package, “Determination of Thermal Performance”, resistance between the

LEDs, electronic components and the printed circuit board was analyzed. Experimental, numerical and analytical methods using LEDs and driver circuit determined the junction temperature of the electronic components and LEDs. Looking at the design of the rear lighting prototype (98mm dia.), by examining the total resistance of the system, new concepts were thought of in the 4th work package named “prototype development and production” and the prototype was designed in the 5th work package: “Preparation of new technology performance map”. The alternative advanced cooling technology was worked on and a new technology prototype was produced by Bergquist, a thermal solutions company (USA).

During the “experimental validation studies” which is the 6th work package, the experimental setup was prepared and tests were carried out and the advanced cooling technology was studied on the prototype. Since experiments are the main part of the study, the experimental investigation was performed in all the packages of the project. Our primary focus in the numerical investigations was predict performance so actual system will operate properly. The effects of different design parameters emerged in the numerical part; partial and total heat resistances were calculated for each model accordingly. An important part of the whole research was the product prototype development. Once a prototype was designed, fabricated and after passed all or part of the tests, the concept of its design could be further improved. Thermal problems of the prototype (similar to the lamp shown in Figure 16) were identified in detail in the early stages and the new prototype was designed so as to solve those thermal problems. During this period, thermal interface materials were also examined for the prototypes and new experimental facilities were purchased. Also, in order to prepare an experimental setup for testing heat pipes in general with major focus on the heat pipe performance comparison in different orientations. Several setup design ideas were discussed and built in the laboratory at Özyegin University. These experiments

provided us with more insight into understanding the heat pipe which allowed discovering the effect of heat pipe when it is inserted into the new prototype. In the final package of the project, metal PCB tests (optical and thermal) were completed. Thereafter, results of CFD were put into comparison with experimental results in the metal-core PCB (validation for experimental studies) and the setup of heat pipe experiment was completed and singular heat pipe assembly of the new prototype was also tested.



Figure 16. Farba LED backlight in a city bus (image taken by author in streets of Istanbul)

3.2 Thermal Design Requirements and Concept Development

The main concept for the system under study is as follows: a multi-functional LED back-lighting lamp with double-sided electronic board inside a plastic housing of 98mm in diameter, the functions being stop, position and signal. This concept is thought to be able to be used as a universal product and meet the needs of the industry in the corresponding sector due to combining three types of light source functions. The lamp essentially consists of the following components: 1. Two-color transparent outer lenses 2. Reflectors 3. Carrier housing (enclosure) 4. Electronic board (PCB) 5. The cable 6. Screw, ventilation, lower parts such as gaskets. Figure 17 shows the components in detailed form in exploded view.

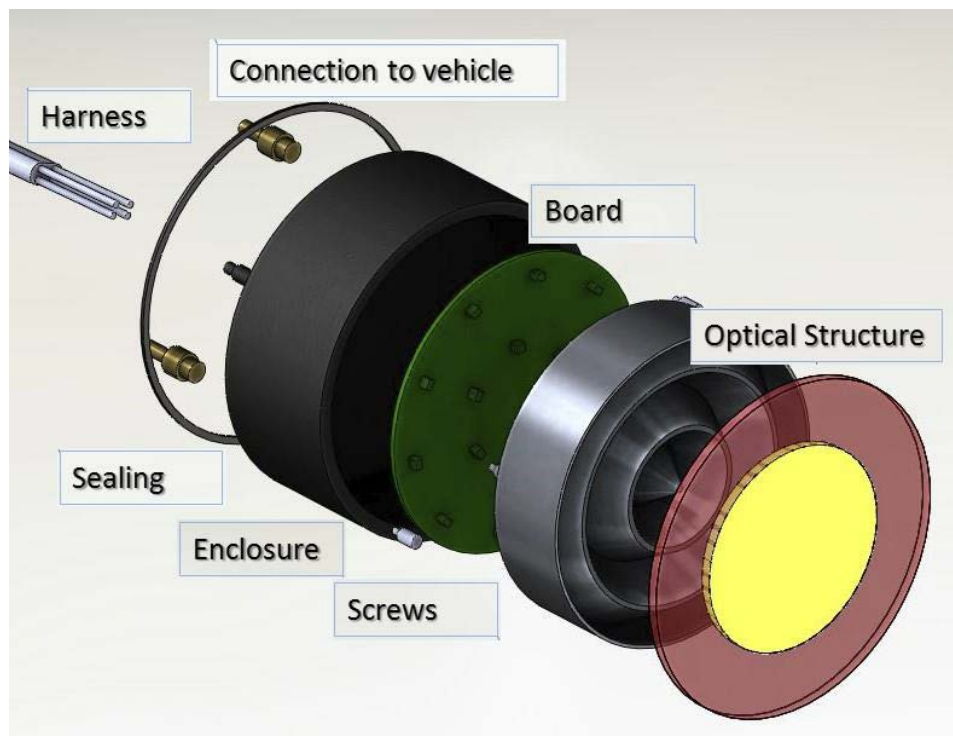


Figure 17. The design concept in exploded view

The driver electronics card which has the LEDs on its surface is concentric with the reflector that is Aluminum coated, optically reflective and is fixed on the board by means of three screws. At one end of the electrical connection between the vehicle and the lamp, vehicle connector is placed and on the other end, the PCB connector is found. The enclosure is assembled using the reflector screw-fixed to the PCB. Ultrasonic welding is then applied to the outside of the incomplete lamp housing and the lens. During the ultrasonic welding process, the welding feet on the lens are perfectly placed such that adequate adhesion is achieved. There are also screws for attaching lamp to the vehicle and also ventilation of the lamp on the rear surface of the enclosure.

Thermal vias in the prototype are filled with copper area which was initially created to help in making the temperature distribution on the board homogeneous. PCB is manufactured in IPC Class III cards according to the international standards. Life testing in electrical tests were made on the prototype board and tests of reverse polarization, such as performance monitoring and circuit boundary conditions were also done. Electrical and optical concept details are also found in Appendix A. In the concept design, required ambient temperatures are between -40 and 60°C, three years of lifetime is aimed for the prototype due to the customers' needs. As can be seen in Table 7, international standards were used for thermal tests. According to test rules, while performing tests on the prototype, melting in any part of the prototype, any type of permanent deformation or discoloration and negative degassing must not be observed; in addition, results of the measurements that are carried out after production of the prototype must be in accordance with relevant optical regulations. Furthermore, during the measurements, tests should be performed with thermocouples placed on the PCB surface and the maximum temperature specified by the manufacturer for PCB material, electronic components and LEDs must not be exceeded. Additionally, in case of LED

degradation tests not being successful, adequate approaches must be taken in this respect in order to eliminate the degradation as a priority.

Table 7. test conditions of prototypes

1	Brake, position and signal functions
2	Total lumen 800 lumen
3	LED chip temperature <100°C
4	Ambient temperature (C) -40 to 60°C
5	Lamp life is 3 years
6	Stop function open time operation 15 minutes
7	Stop function off time operation 30 minutes
8	When running, it should always be operated as a function of the signal flasher at 1.5 Hz
9	When starting, the position function must be operated continuously
10	13.5V voltage range can be applied to the product
11	Testing must be continued for 96 hours

3.3 Single Package Analysis

As a starting point, in order to create a three dimensional model of a commercially used LED packages that is also a part of the prototype, different investigations were performed; in other words, reverse engineering was done to an LED package to determine its exact measurements and inner elements. In the following section, the effort to cut this package is explained step by step.

3.3.1 Slicing an LED Package

During the first trial of understanding the LED package used in this project, it was carefully cut layer by layer so that package components were seen in detail. Figure 18 illustrates the variety of methods used as well as view angles under microscope.

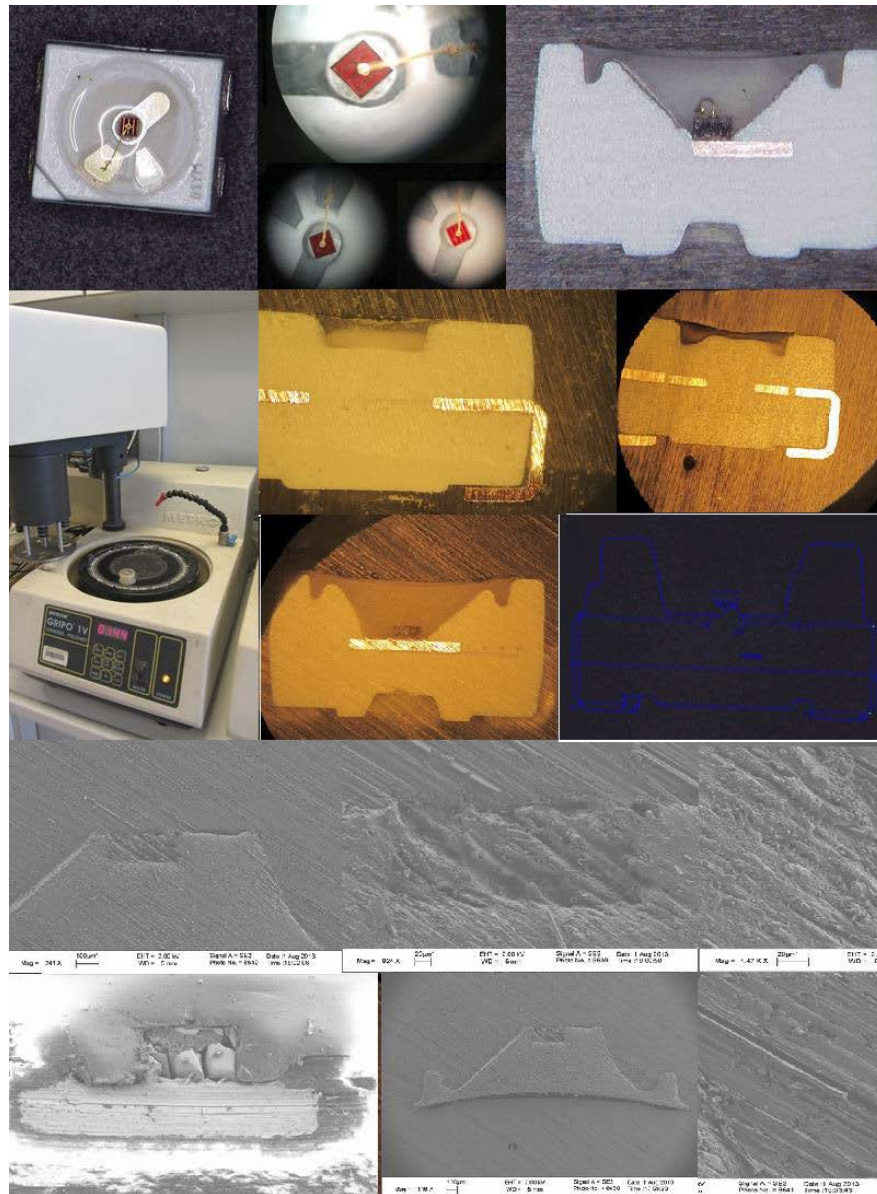


Figure 18. The package under microscope; various methods, different angles (all taken by the author)

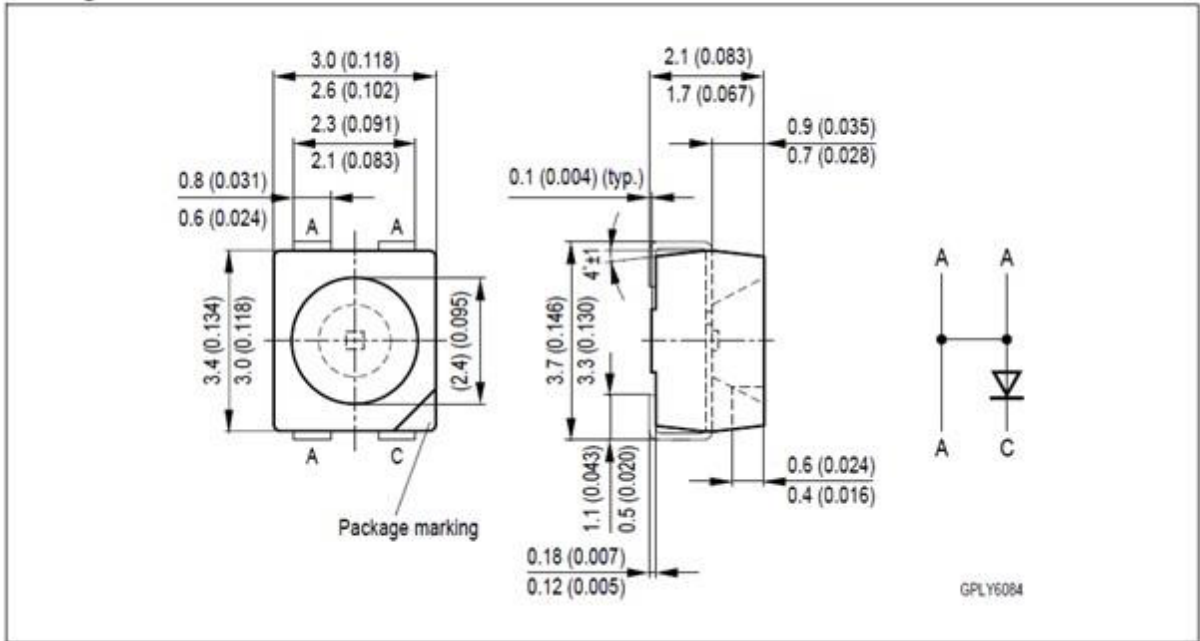


Figure 19. Data sheet provided by the LED Company [Osram]

The methods tried for cutting include diamond saw blade, specimen cross-section preparation for electron microscopy (Leica Microsystems) and sandpaper and were each checked at least two times in order to achieve precise dimensions which were not provided in the data sheet. For the sandpapering method, the sample was prepared in a 5ml cylindrical container, the LED package on the bottom and the silicon polymer mixture poured on top of it and cured for few hours; the lower surface of the working LED package was fixed by carbon tape. Thereafter, the cured sample was polished and removed and decreased layer by layer. Derived images were investigated under SEM and optical microscope for possible deformation and changes throughout the cutting process. The exact mid-cross section was taken later on. Chip and silicon measurements are derived through images. The chip is placed inside the silicone encapsulant, over the copper cathode. The lines created using the sandpaper are almost at 50 μ m order of

magnitude. The sandpaper used to finish the polishing may have been too harsh, but in the modeling, the scale of uncertainties is considered as acceptable. These measurements derived through the cutting were used along with the outer general details given by the producer (Figure 19 and Figure 20) to create a 3D finite element model for a numerical thermal analysis of the package. Here, the data sheet provided by the LED Company is also presented.

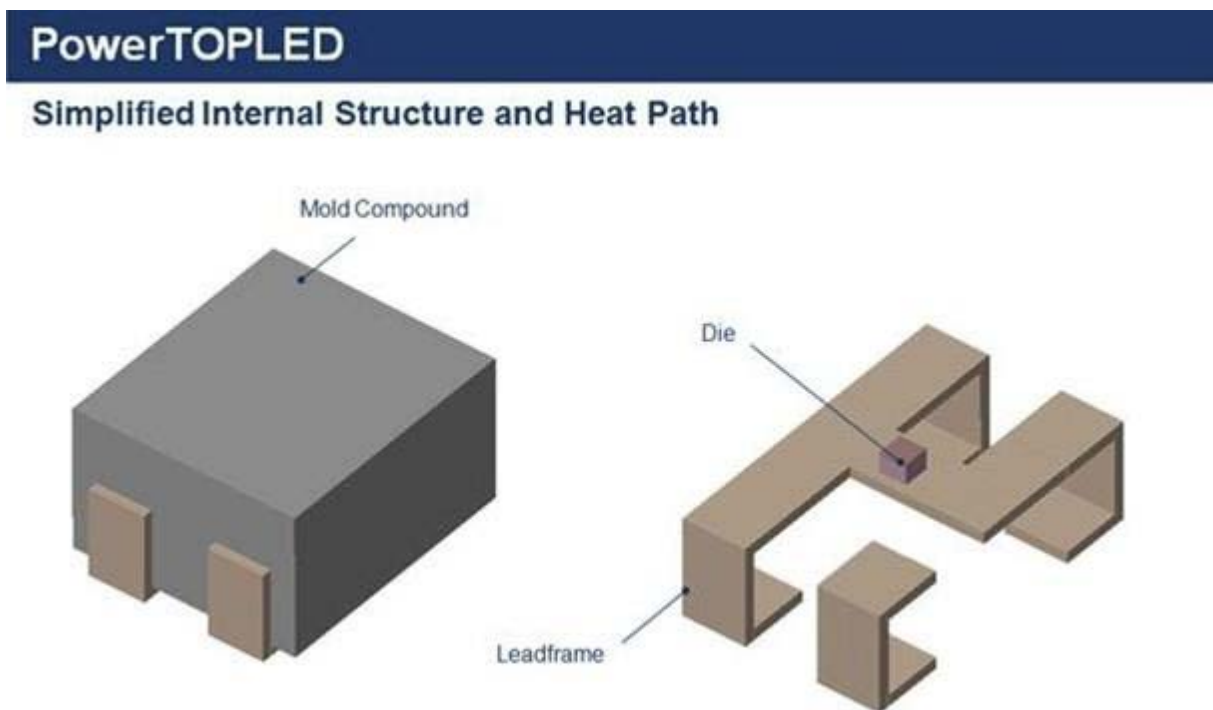


Figure 20. Leadframe in its most simplified geometry as given in the data sheet [Osram]

3.3.2 Analytical Study

Figure 42 shows a typical thermal resistance network for an LED system. The heat path traversing from the LED junction to the ambient is usually a long path of conductive

elements through the full system, at which point convection dissipates heat to the air and the surroundings [27]. Each part of this path must be properly manufactured and assembled so that thermal resistances are minimized. Individual parts or elements must use the proper materials (for thermal conductivity) and geometry (controlling the area for conduction to occur and the overall path length), as well as have proper interfaces to other parts for low interface resistances. For illustrative purposes, one can evaluate a simplified thermal network to understand a systems performance. Using Figure 21, thermal design parameters about a typical LED were investigated for each component inside an LED.

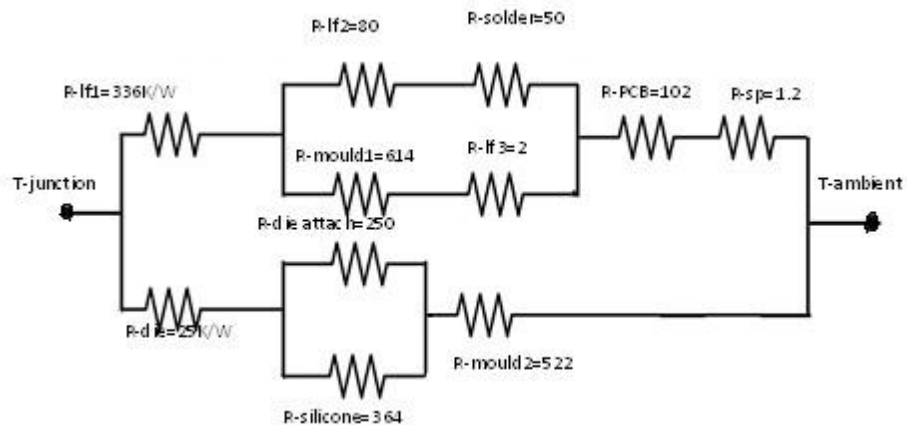


Figure 21. A sample thermal resistance network

As shown in Figure 22, the suggested thermal resistance network which is drawn by simplifying the conduction heat transfer paths connecting junction point to solder pads, given thermal conductivity values of 0.26 W/mK for die attach, 60 W/mK for solder, 401 W/mK for aluminum leadframe, 0.26 W/mK for moulding compound and 0.9 W/mK for silicone encapsulant. The resulting total resistance is reasonably close to

what is reported in the LED package data sheet provided by the manufacturer. This validates the model as well to an acceptable degree.

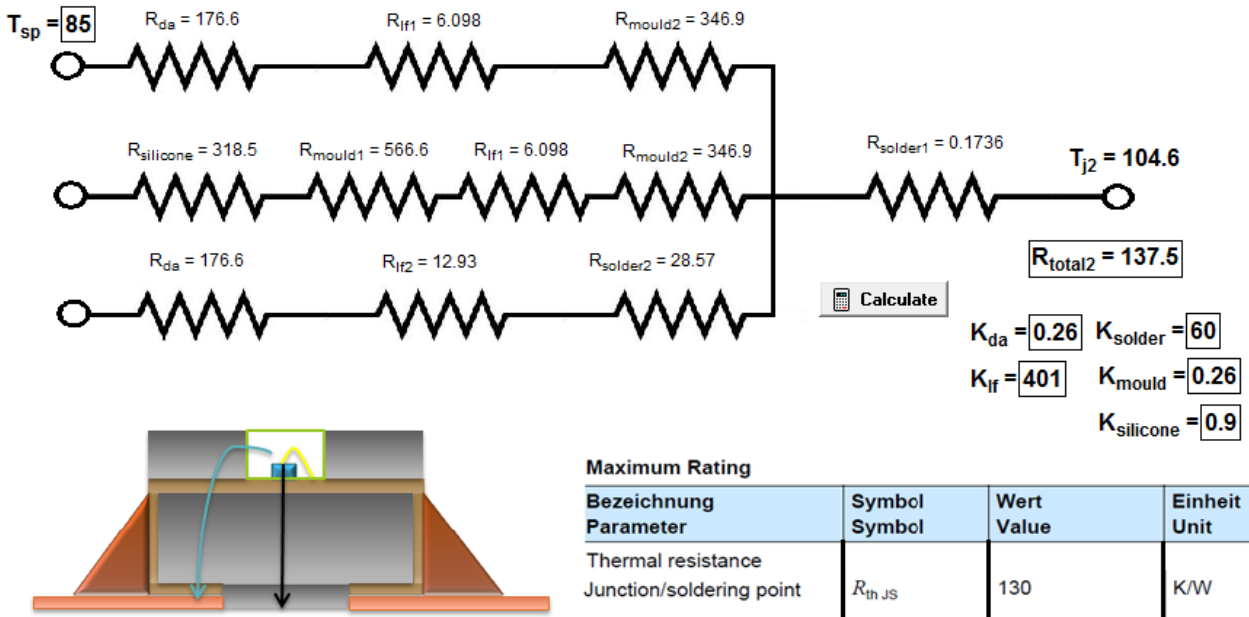


Figure 22. Analytical model (suggested) results compared with the table from the LED's data sheet

Table 8. Package thermal resistances obtained from numerical and analytical models

	Data sheet	Numerical	Analytical	Deviation (%)
$R_{jsp}[K/W]$	130	130.1	137.5	5.7
$R_{ja}[K/W]$	300	306.7	-	2.2

3.3.3 Numerical Study

The primary purpose of single package thermal study is to review the thermal performance of a commercial LED package and identify the performance bottlenecks via detailed 3Dcomputational models. In this study, we investigated the effects of each

component inside the LED package from thermal point of view. First, in the numerical study, different boundary conditions are implemented as different states and in each boundary condition (BC), each component is studied individually for its thermal impact (by its thermal conductivity). This is plotted as percentages versus the resultant thermal resistance. At the end of each study, a conclusion table is developed for that special BC. In the second part of this study, analytical models were developed for the same geometry and same components. Results and percentages of influence are once again obtained and compared with the numerical results.

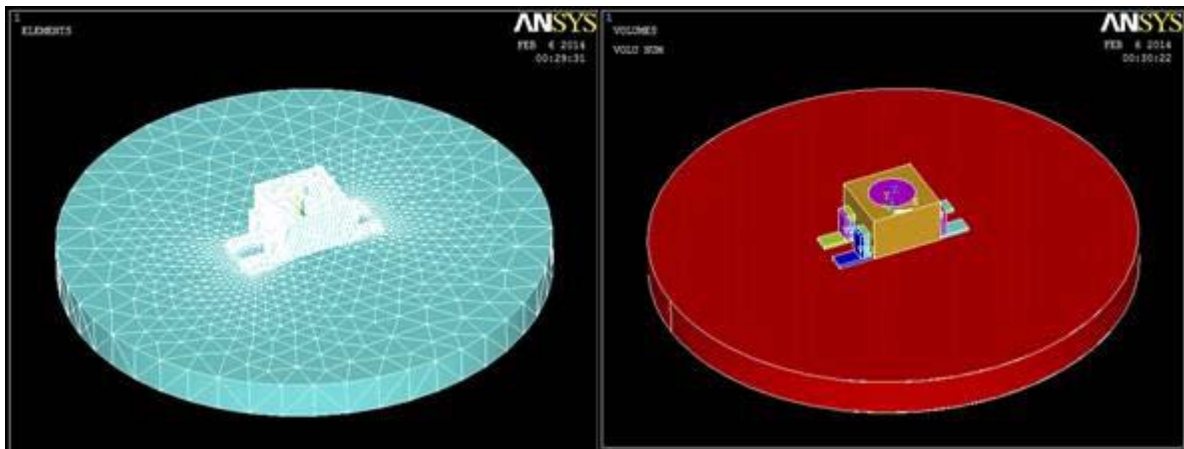


Figure 23. Geometry of the LED package on board and mesh elements

In the computational models, conduction heat transfer is of interest and bottom of the package (solder included) is assumed at a constant temperature since the conduction is the only mode of heat transfer in the package. The geometry used on the computational models is similar to the shape seen in Figure 23. The model consists of an LED package soldered on a cylindrical board of 20mm diameter. Heat flux through chip is almost 400000 W/m^2 and ambient temperature is $27 \text{ }^\circ\text{C}$. Four solder pad legs (where they sit on the board, touching) is set as fixed temperature surface and the chip surface is chosen

as heat generation part. Our primary goal is that we can validate manufacturer's data with the finite element models. The details of the numerical model (different elements) on ANSYS Mechanical APDL and the comparison of resistance with data sheet are presented in Table 9. The sample temperature contours are seen in Figures 24 and 25 where the component conductivities are set in a way that the resulting thermal resistance of the package is the closest to those provided by the data sheets. Finally, all of the boundary conditions are compared in a graph. FR4 PCB and Aluminum PCB are also compared.

Table 9. Properties of elements in LED package

	Temperature gradient [K]	Conductivity [W/mK]	Approximate volume [mm ³]
Moulding compound	29	0.2	16
Lead frame	29	380	1
Silicone encapsulant	27	0.7	2.5
FR4 board	45	0.3	125
Die (chip)	1.3	0.2	0.001
Die attach	16	20	0.0005
Solder	25	58	0.8
Solder pads	26	58	0.5

Geometry of the package was created in ANSYS Mechanical software. Implement component power levels and modeling details are found in Table 9. Input power of a

single LED package is found to be 0.125W. Heat generation is almost 75% of the input energy.

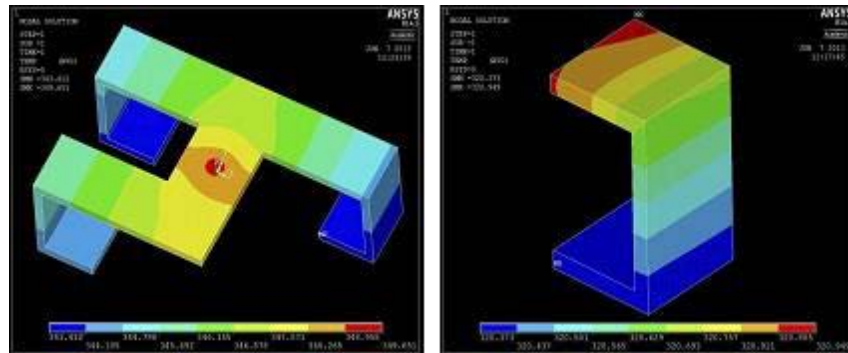


Figure 24. Temperature contours of anode and cathode with thermal resistances

Mesh independency study was performed and more than 150 000 elements were found to be adequate (Figure 26). Conduction is assumed to be the only heat transfer mode in the single package model. The package was soldered on a printed circuit board and therefore, both solder pads on the board and solder surfaces covering the lead frames outer parts were considered in modeling. Lead frame was expected to be a highly conductive material and it has a strong contribution to heat flow. The chip, die-attach and the silicone encapsulant also located above the lead frame were modeled in detail.

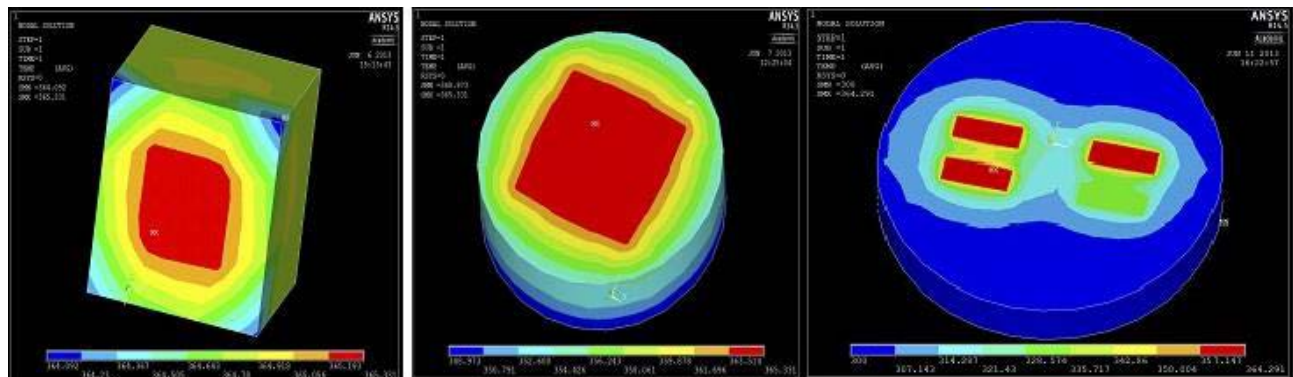


Figure 25. Chip, adhesive and printed circuit board temperature contours

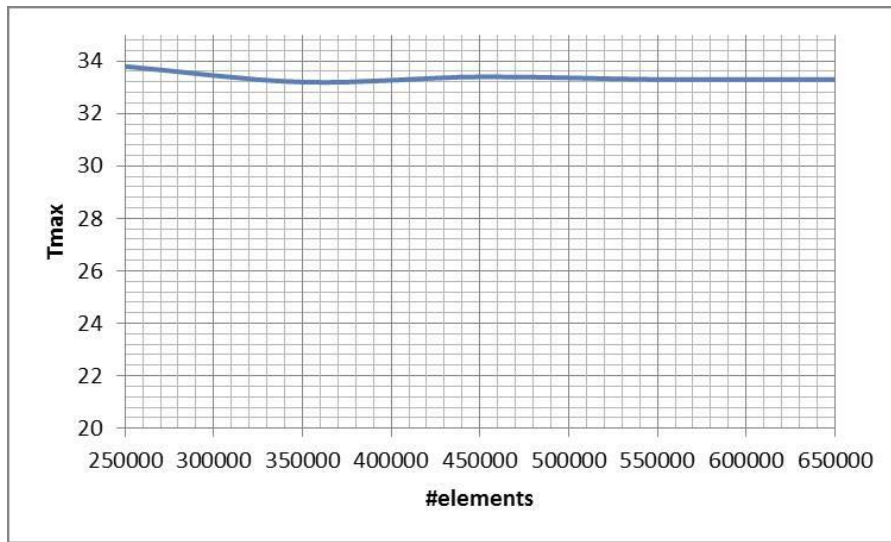


Figure 26. Maximum temperature versus the number of elements in MAPDL model showing mesh-independency

The components are then held inside the package with a plastic compound. Figure 27 gives a comparative bar graph of temperature gradients on each component in cases of aluminum board and FR4 board.

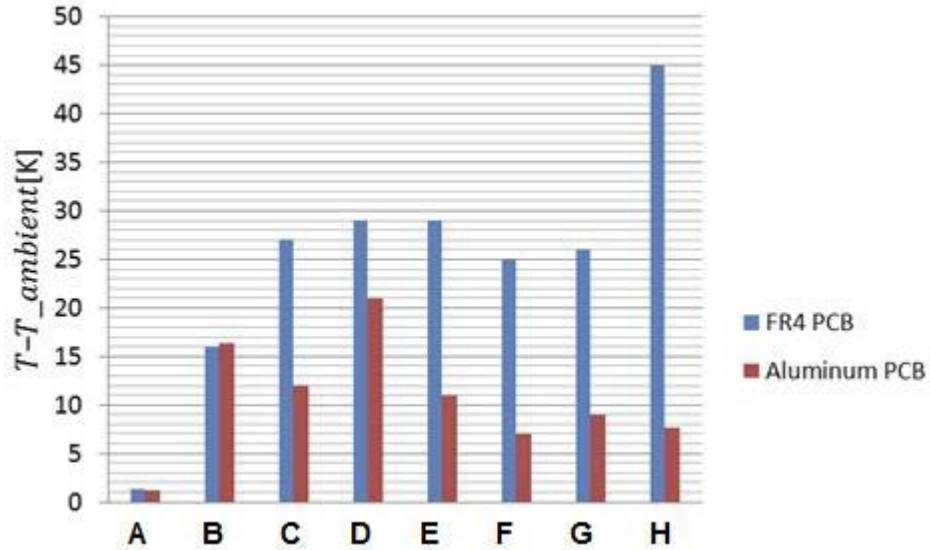


Figure 27. Basic comparison between Aluminum vs FR4 PCB constant heat flux is applied as thermal boundary condition on the area between; A: chip, B: die attach, C: Silicone encapsulant, D: Lead frame, E: Moulding compound, F: Solders, G: Solder pads, H: PCB

Table 10. Initial conditions of FE model

Package input power [mW]	125
Package heat generation [mW]	94
Ambient temperature [K]	300
Heat flux [W/m^2]	405493
Element numbers	171387

The chip and its adhesive, and an isothermal surface is considered to be at constant temperature, which is applied to different areas in each case. Two types of boundary conditions are applied as two different cases (Figure 28). In the first case, back surface of PCB is isothermal and in the second case, back surfaces of solder pads are assumed to be isothermal.

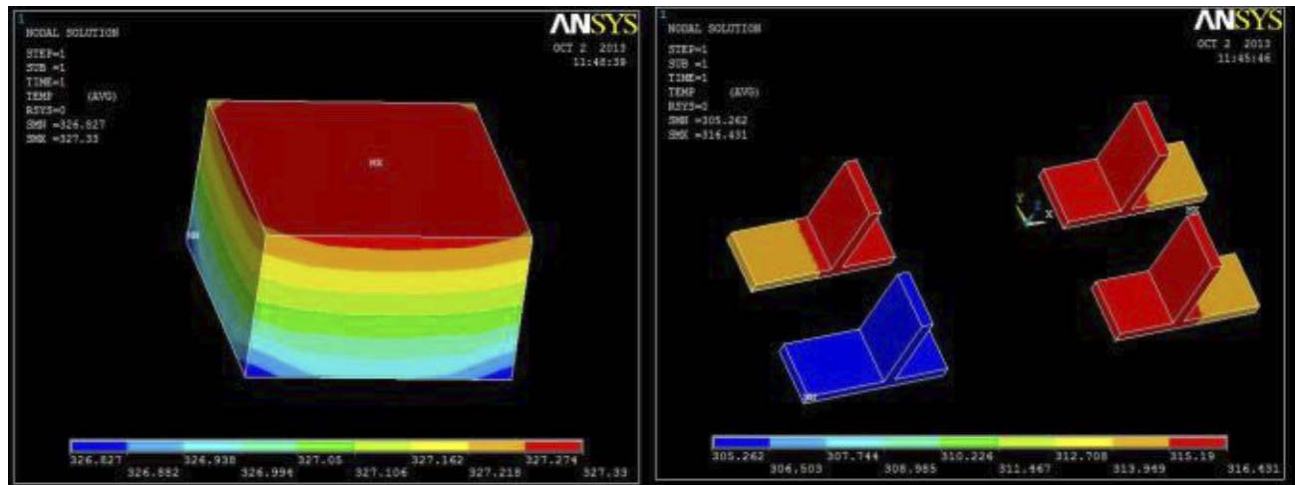


Figure 28. Two cases of single package numerical model analyses with different boundary conditions

Numerical models were run to determine local temperatures and temperature gradients and two different resistances are derived according to the maximum temperature in the chip and the maximum temperature on the solder (which is called solder point, Figure 29); leading to calculation of junction to solder point resistance and junction to ambient (or board) resistance. There is no difference between the definition of junction to ambient and junction to board because there is no convection and therefore no ambient resistance in the model. The reason why we do not consider convection is the very low percentage of its role in dissipating heat in comparison to conduction. A range of thermal conductivities of package components were set in a way that it could exactly conclude in the given values of thermal resistance in the data sheet. Table 11 lists the components and their conductivities. An analytical model capturing essential features of the package according to data sheet was built as well. However, the analytical model was created for the junction to solder point only.

Table 11. Chosen conductivities of the components (according to thermal resistance reported in data sheet)

Package component	Conductivity [W/mK]
Phosphor	12
Leadframe	370
Die	400
Die attach	0.8
Solder	100
Silicone encapsulant	0.7
Plastic moulding	0.2
Board	0.6

The reason for the junction to board (or ambient) not being discussed is mainly due to the unpredictable effect of spreading resistance, which cannot really be modeled using one-dimensional analogy, and it was not the primary goal of the current study.

The analytical and numerical resistance values for both junction to solder point and junction to ambient are compared with the manufacturer's data. It is found that junction to solder point thermal resistance is about 130K/W, which is much higher than conventional power packages. Both analytical and numerical models were able to predict the resistance within 5.7%. A number of cases were studied to derive the sensitivity of each of the resistances to each components thermal conductivity. Figure 30 and Figure 31 illustrate the sensitivity plots of various components. For every component, junction to ambient (board) and junction to solder point resistances resulted from computational model of a single package for both boundary conditions were obtained.

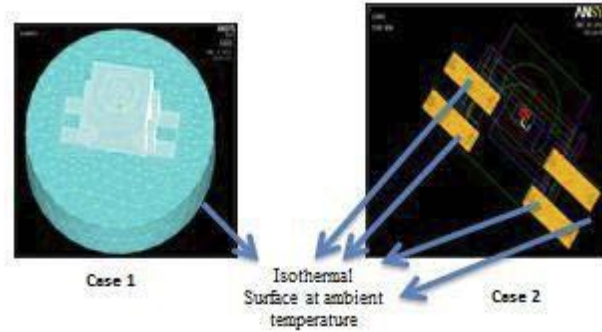


Figure 29. Temperature contours in (a) chip and (b) solders (scales are different)

A sensitivity term has been defined as $\Delta R/\Delta K$. A close examination of the sensitivity plots for resistance to die attach conductivity shows that as the conductivity increases from 0.2W/mK to almost 0.5W/mK , slope of resistance decreases abruptly with $370\text{m.K}^2/\text{W}^2$. Die attach is the adhesive connecting the chip to the lead frame and is also called die/chip adhesive (or sometimes silicon). As die attach conductivity was increased to 2W/mK (running a steady case for each die attach conductivity), resistance gradient model gradually decreased in each case, dropping with slope of almost $17\text{m.K}^2/\text{W}^2$. This slope is close to 22 times smaller than the slope of first part of the plot. If a factor is to be created for sensitivity of package resistance to thermal conductivity of die attach, we can say that with 4W/mK increase in die attach's conductivity, 250K/W decrease in resistance was achieved and therefore, sensitivity factor for this package to die attach from thermal conductivity of 0.2W/mK to 4W/mK is almost $63\text{m.K}^2/\text{W}^2$. However, it is better to deal with sensitivity factor more precisely. In other words, the factor should be reported when the resistance conductivity plot has the closest behavior to linearity. This way, we report two different sensitivity factors of the typical package under study to its die attach; one for lower thermal conductivities and the other for higher conductivities of this component.

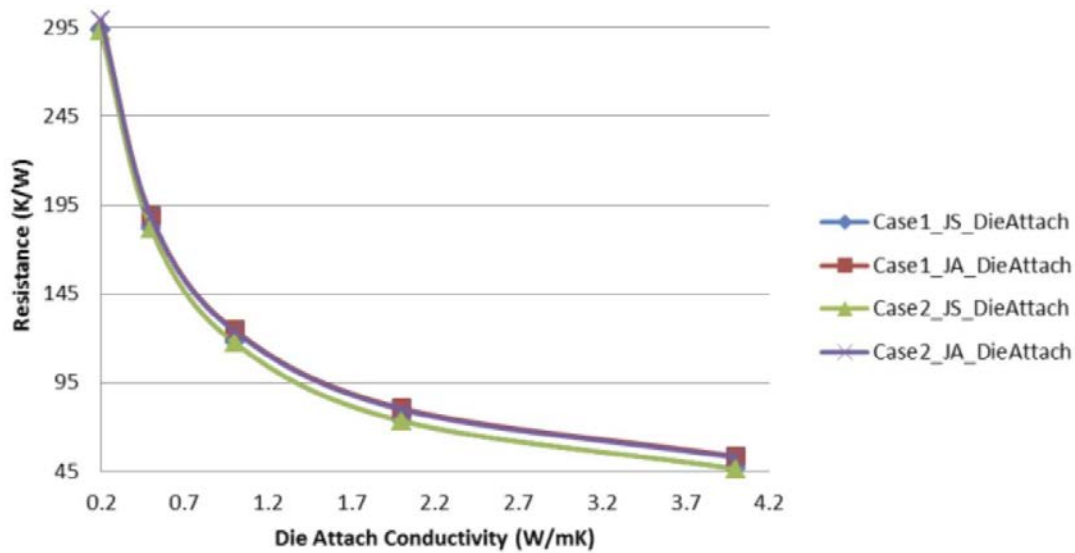


Figure 30. Sensitivity of a single packages thermal resistance to die attach conductivity

Plastic molding compound (which encapsulates the leadframe and the chip/die, die attach, phosphor, silicone encapsulant and is usually made of plastic or ceramic) has a more linear tendency when it is studied for its impact on package thermal resistance and shows higher potential to vary in conductivity compared to die attach. The slope of package resistance decrease according to case-1 boundary conditions is almost $1m.K^2/W^2$ which is again the sensitivity factor for plastic molding. It is seen that this sensitivity is a lot lower than the die attach's sensitivity. Lead frame which has the highest conductivity after the die itself is normally expected to be influenced the most when altered in conductivity. According to Figure 32 though, the slope of the line (which is the same as the mentioned sensitivity factor), shows the slightest sensitivity with almost $0.04m.K^2/W^2$. Lead frames high conductivity, which is the major heat path flow inside a LED package, is enough by itself and altering the conductivity range does not change the resistance to a great extent.

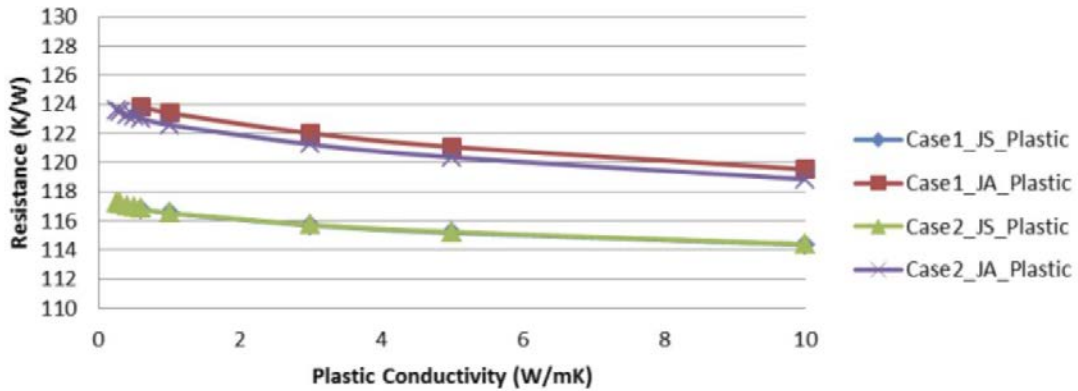


Figure 31. Sensitivity of a single packages thermal resistance to plastic conductivity

Silicone (the component encapsulating the chip/die, die attach and the phosphor) exhibits two different behaviors when low or high ranges (less than 10W/m.K and more than 50W/m.K respectively). For low thermal conductivities, silicon causes a dramatic drop in the package resistance with a decrease close to almost 100K/W of decrease. From 50W/m.K to higher conductivities, though, silicone affects the package resistance minimally with almost 0.16m.K²/W² slope of decrease. Therefore, silicone has two types of behavior, showing sensitivity of 10m.K²/W² in lower conductivities and 0.16m.K²/W² in higher.

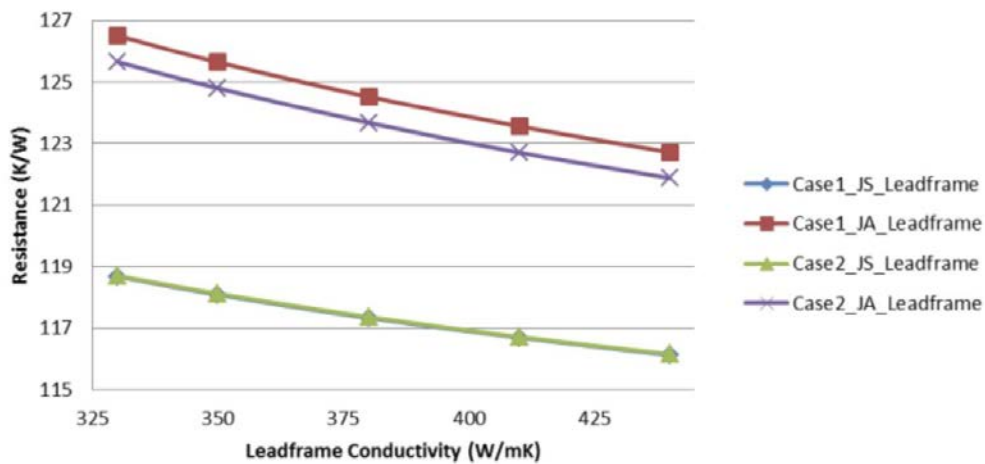


Figure 32. Sensitivity of single packages thermal resistance to leadframe conductivity

It is evidently clear from the boundary conditions definition that thermal impact of PCB on LED package is actually ignored in the second case. Figure 34 illustrates the sensitivity factor for the board. As for the silicone impact on the total resistance, board is also showing two different behaviors in different conductivity ranges. For a low range of around 0.3W/mK which is the typical conductivity for an FR4 board, the drop is even steeper than it was for lower ranges of die attach conductivity. The sensitivity factor is around 1700 mK²/W². But when the conductivity is in the tenth orders (specially starting from 20W/mK), the sensitivity behavior changes and much lower sensitivities are achieved up to very high values. The board, therefore, shows the largest changes compared with other components. As can be derived from Figure 33 and Figure 34, percentage difference between these two cases are in the order of 5% of the highest values. But both JS resistance and JA resistance are of utmost concern in the second boundary condition case. Basically, for the solder pad isothermal condition, JS is calculated using the maximum temperature on solders and JA from their minimum.

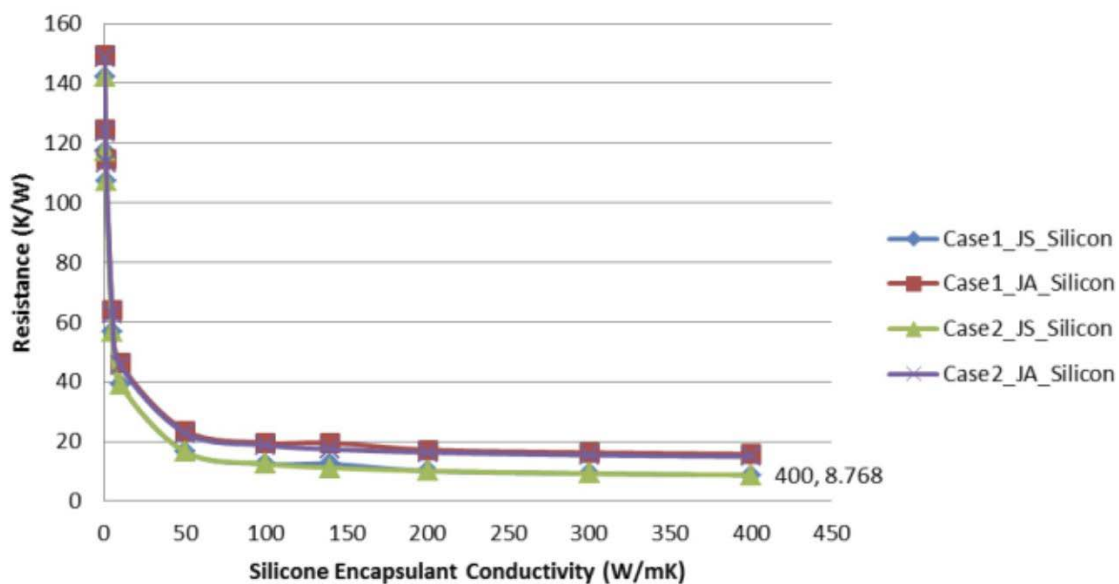


Figure 33. Sensitivity of a single packages thermal resistance to silicone encapsulant conductivity

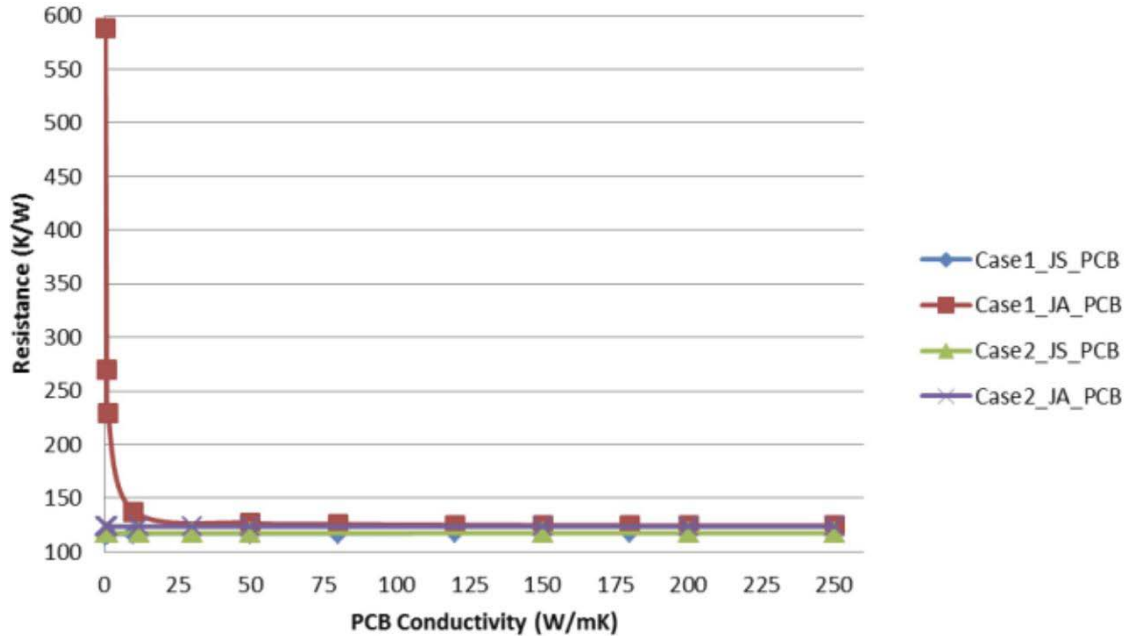


Figure 34. Sensitivity of a single packages thermal resistance to board conductivity

In order to study the sensitivity of solder, the only resistance which can be relied on is the JA which is due to the fact that the point of maximum temperature on the solders cannot give a precise view of the sensitivity of the LED package to the solder itself. According to Figure 35, JA resistance for both case 1 and case 2 can be the study point for the solders conductivity but the behavior of solder is the same in both. With a changing pattern close to linearity, package resistance reacts to increase of solder conductivity with a slope of almost $0.03 \text{ m K}^2/\text{W}^2$. This way, solder shows the least impact possible among the components studied so far. Overall, according to the plots, die attach and silicone (encapsulant above the die and phosphor) reveal their importance as two components playing the most significant roles from thermal conduction point of view inside a typical commercialized LED package. In order to make the sensitivity factor comparable for individual studies of various LED package components, a new

parameter is defined. This time, logarithm of the sensitivity factor is used. Thermal impact of each component is then plotted in a bar chart as logarithm of sensitivity.

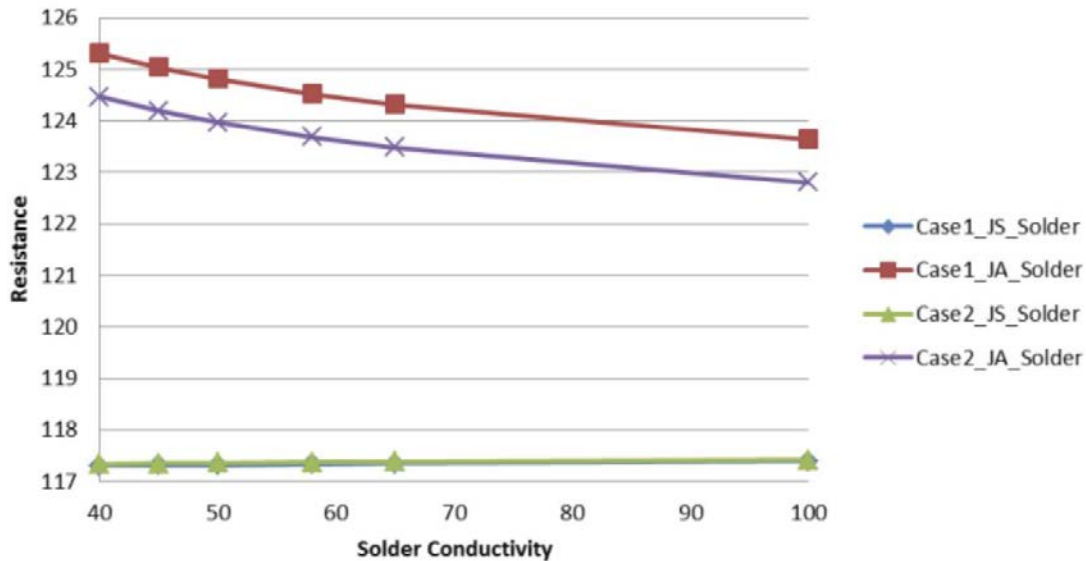


Figure 35. Sensitivity of a single packages thermal resistance to solder conductivity

Plastic molding with a low sensitivity will be standing in the center and negative values of logarithm will mean the factor is in the range of 0 and 1m.K2/W2. The lower the value for each component, the closer their sensitivity is to zero. Figure 36 depicts the so-called conductivity sensitivity factor or CSF for all the described parts in logarithmic scale. In other words, logarithm of CSF is plotted as pie chart for each component. Since the sensitivity differs in lower conductivity ranges and higher ranges for some of the components, bar chart is divided in two ranges: low range and high range. According to the results, the board has the largest effect and its sensitivity impact is very strong especially when designed to produce with low-range conductivities (such as in FR4). This is already applied by sprayed copper layers in the end of board and by added thermal vias. Die attach and silicone are the next two sensitivity creating parts leading to plastic (molding compound) and the lead frame. Moreover, in higher ranges,

die attach and plastic are the two major sections requiring thermal attention. Board, silicone and leadframe are respectively the next. A very crucial point which cannot directly be understood that the high conductivity range differs for every component, i.e. 20 to 250W/mK for PCB, 100 to 450W/mK for silicone and 2 to 4.2W/mK for die attach. But the low range is almost up to 1W/mK for all. Plastic mold is seen as zero which implies that magnitude of CSF for mold is equal to 1.

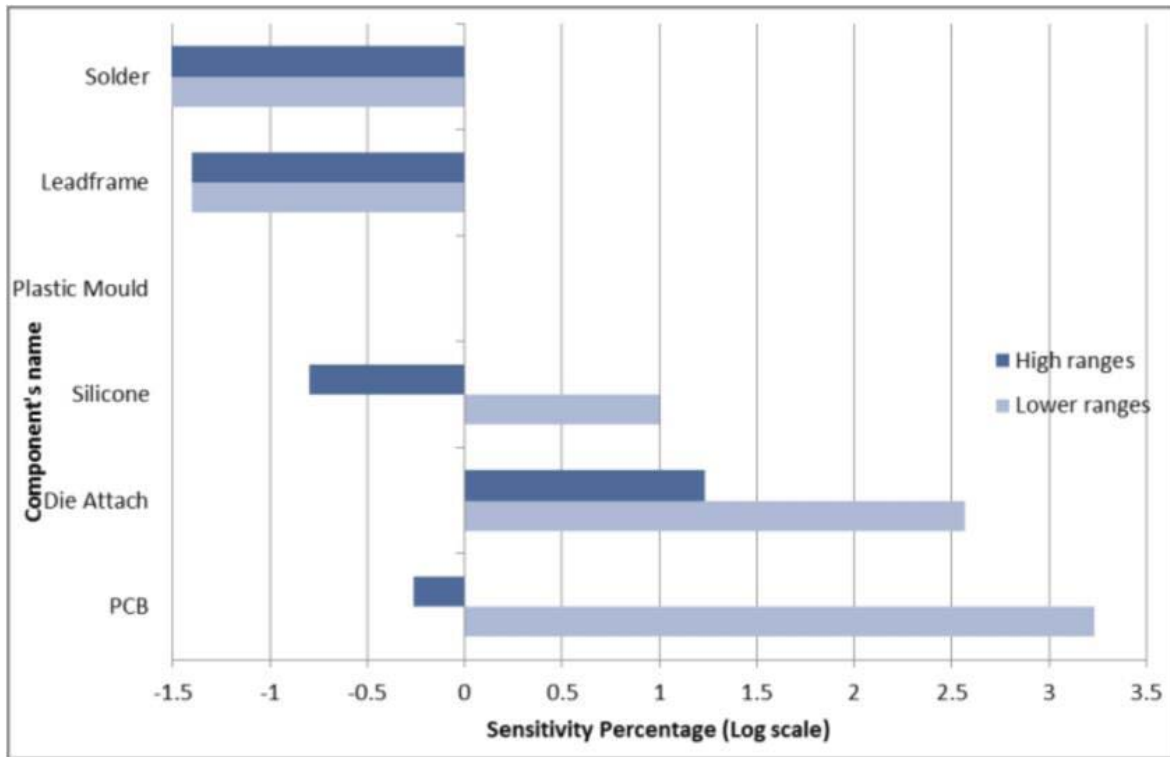


Figure 36. Effect of components conductivity on junction temperature sensitivity

3.4 System Level Analysis

While package level analysis can identify key parameters at the LED package level, a system level analysis identifies the hot and cold spots in a larger scale. In system level modeling, a number of electronic components with different heat fluxes are located at

the rear of the LED PCB board. Although the heat dissipation rate seems low compared to conventional electronics, thermal margin for design engineers and aggressive ambient conditions poses significant challenges.

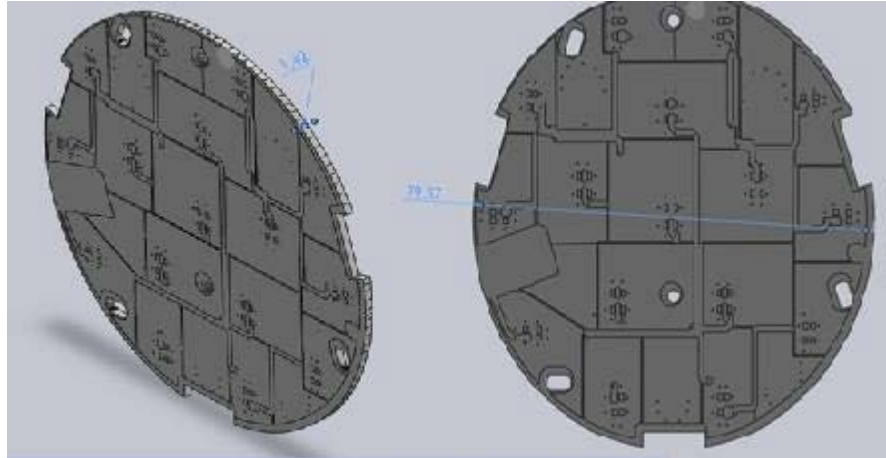


Figure 37. Geometry created in Solidworks CAD

The System CAD models were both created in ANSYS and in CAD software, Solidworks (Figure 37). Due to numerous details of the board (with all the layers, components, solders and vias), the CAD model must be idealized. Particularly when modeling in Icepak (ANSYS 14.5 [28]), details are simplified up to a level that it is both verifiable and compatible with ANSYS modeling. After creating the CAD model, boundary conditions were applied and solution was run. All results are explained in the final chapter.

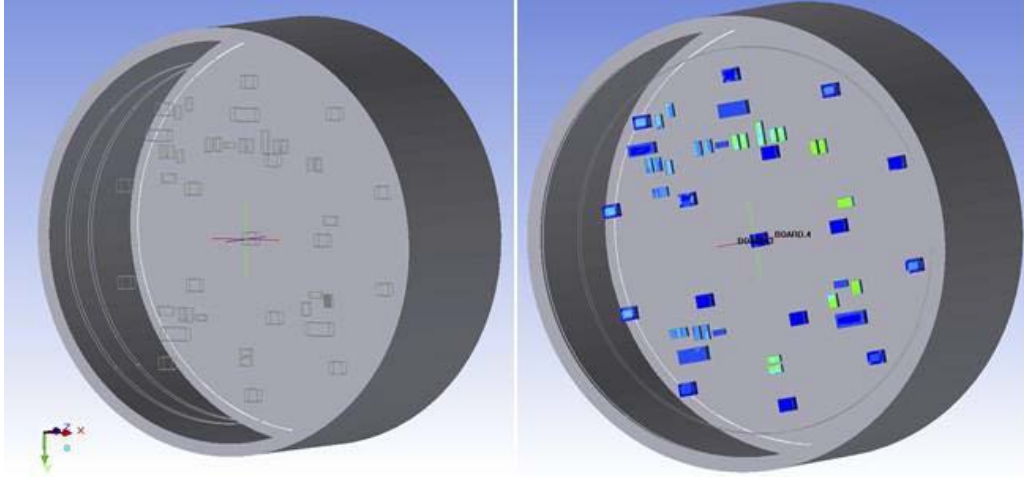


Figure 38. Geometry of Board inside its plastic enclosure along with initial temperature contours

Geometry of the system is modeled as shown in Figure 38. The lens and closing wall of the plastic housing are viewed as transparent so that the inner details of the modeling is seen. Figure 39 shows initial results of the CFD modeling. The model is solved for different board materials, different component arrangements (according to different arrangements of the prototypes), with the board inside/ outside the enclosure (i.e., in free-space) and different ambient conditions.

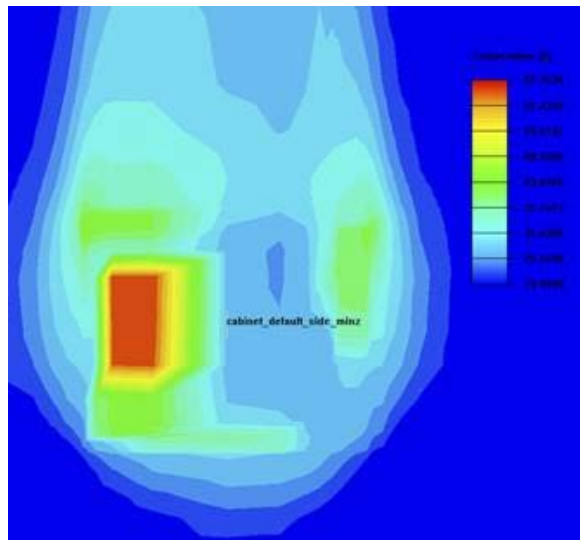


Figure 39. First numerical results of CFD modeling

Table 12. Power rate and heat dissipation for each function

Function system	E [W]	Q [W]
Function-1	0.43	0.39
Function-2	2.98	2.58
Function-3	4.22	3.78
Total	7.63	6.75

Total current to the board is close to 400mA with components legs sitting directly on one of the metallic layers of board. LEDs power input is up to 400mW, transistors 840mW and resistors up to 200mW. Details of electrical and thermal power are summarized in Table 12. Vias are holes around local hot spots and are covered by a copper layer of 70 μ m thickness, playing an important role in enhancing board spreading conductivity with lowest cost possible. The board geometry is shown in Figure 40 while being tested. The system is supposed to operate in an aggressive environment of between 40°C to 80°C in a tight thermal envelope. Farba Company expects lifetime of about three years for the prototype under full functioning conditions.

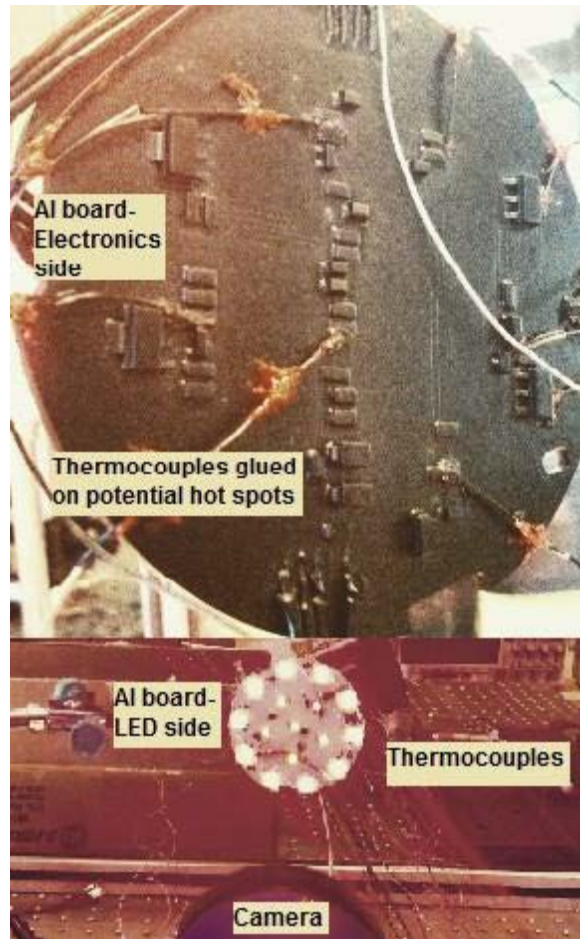


Figure 40. Multi-functional LED backlight board with thermal vias, (a) front layout, (b) back layout

3.4.1 Analytical Study

A simplified analytical network of thermal resistance was proposed for the current system as shown in Figure 41 (this figure is only a sample since the real values of resistance for each part differ in each prototype). In the figure, junction temperature on the left is connected to the ambient temperature by external resistance, normal LED resistance (4 K/W for each type of LED), PCB normal resistance (less than 1 K/W) and electronic components' normal resistance (the highest being 18 K/W). The simplifications turn the resistance network into a different system where spreading

resistance is excluded. However, the model could still be utilized to get an understanding of how sensitive the whole network of zero spreading resistance reacts to the normal board resistance. This sensitivity was found to be more than 300 percent when compared with any other resistances (LEDs, solder pads, electronic parts or external resistance). Since the analytical problem in this case is totally different than the system model (since shifting from 3 dimensional to two dimensional problem), the results are not compared with the ANSYS results. The only conclusion is that when simplifying the system resistance to a 2D network, the board resistance still has a much higher influence on the total system and this adds value to the focus of the current study (increasing the resistance of board).

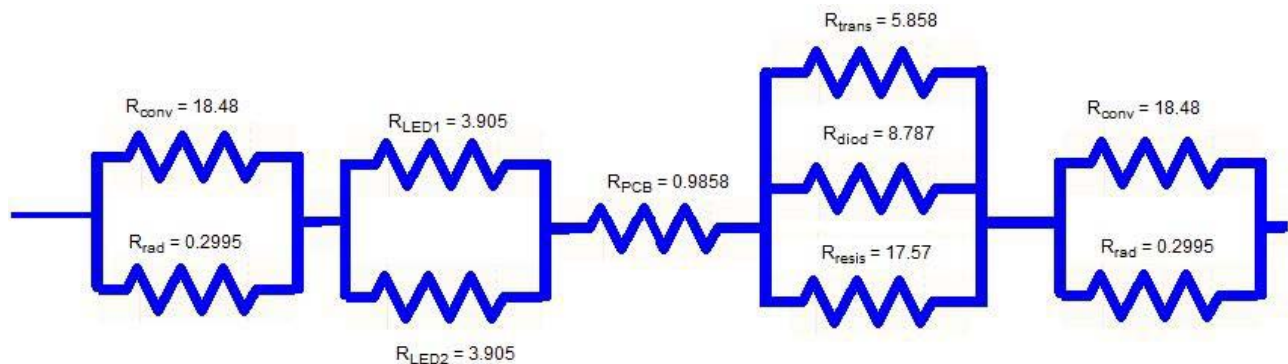


Figure 41. A sample thermal resistance network for the automotive lighting system board in free-space

3.4.2 Numerical Study

After creating the geometry of FR4 and thermal clad board, mesh sensitivity of Icepak model was checked. Figure 42 shows the residuals and solution details. When increasing the number of elements in mesh, the temperature results are sensitive up to a certain number of elements. This number is 500 000 as seen in Figure 43. The results

are independent from the number of elements and mesh type after this certain point. The model is solved using 703481 number of elements in the free-space.

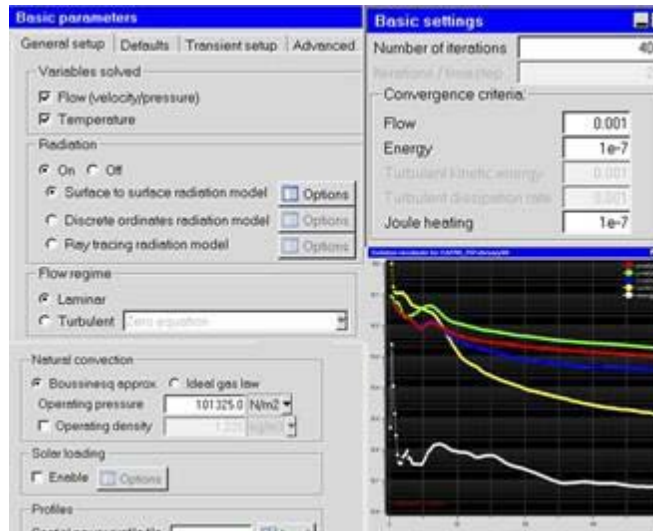


Figure 42. Basic parameters and settings of Icepak model

The CFD model is checked for mesh-sensitivity, resulting in the model being mesh-independent. Mesh sensitivity is checked according to one of the components (i.e. Q3) which creates one of the local hot spots on the board. Model is checked for independency to mesh (Figure 43).

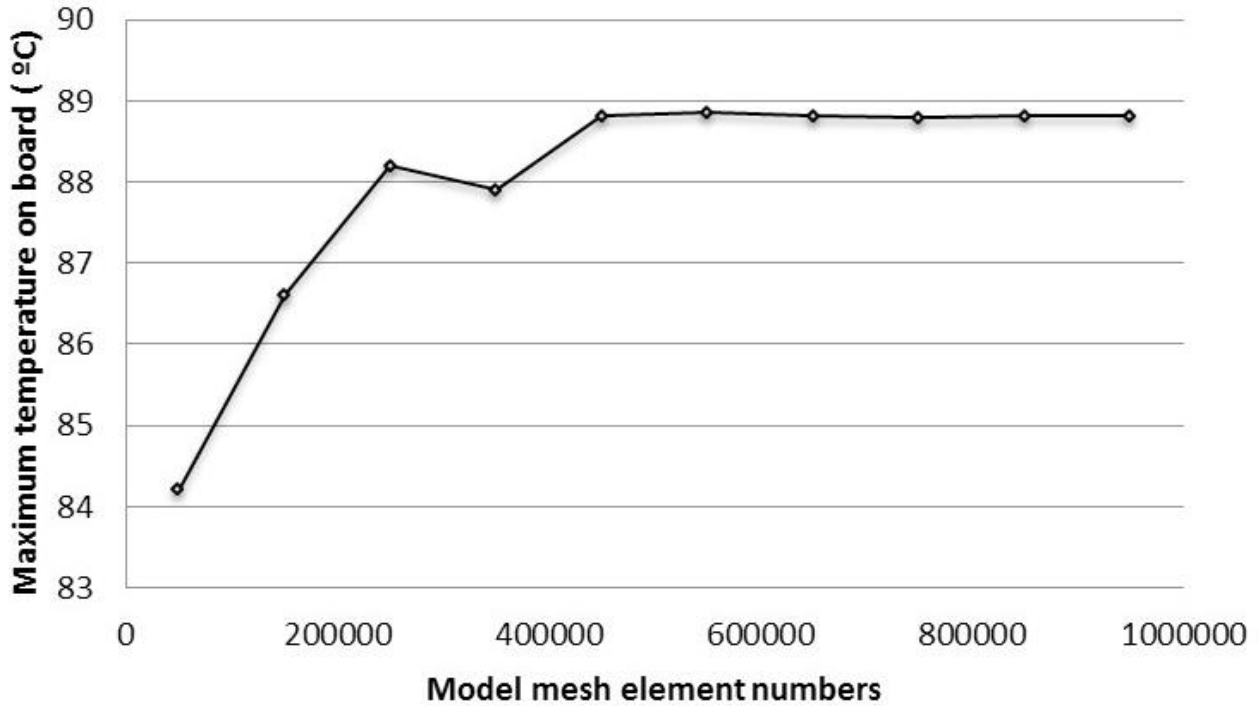


Figure 43. Mesh sensitivity plot for Icepak model

Temperature results are then derived. First, each board is solved without any enclosure and then a plastic enclosure along with the simplified optical structure is modeled to represent the thermal behavior of those parts in the tightly packed system.

Temperature results for the double-sided FR4 board shows that maximum local temperature occurs on the electronics side where the high flux components are densely populated. This configuration is also dependent on the structure at the other side of the board (LEDs side) where the maximum local temperature (which is less than the total T_{max}) happens about the same place. As previously mentioned, this local area is also dependent on orientation. Overall, hot regions locally vary strongly and are more on the electronics side (transistors and resistors) due to higher fluxes. Total maximum temperature is found to be 110°C and minimum 46°C. When the board conductivity is low, it responds significantly in terms of temperature distribution to a slight increase in

conductivity. But when the board is more conductive, the slope of decrease in maximum temperature drops as. On the next level, double-sided thermal clad of this study is tested so that we compare FR4 results with results of compact LED lighting system that is suitable for a high performing economical automotive exterior LED lighting approach. Thermal clad board model results demonstrate a more uniform temperature distribution on both electronics and LEDs side. These results show that metal core board clearly has a uniform temperature of 70°C and minimum of 63°C.

According to the temperature results, maximum junction temperature is decreased by 34°C only by changing the board from FR4 to thermal clad. We have observed that local hot spots are dependent on orientation, heat flux density of both sides (LEDs, transistors, resistors etc.) but this sensitivity is decreased when using thermal clad board since the distribution is uniform (temperature gradient on the board is less than 7°C). Due to the fact that electronic component suppliers estimate doubling the rate of failure for each 10°C rise in the junction temperature, thermal clad board is a more promising approach here with less than 10°C all through the board which means the waste heat generated in each component is efficiently removed and is highly reliable. These computational results will be verified with the experimental results in next section. Using these results we can have an image of change we should expect in maximum temperature on the board, when using high-conductive heat spreaders such as heat pipes (Figure 45).

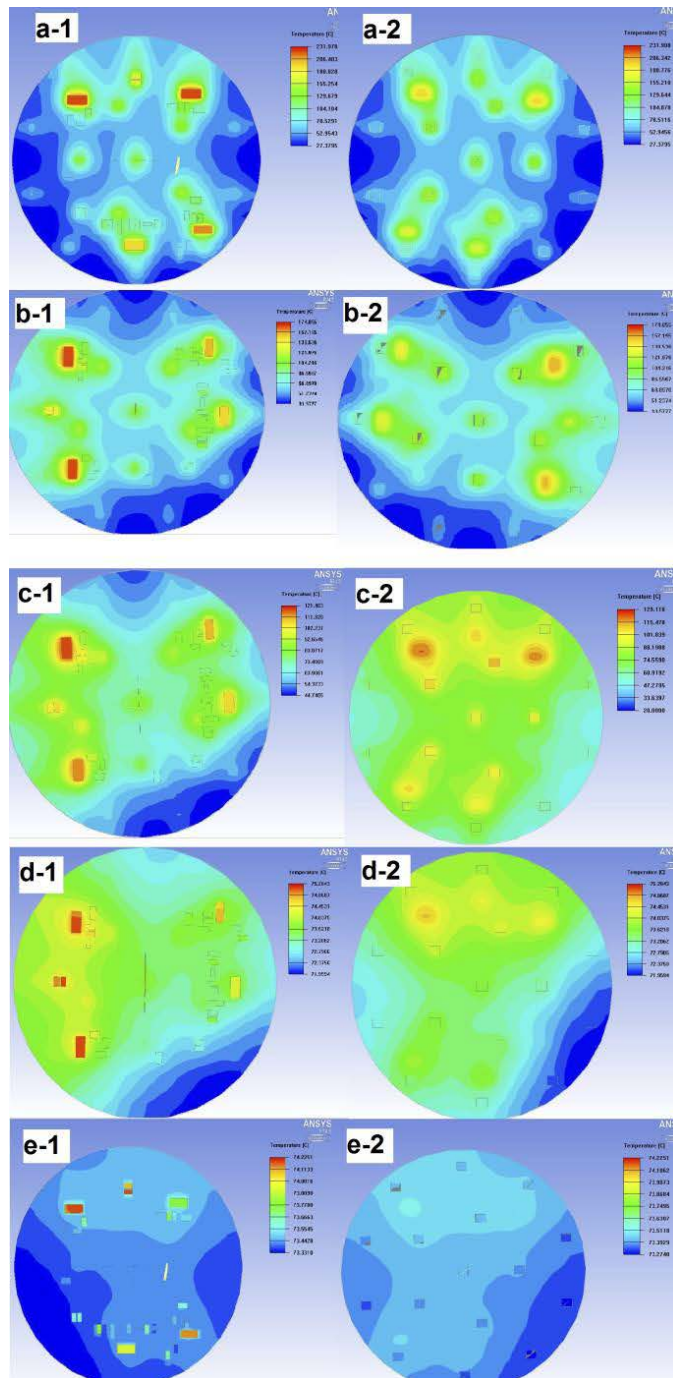


Figure 44. The temperature contour in post processing of the lamp model, (a-1) board conductivity 0.2W/mK, electronics side, (a-2) board conductivity, 0.2W/mK, LEDs side, (b-1) board conductivity 0.8W/mK, electronics side, (b-2) board conductivity 0.8W/mK, LEDs side, (c-1) board conductivity 2.5W/mK, electronics side, (c-2) board conductivity 2.5W/mK, LEDs side, (d-1) board conductivity 160W/mK, electronics side, (d-2) board conductivity 160W/mK, LEDs side, (e-1) board conductivity 1000W/mK, electronics side and (e-2) board conductivity 1000W/mK, LEDs side

3.5 Developing Other Concepts for the Prototype

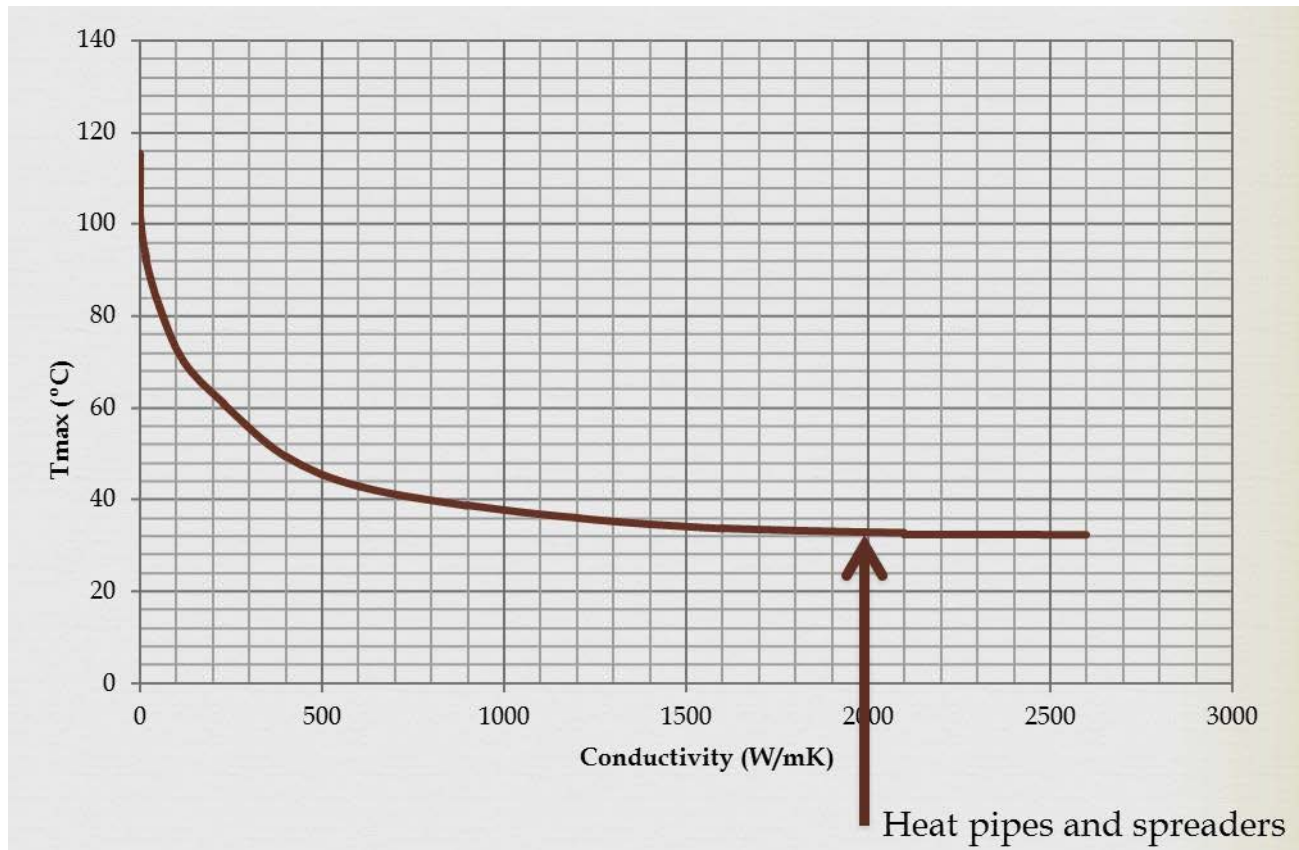


Figure 45. Basic comparison between the max. Temp. in different board materials

At the final stage of this study, a number of concepts are developed to enhance the thermal performance of the system. Initially, a prototype is made with Thermal Clad board. Thermal performance is checked (this will be explained in detail in the next chapter). Thereafter, heat pipes are modeled in order to be checked in terms of thermal performance embedded inside the board. Initial models were created and the results were recorded. A simple geometry of the board inside the enclosure with two vertical heat pipes is seen in Figure 46 and Figure 47 (mesh independency checked).

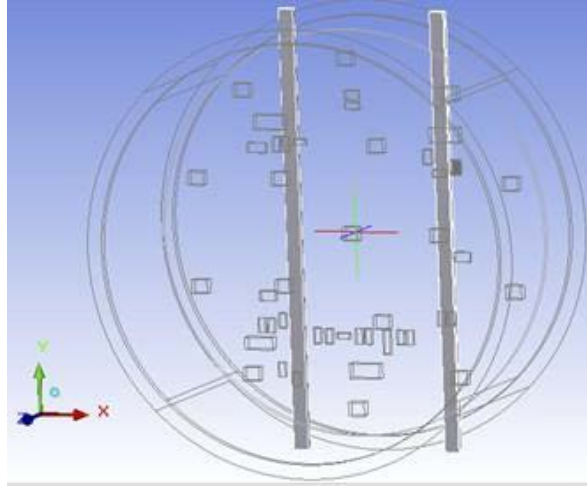


Figure 46. Initial modeling with heat pipes

Due to the high temperature gradient created in this board (FR4), highly conductive bars and heat pipes lead to achieving higher uniformity of temperature. But the final results will be available when every possible case is created and checked for feasibility.

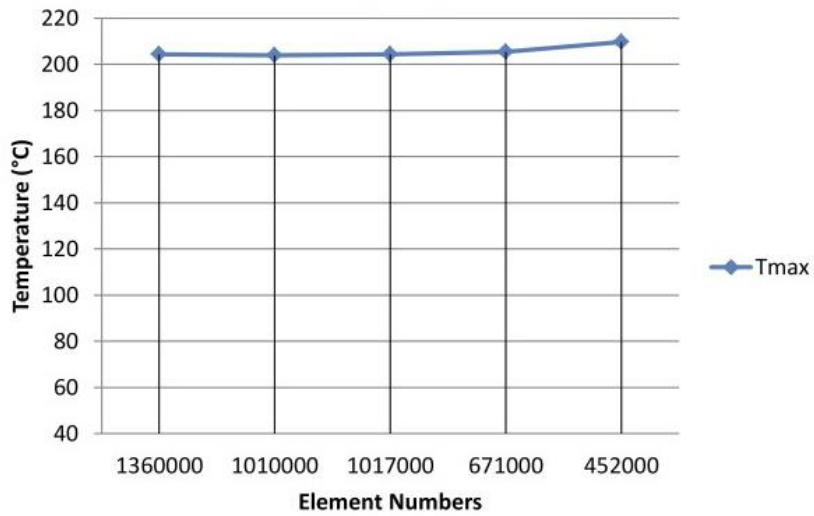


Figure 47. Mesh independency plot

CHAPTER IV

EXPERIMENTAL ANALYSIS

In this chapter, the system of measurement is introduced both for the automotive lighting prototype and the heat pipe performance test. Experimental procedure is given in detail along with standard deviation analysis and uncertainty analysis for each.

4.1 Measurement System

Measurement system design is one of the important tasks in experimental tests of electronics cooling. In order to measure the performance of an experiment, basic parameters have to be measured. These parameters are: temperature at various points, flow (in forced convection), and electrical input power. When cold plates (forced convection cooling) are used, temperature in and out from the cold plate or water tank, ambient temperature to calculate heat loss from the system, and sometimes insulator and cover temperature are some of the variables that must be checked. The systems have been designed and calibrated to measure all these parameters. Temperature measurement thermocouples were used in measuring liquid, insulator, surface and ambient temperatures. T-type thermocouples with calibrated data acquisition system were used for the whole measurement set up that is shown in Figure 48. The digital

display data logger was used for reading the temperature scale. The data logger was designed for other heat transfer measurement and had to be calibrated for this experiment. It was calibrated using thermometer of a hot plate as a reference.

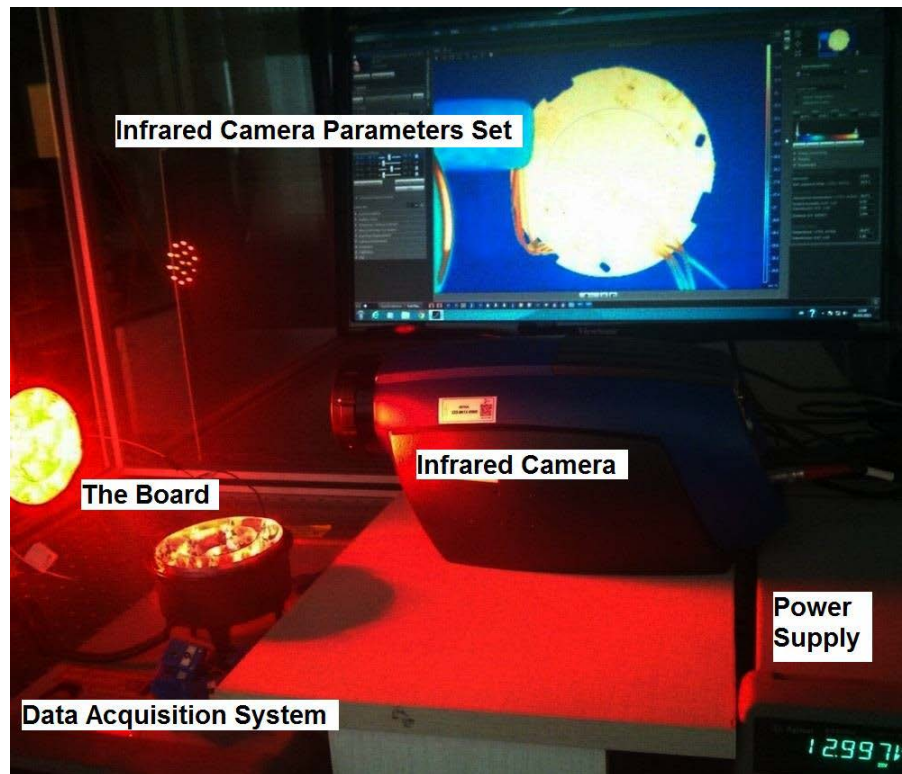


Figure 48. Experimental Setup Parts: IR camera test

4.2 Experimental Testing Procedure

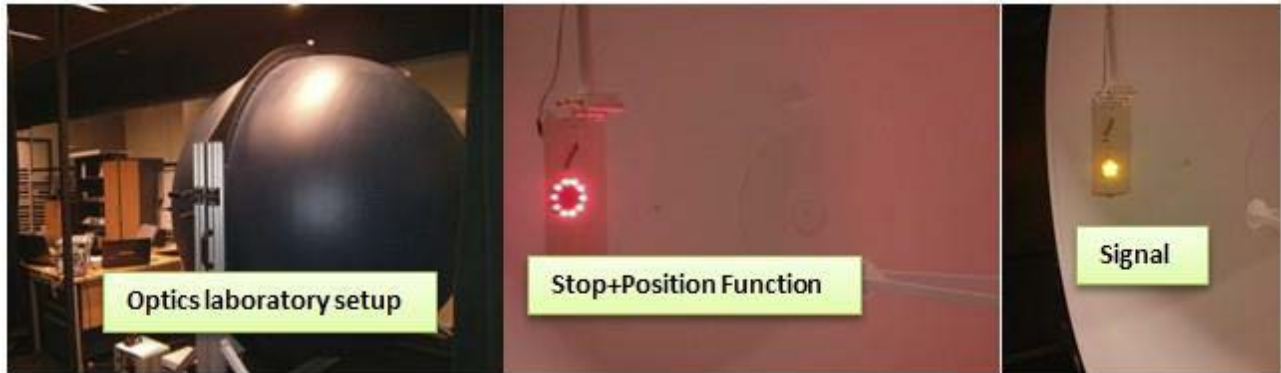


Figure 49. Experimental setup parts; integrated sphere test

The setup consists of power supply, data acquisition, a number of thermocouples attached to surface of the prototype (board along with the enclosure), the FLIR IR camera and the FLIR software for measurement. As is clear in Figure 48, the setup components are put together inside a full-wall 1m³ cabinet in which each test is performed. Three functions of the system along with their measured optical output are seen in Table 13 (measured in Evateg optical laboratory's integrated sphere).

Table 13. Function modes of the system

Functioning mode	Voltage (V)	Lumens
3i1 (simultaneous)	28	90
Signal	28	33
Position	28	7.5
Brake (stop)	28	51

In the tests, thermocouples are glued to surface of the prototype using RTV Red high temperature silicon gasket maker. This is due to the fact that the point for which the temperature is being measured by both thermocouple and camera must be visible to IR rays by means of a substance that stands to high temperatures. Figure 49 shows the optical setup (more optical details can be found in Appendix). Electronic components are given more attention due to their hot spot issue. The system works with 28 volts and for each test, steady-state condition is achieved. Reaching steady-state condition as seen in Figure 50 takes 20 to 30 mins but in order to make sure that the results are not changing out of the 1% range, 120 min of steady-state time is considered as suitable.

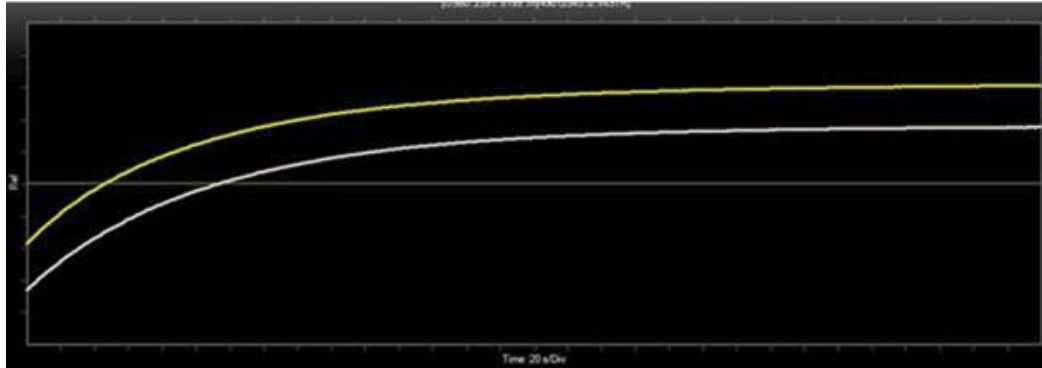


Figure 50. Reaching steady-state by temperature sensors

An infrared camera is a very important diagnostic equipment capable of measuring system components used in various industries and their apparent temperature distribution interface. Thermal imaging equipment is a device that detects the temperature distribution without direct contact in infrared wavelength spectrum. A sample thermal image is seen in Figure 51.

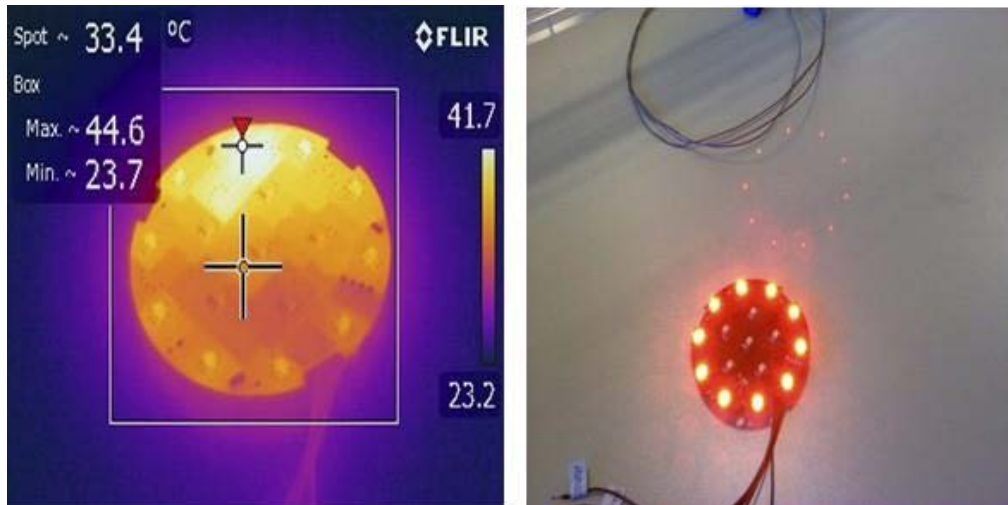


Figure 51. Sample R images of the first prototype

Thermal camera comes along a display device in which features and parameters are set so that analysis can be done using the software. Analysis software allows determination of the temperature distribution range, coloring etc. The most important parameter which must be calibrated prior to any measurement is surface emissivity. Depending on the type of surface material, the emissivity can be determined almost accurately.

4.2.1 Validation of Computational Results; Board Testing

An experimental system has been designed and built for the current study. The experimental apparatus is set in the same conditions as in the simulation. The surface parameters for IR camera are first calibrated using the T-type thermocouples that were individually calibrated. The surface is covered with a layer of a black paint (as seen in Figure 52) with a calibrated emissivity.

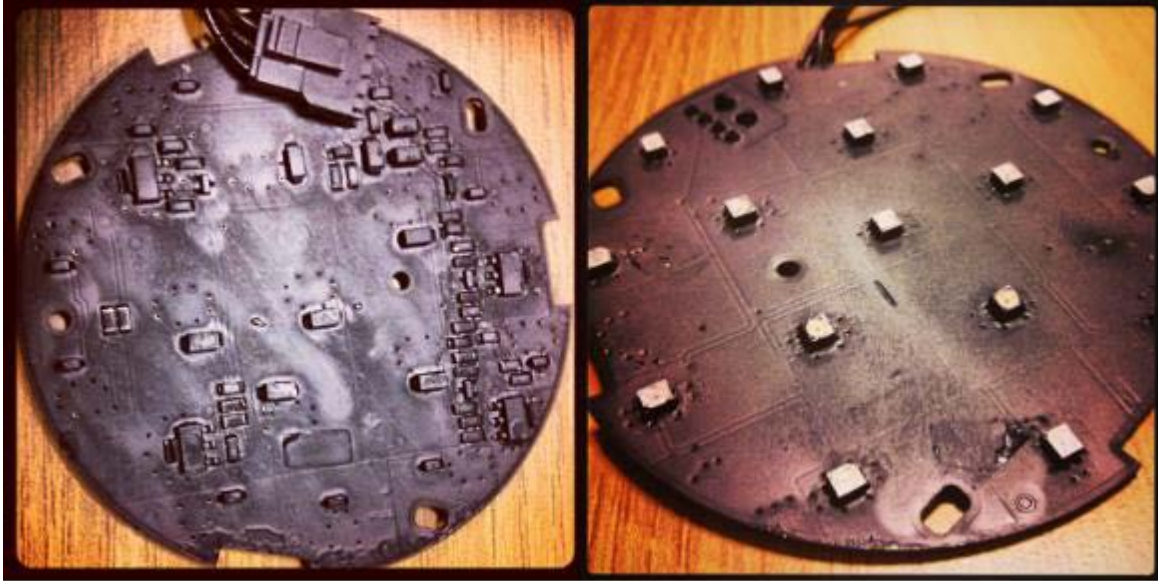


Figure 52. A painted version of the board

For a sample point chosen on the surface of MCPCB, emissivity values of 0.98, 0.99, 0.83 and 0.96 were found for four different points, front and back. Emissivity is therefore calculated as average of these four points of 0.94. The system was designed and tested as a conventional FR4 PCB in the first part of this study and then thermal clad board was tested.

Table 14. Experimental vs CFD results of the FR4 prototype

		Board alone		Board in enclosure	
<i>Component</i>	Flux (*10 ⁶ W/m ²)	Exp. ΔT (K)	CFD ΔT (K)	Exp. ΔT (K)	CFD ΔT (K)
R ₁	50,3	60	67		
R ₄	50,3	58	60		
R ₆	78,4	74	78	100	108
R ₁₂	78,4	104	110	117	126
R ₁₈	134	87	93	118	123
R ₁₉	134	88	89	111	115
R ₂₂	50,3	66	72		
Q ₁	127,3	63	65	100	110
Q ₂	127,3	46	46		
Q ₃	127,3	53	59		
Q ₄	1,178	45	46		
Q ₅	153,9	73	82	117	128
Q ₆	159,6	75	80		
Q ₇	2,3	48	51		

Table 14 gives experimental results of FR4 prototype in comparison with the CFD results, noting an uncertainty of 2-10% depending on the spot location on the board. In the table, “Exp.” refers to experimental results (using both IR and T-type thermocouple) and “CFD” represents the results derived from simulations in Icepak.

Table 15. Verification of IR data by thermocouple readings

Component	Temperature by IR (°C)	Temperature by Thermocouple(°C)
R_{13}	63.0	61.6
R_{16}	63.5	62.0
Q_5	61.7	64.9
R_{19}	62.7	64.5
R_{22}	62.6	61.8
R_2	62.0	62.0
Q_1	60.5	62.1
Q_6	61.6	64.1
LED_5	60.1	56.1
LED_{14}	60.6	57.4
<i>Ambient</i>	25.4	25.4
<i>Max.</i>	70.4	65.0

Uncertainty analysis for this experiment is done in a way that the test is repeated at least twice for exactly the same ambient condition. After averaging the results for certain chosen spots, the hot spot temperatures are compared as shown in Table 15.

Figure 53 show the temperature distributions obtained with a FLIR IR camera SC5000. The LEDs side layout of temperature distribution images by camera is shown in Figure54. The hot spots are clearly observed and similar to the numerical results with standard deviation of 3%. Thermal clad board, on the other hand, has a more uniform temperature distribution as previously discussed.

Figure 53 shows that the local hot spots are similar to the hot spots in thermal clad board prototype at the electronics components side. Overall, the distribution of temperature is close to uniform within 3°C whereas in FR4 board, there exists an almost 50°C. This temperature difference is more than 10 times the temperature difference found in thermal clad prototype.

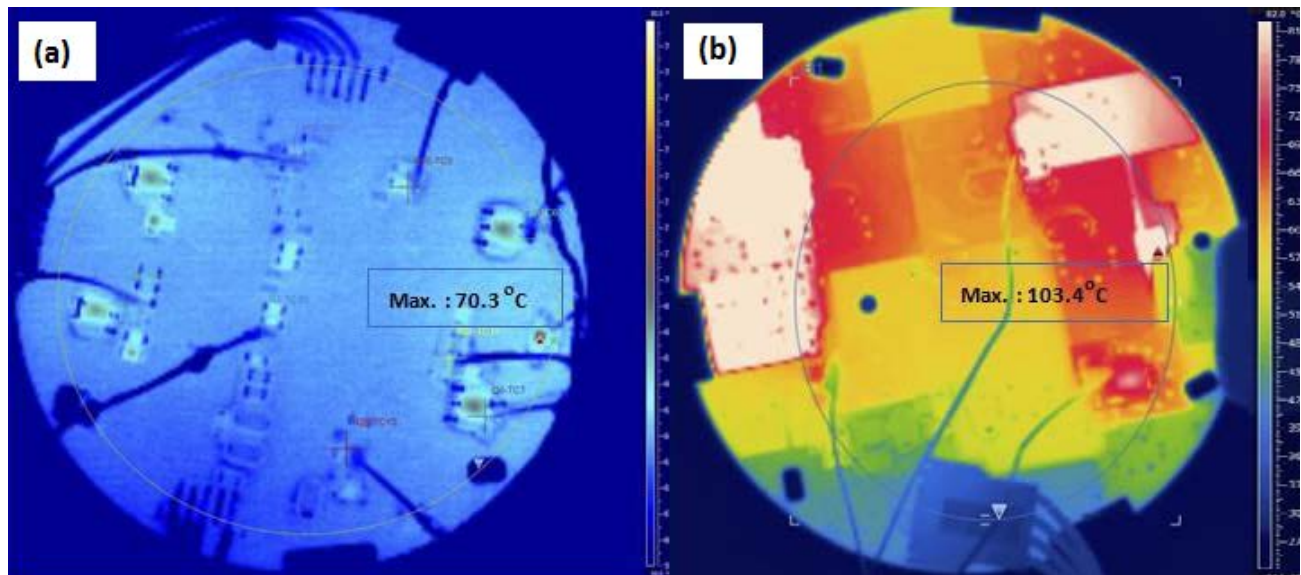


Figure 53. Temperature contours comparison for the Electronics Side for (a) FR4 vs. (b) thermal clad Board

Free-space results (i.e. the board with no enclosure packing the board and electrical and optical parts as a system) are first discussed here. According to results of the idealized system model after local hot spots were specified, the conductive plates were placed in three different forms: embedded inside the board, standing outside the board or attached to it, making a connection between board and enclosure. Results of different plates (in terms of geometry, placement and conductivity) show that embedding the heat pipe is the best choice to remove the local temperature differences on the board.

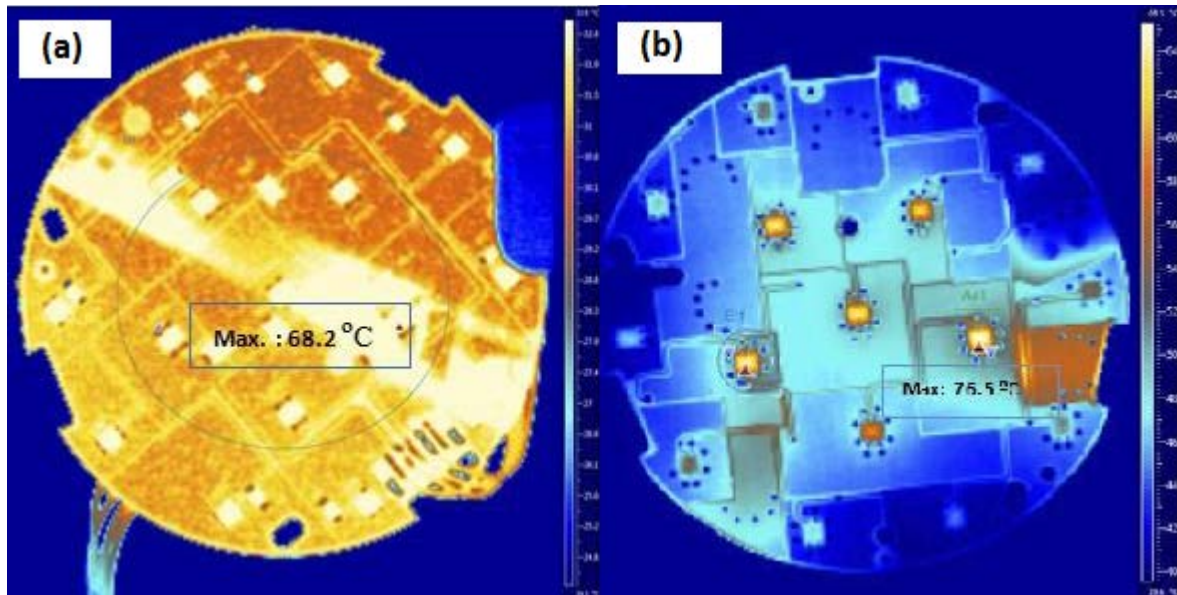


Figure 54. LEDs side of temperature distribution in (a) thermal clad prototype and (b) FR4 prototype

As a conclusion, The LED lighting system with double-sided FR4 board was closely examined for the sensitivity of the system to thermal conditions computationally and experimentally. It is found that maximum temperature gradient on the board was 35 °C and 48 °C for LED and driver circuit sides. Maximum temperature on the board is found to be 104 °C. Next, a double-sided metal board was studied computationally and experimentally validated. It is found that maximum temperature gradient on the board was 6 °C and 9 °C for LED and driver circuit sides. Maximum temperature on the board is found to be 70 °C. The uniform temperature distribution as a result of this change in the board is reported as highly critical and trustable in terms of eliminating possible thermal failures, especially for high brightness LEDs. Even further, the local hot spots were also abated by means of embedding a conductive structure inside the board for which the models show that homogeneity is even higher.

4.3 Experimental Testing Procedures: Heat Pipe

The experiment was designed to collect basic parameters to evaluate the heat pipe's performance. Heat pipe tests were done using the experimental setup illustrated in Figure 55. This consists of a data acquisition system, with analog to digital converter attached to seven thermocouples; this data was acquired and interpreted using a software package referred to as Agilent (IO Libraries), which can acquire and plot data from near to 50 channels and acquire near to a 10e6 package of samples per channel, in addition to allowing for the acquired data to be exported to Microsoft Excel. For this experiment the software was set to record temperature in degrees Celsius with seven channels as input. The frequency of recording data was set to 2Hz, with each test acquiring up to 7200 individual data points per thermocouple channel for a two hours' time span, for a total 28,800 data points per test.



Figure 55. Experimental setup for heat pipe performance test

The evaporator section of the device was attached using screws and an Aluminum cubic block with two Cartridge Heaters, with diameter of 5mm and the heated length of 1 inch. The device was rated for 50W at an input Voltage of 12V. The schematic of the heater can be seen in Figure 56.



Figure 56. Cartridge heaters

In order for the thermal resistance between heater and interfaces of the aluminum cylinder to be reduced, high temperature and high thermally conductive paste (5-min epoxy) was applied to fill potential gaps. RTV paste was used to mount the thermocouple assemblies to their proper locations. The amount of applied voltage was adjusted manually. For the experiments performed the strip heater was supplied different voltages between 6 and 12VDC, which was determined by measurement through the power supply itself, with an accuracy of +/- 1%. Water is used as cooling fluid inside an Aluminum tank of 1000cm³ which cools by natural convection. There is some variation in the performance of the cooling tank, due to the system being open to atmosphere, but with a variation of 2-3°C temperature difference throughout the

experiments the effects are assumed almost negligible. The thermocouple assemblies, which have a variation of $\pm 0.25^{\circ}\text{C}$, were mounted at strategic locations to accurately measure the points in this system as well as to record the temperature change in the cooling fluid in the condenser box. On the evaporator section, a tiny hole was mounted inside the insulation cube which aims to minimize the heat loss of heaters. Holes were then filled with the paste to reduce thermal resistance developed at the interface. The heat pipe adiabatic section is insulated using glass wool and some tapes around it. After the above steps, tests are performed and data is analyzed to measure the performance of heat pipe in each orientation. To determine how much of input power as heat is transferred to the condenser block (and how much is lost), an Icepak simulation is done. The condenser is cooled using water inside a small tank. Having reached the steady state, the temperatures of the earlier mentioned points on surface of heat-pipe are recorded. The thermocouples are also attached (Figure 57) on the insulation surface and other related positions by adhesive tapes and silicon, so that heat loss can be estimated.

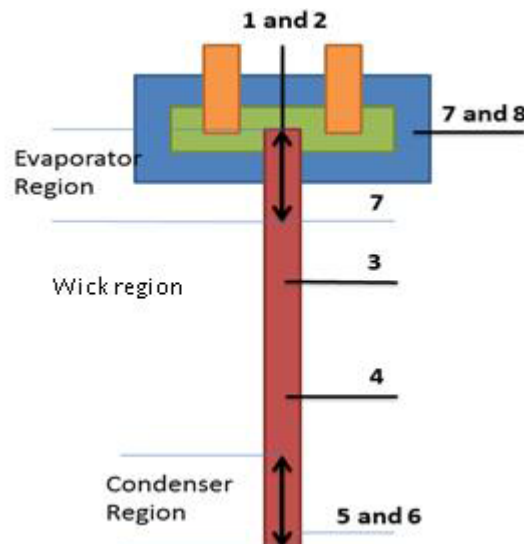


Figure 57. Thermocouple placement in the heat pipe test set

Each experiment is repeated three times and average values are reported. The heat pipe circulates vapor and liquid in a copper/water unit which is the same pipe line.

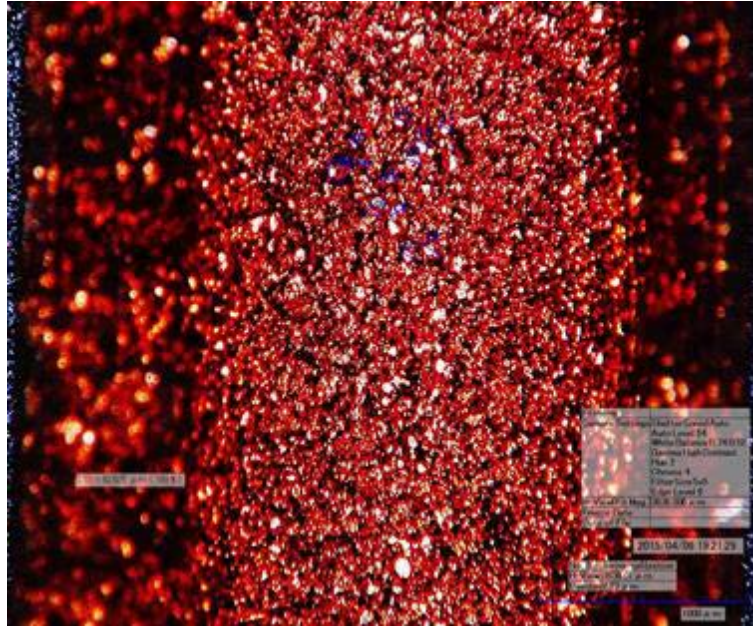


Figure 58. Estimation of pore diameter using a high-resolution microscopic system

Copper powder is the wick-structure in this case for which the porous diameter is measured $d_s = 64.8024$ (μm) under the microscope as given in Figure 58. When enough amount of heat is supplied to the evaporator, the heat pipe acts as a super conductive rod.

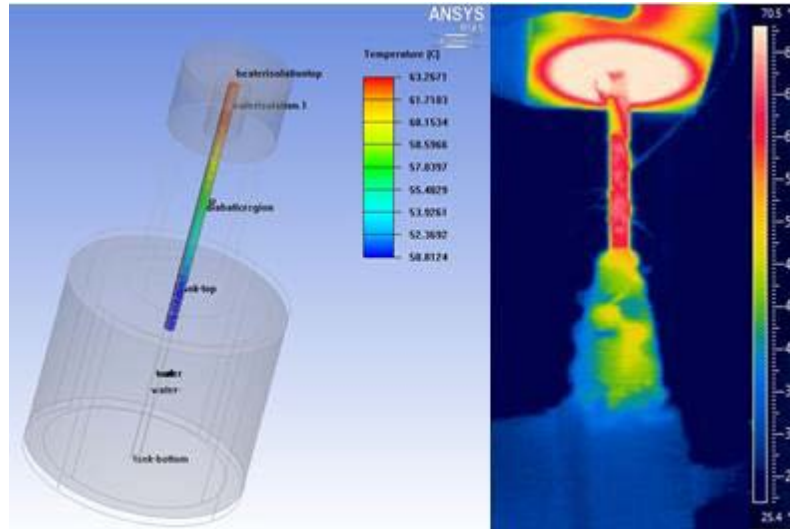


Figure 59. Simulation of a heat pipe equivalent in CFD model (left) and IR thermal image of the actual measurement setup (right)

The numerical model (Figure 59) simulates the heat pipe system with blocks of the same properties as in experimental setup (heater block, heater container block, the rod as a copper cylinder, insulations and water tank). Therefore, when simulated in 3D, results are expected to show similarity to those experimental and analytical studies. Mesh sensitivity study shows that the results are independent of mesh size for mesh greater than 128,000 elements. When heat is applied as input power in the same ambient conditions, the temperature contour shows similar results. In other words, when conductivity of the rod is set to be the same as effective conductivity of heat pipe which is calculated in experimental part, temperature difference between condenser and evaporator are in the same range. In the study of heat pipes embedded inside the boards, two plates of 200x100x7 (mm) are prepared and the previously tested heat pipes are flattened and embedded by gradual pressing inside a groove of the same perimeter as circular-heat-pipe's cross-sectional perimeter. In order to avoid gaps between the

groove and heat pipe, a thermal interface material is applied prior to embedding at the contact surfaces.

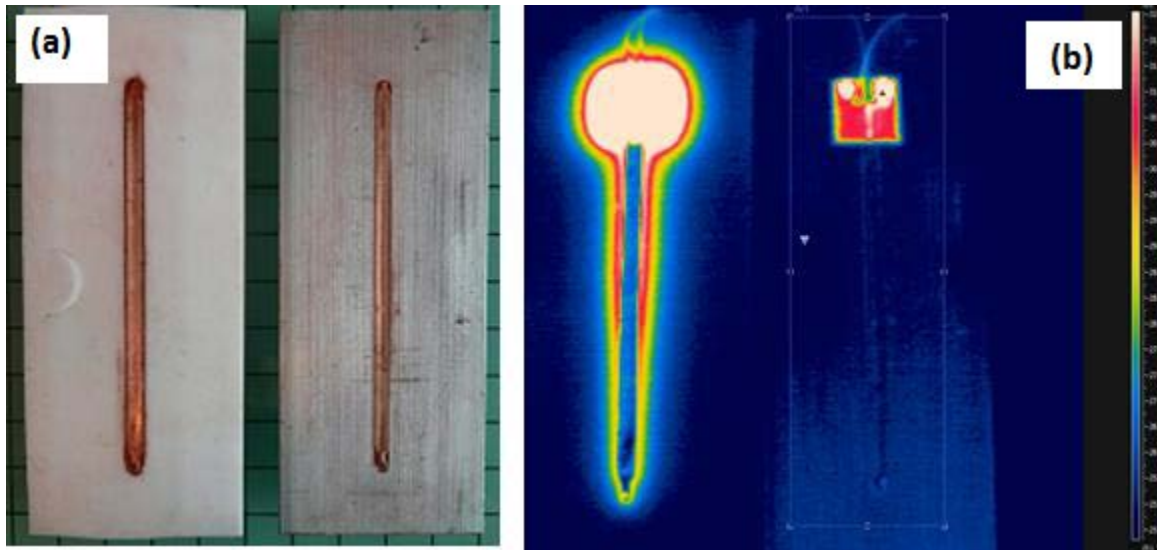


Figure 60. (a) Embedded heat pipes in a polymer (left) and an aluminum board (right) along with their (b) temperature distribution by IR camera

Heat pipes were embedded inside two plates with different thermal conductivities. Aluminum plate with (210 W/mK) conductivity when heat pipe embedded inside is on the right side of Figure 60, and polymer plate (conductivity of 0.25 W/mK) with embedded heat pipe is on the left. A 17.8 °C temperature span is observed in the Aluminum plate (on the right) in which the heat pipe performance is not observed much. But it is observed that in the polymer plate (left) a higher range of temperature exists and the heat pipe is obviously playing an important role in heat spread.

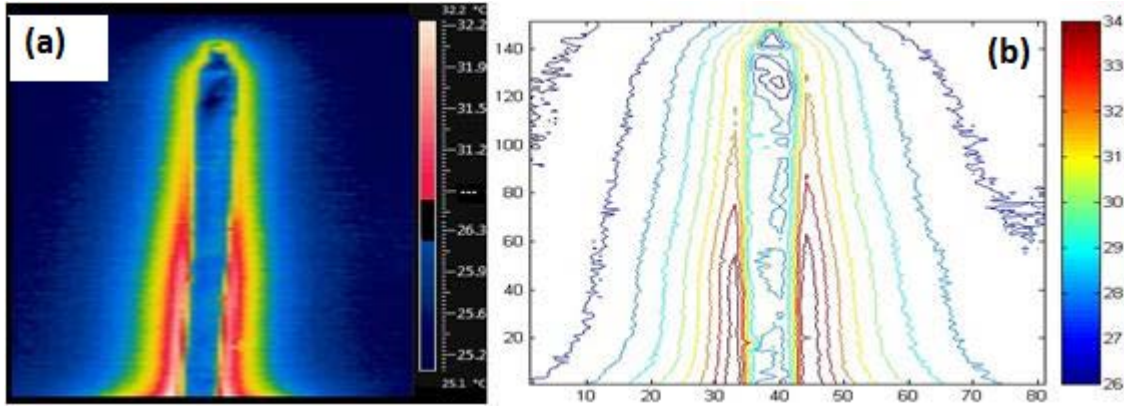


Figure 61. Temperature gradient of 2K obtained when manufacturing conditions are not optimum in a Teflon plate (a) IR image and (b) contours extracted with MATLAB for a similar case

When a heater is used to give input power in the evaporator region, with natural convection cooling the condenser region, infrared camera gives a temperature distribution as expected, while the contours are developed using MATLAB software. Figure 61 shows the temperature distribution for a heat pipe embedded Teflon plate. It is expected that substrate's thermal conductivity is less than 0.5 W/mK.

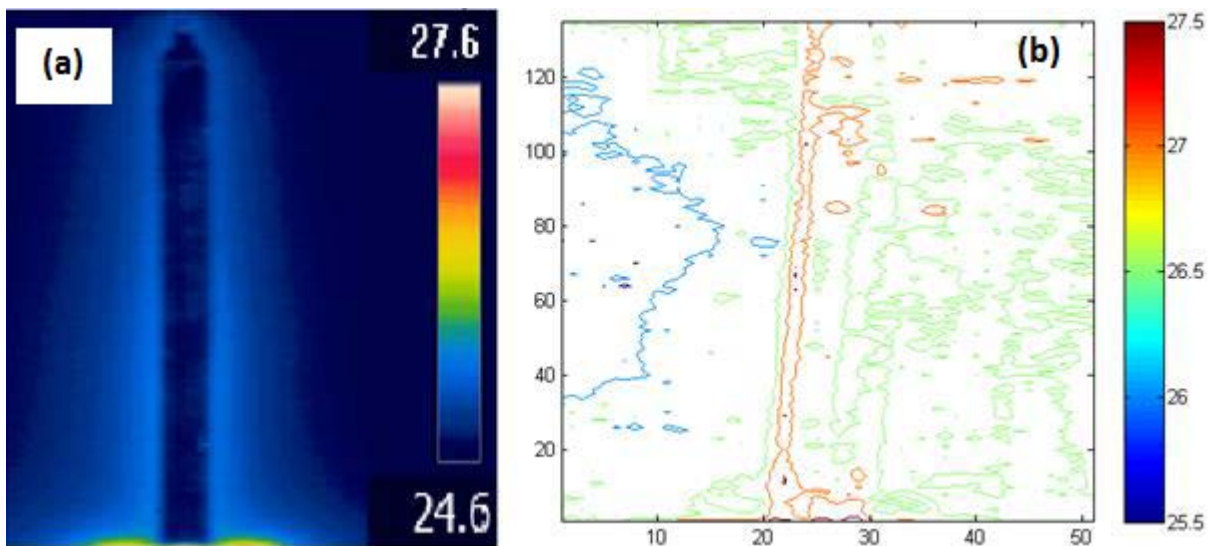


Figure 62. Aluminum-based substrate with a single heat pipe at the same heat removal condition; (a) IR image and (b) temperature contours extracted with MATLAB



Figure 63. Comparison between a heat-pipe embedded in a plate using IR image (right); Line 1 representing a heat pipe embedded in board and Line 2 a simple heater on a simple board (no heat pipe)

Figure 62 shows the aluminum-based substrate. Therefore, large distribution is expected without a heat pipe. It is found that even for a low heat removal condition a temperature gradient of 8K is obtained. Figure 63 shows the infrared thermal experimental results for the baseline test without a heat-pipe and with a heat-pipe for a Teflon substrate. It is shown that heat pipe embedded plate experienced a much lower temperature than baseline case. The temperature difference between condenser and evaporator, the thermal resistance and the effective conductivity under different heat load and orientation are plotted and results are comparable with what is reported in literature [29] of a 200 mm heat pipe (copper, water), 6 mm in diameter. To show the validity of the experimental test, Figure 64 is constructed to compare with published work by Loh et al. [33]. The results indicate that our test setup and measuring procedure are predicting similar performance as the one published in literature. The increase in temperature difference when heat load increases is due the increase in the amount of evaporated fluid which require higher pressure difference driving vapor from evaporator to condenser. In summary, an experimental and theoretical investigation of a heat-pipe-embedded printed circuit board technology has been achieved for its thermal performance.

A commercially available heat pipe first considered and followed by a series of testing for different orientations. The experimental setup is built and its results are then validated by analytical and numerical results. Due to effective heat spreading, when heat pipe is flattened and embedded inside plates of known conductivities, spreading resistance is significantly low so that temperature difference between minimum and maximum points on the surface decreased abruptly (when comparing with a non-embedded board). Thermal resistances in each case are compared with conventional cooling method for a plain PCB made up of polymer or Aluminum and results showed reduction of 50% in the overall resistance.

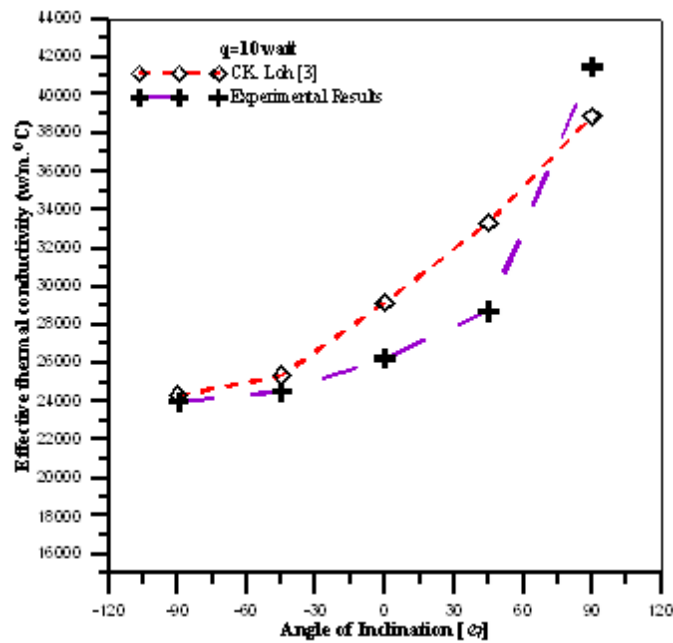


Figure 64. Comparison of results with literature (Loh et al. [29])

4.4 Deviation and Uncertainty Analysis

Various experimental investigations were performed to observe the performance of heat pipes given a certain watt density heat source, at various orientations. Additional testing was performed on the forced-convection with a micro water pump, at varying flow rates. As stated previously each apparatus was mounted in the 90, 45 and 0 degree orientation. The reason behind this choice of inclination angle was to observe the heat pipe effective conductivity in various orientations, while we expect that 90 degree must be the most efficient one.

CHAPTER V

LOCAL ENHANCED CONDUCTION MODELS

In order to see the temperature over hottest and coldest points on thermal clad board, temperature line function is created (see Figure 65). With a close examination of this distribution, the best placement for the heat pipe embedded board structure is determined. According to experimental results, in the state when hottest spot of thermal clad board is standing in the highest point against gravity (in that case heat pipe will also be at its maximum efficiency), maximum temperature difference is achieved and the embedded heat pipe is expected to be of the optimum efficiency in that orientation.

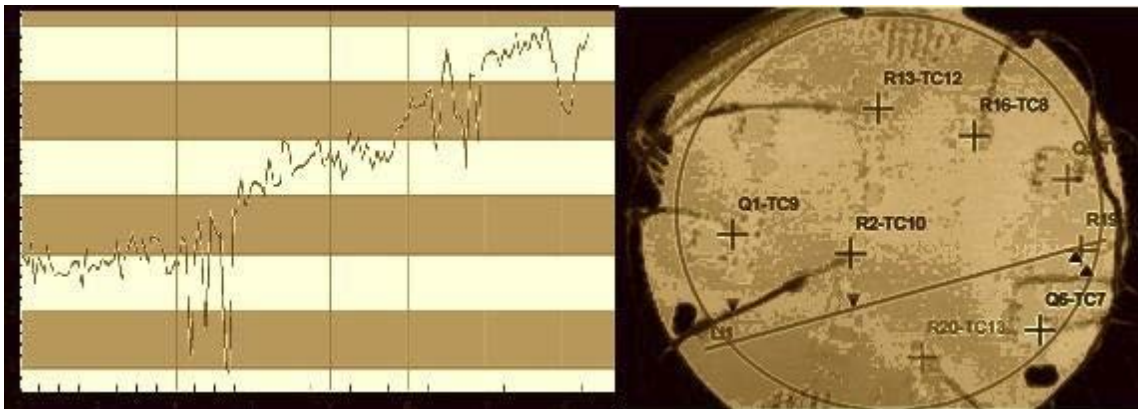


Figure 65. Using line function to determine the maximum temperature difference on thermal clad board (line that is drawn on thermal image on right side gives temperature plot on the left side: temperature versus X-position on the line)

While metal clad board provided a better heat spreading, a further study has been performed to obtain more uniform temperature on the board. Therefore, heat pipe technology is of interest. Heat pipe as a type of heat transporting system has been developed remarkably over the last sixty years, appearing in a large number of publications. The ease of design and simplicity for production, dropping the temperature gradient between two local hot spots, and transporting high heat fluxes at even high temperature gradients are characteristics of heat pipes, all special to them [14]. Here, a typical standard heat pipe is simulated as conductive elements, which is simplified as a highly conductive block. Figure 66 illustrates one of the heat pipes modeling when embedded inside the board in Icepak/ANSYS software.

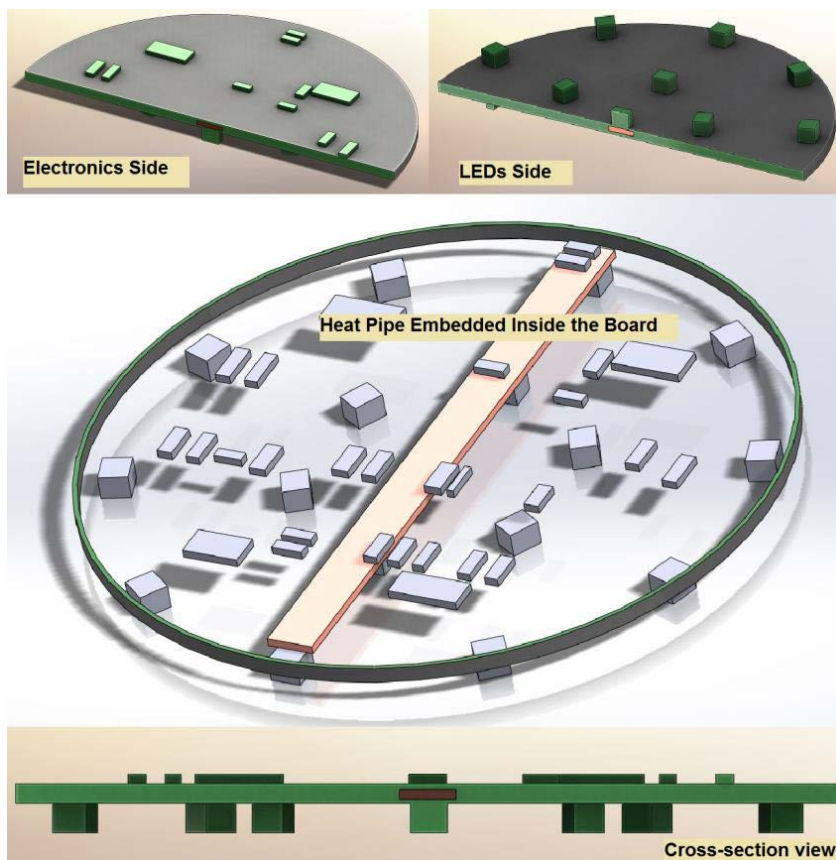


Figure 66. Embedded highly conductive plate analogous to heat pipe in the model, cross sections from different views

In the computational model with heat pipes, various orientations and placements are modeled and investigated. These include two short high-conductive bars between several hot spots (as seen in Figure 67). The same model was updated for other conductive plates as well. Different models were then created in terms of quantity and shape and position according to the board (either embedded inside it, placed on its surface, connecting several components or acting as a spreader between system parts). Figure 68 shows the results for one of these cases.

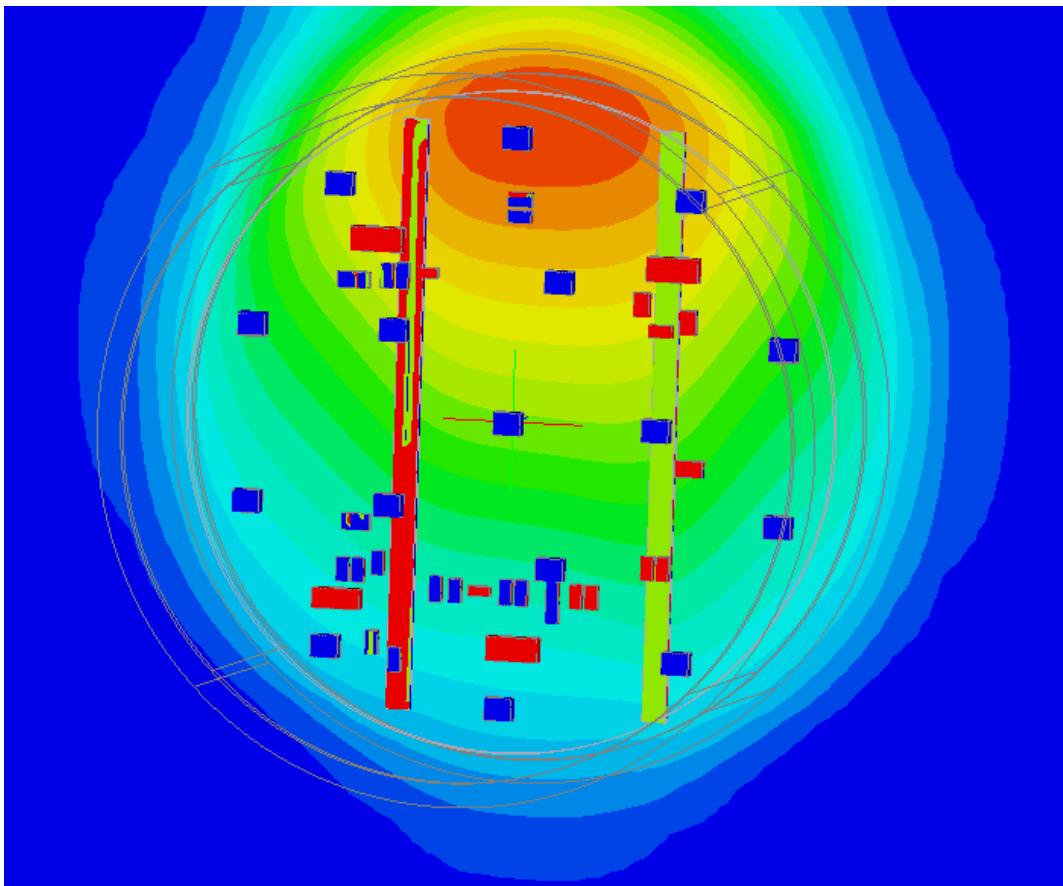


Figure 67. Temperature contour of the automotive lighting system when two short super-high-conductive bars are placed on the board surface, acting as heat pipes

When comparing temperature results of all the mentioned models, best performance and the lowest temperature difference on the board (most uniform one) is when a highly

conductive geometry is embedded inside the board and is circular (as is geometry of the board). This result shows that uniformity is 50% higher when highly conductive plate is embedded.

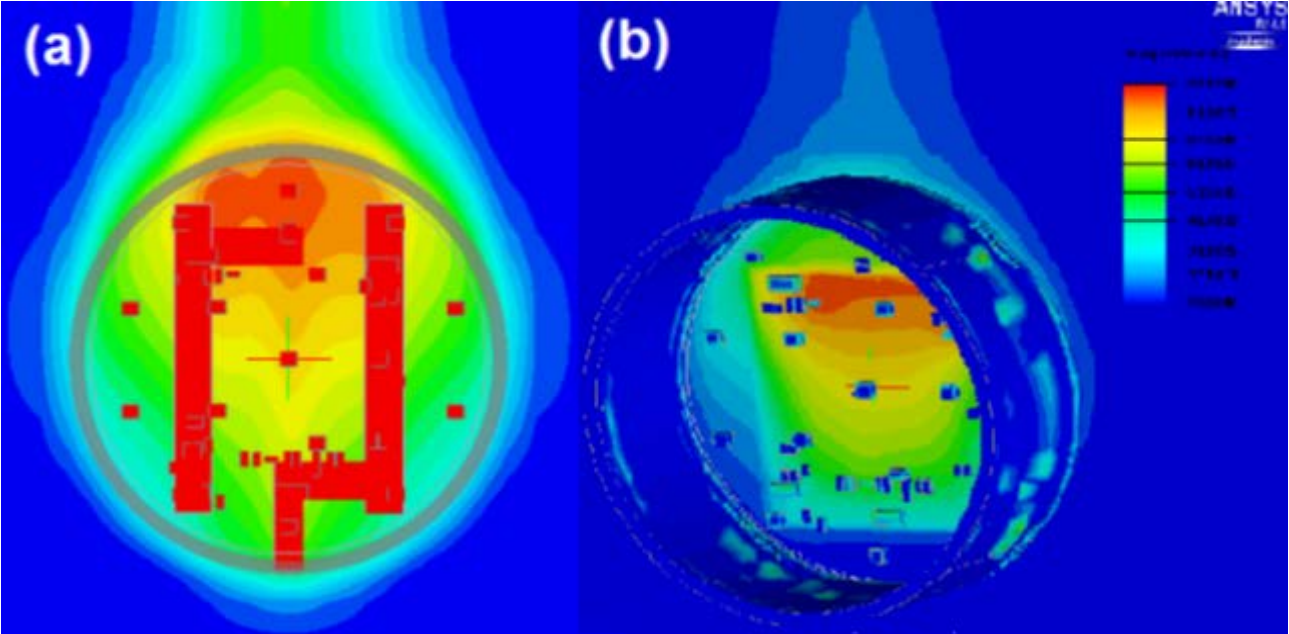


Figure 68. Temperature distribution of several high-conductive plates embedded in board; (a) components: LEDs and electronics components, plates, (b) board and plastic enclosure around it

CHAPTER VI

CONCLUSIONS

Among the most important challenges of thermal management in LED lighting systems, the ratio of power density to the surface area available leads to heat flux rates higher than threshold which creates temperature gradients larger than that of the Sun even when the cross sectional area is merely a thousand micron square. While conventional plastic PCB technology is still widely used for LED system packaging, it may lead to local hot spots and temperature non-uniformities. In this thesis, the first analysis shows local hot and cold spots occur even in conventional designs with thermal vias. In particular, this happens in harsh environments where the LED junction is highly susceptible to cause failures if temperatures are above the safe limits. The main goal in this study was to find the heat transfer effects of every component producing heat in a LED based light engine designed to be used in automotive exterior applications. The work was built upon a single package thermal analysis both analytically and numerically with pure conduction as the dominant heat transfer mode. Sensitivity of the package resistance to conductivities of each component was analyzed. Then, a three functional system of LED lighting was studied computationally and experimentally. A double sided PCB is the subject of study on which one side is specified for LEDs and the other for electronic components is placed in a sealed enclosure which is supposed to be functioning near the engine of vehicle. The system posed challenges both thermally and mechanically due to high local ambient temperatures. A series of

experiments were done (along with analytical and numerical validations) for system level analyses. Effect of PCB on the package thermal performance is significant especially when it is a conventional low conductivity material like FR4. Transistors on the PCB show local hot spots and the heat has to be spread uniformly so hot spots can be abated.

The LED lighting system with double-sided FR4 board was closely examined for the sensitivity of the system to thermal conditions using computational and experimental techniques. It was found that maximum temperature gradient on the board was 35°C and 48°C for LED and driver circuit sides. Maximum temperature on the board is found to be 104°C. Next, a double-sided metal board was studied computationally and experimentally validated. It is found that maximum temperature gradient on the board was 6°C and 9°C for LED and driver circuit sides. Maximum temperature on the board was found to be 70°C. The uniform temperature distribution as a result of this change in the board is reported as highly critical and trustable in terms of eliminating possible thermal failures, especially for high brightness LEDs. Furthermore, the local hot spots were also abated by means of embedding a conductive structure inside the board for which the models show that homogeneity is even higher. Different approaches in the board were also compared and the uniformity reached 3°C leading to best thermal performance.

APPENDIX A

OPTICAL AND ELECTRONIC CONCEPT DEVELOPMENTS

In the optical structure, the reflector, lens and the enclosure play important roles. LED chips (10 chips) of LAE6SF type are amber in color and function as stop and rear positioning, while 6 yellow LEDs of LYG6SP type function as signal. Table A-1 shows the system functions along with the regulation name or detail for the FR4 prototype produced by Farba Company.

Table A-1. The three functions and their details

System function and regulation	Details
Stop and rear positioning LED type	LAE6SF- Amber
Stop functions- electrical current	50 mA
Rear position function electrical current	5 mA
Standard regulation for stop and position	ECE7
Signal LED type	LYG6SP- Yellow
Signal function- electrical current	140 mA
Standard regulation for signal	ECE6

The stop function, light intensity of HV (origin) is desired to be between a minimum of 60 cd and a maximum of 260 cd, for rear position function. In the experiments, while waiting for sufficient time to reach to steady state conditions, Figure A-1 shows the system to come to steady state, when the optical output that was measured using integrating sphere. As we have seen, about 500 seconds after the start, the optical output is reduced to 50%.

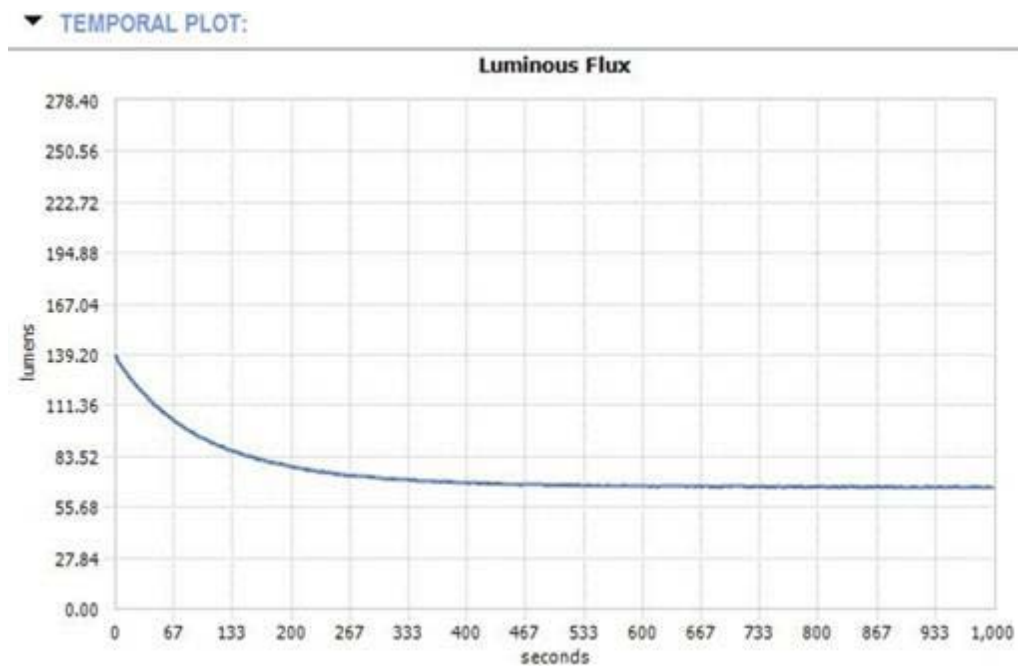


Figure A-1. Reaching steady-state by optical output

The product has two versions, operating under 12V and 24V electromotive forces which is because it will appeal to different customers and preparation is done according to the electronic concept of common international standards and customer preferences. The LED placement is the same in both versions and the electronic

component placements are modified according to system requirements. The LED components are located on the PCB top layer (reflector is also designed to match them).

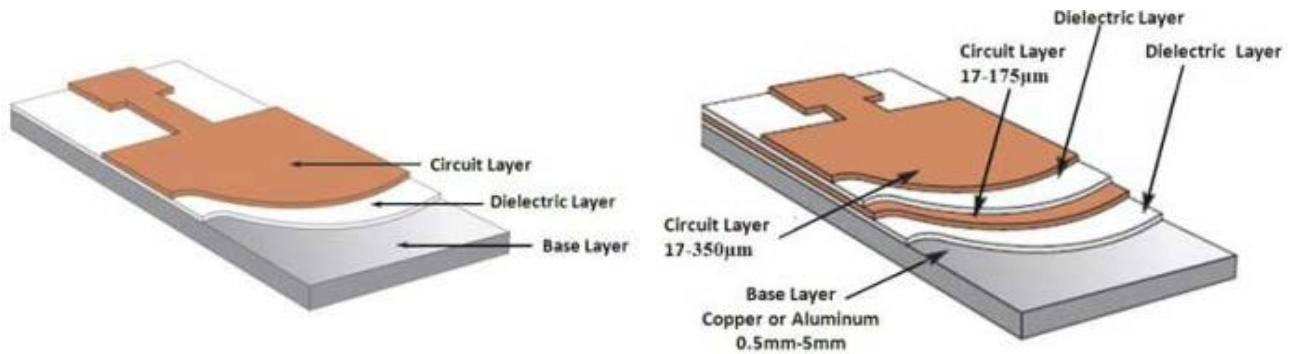


Figure A-2. Board technology [Bergquist]

On section about novel PCB technologies, we described how important the choosing process of an appropriate MCPCB material is for the stack-up. The reason for the utmost importance of selecting the material is that it is dependent and somehow proportionate to the LED that is being used in the product. If LED's thermal resistance is low enough to make the product thermally efficient, the substrate must not be a one with low performance. For this, carrying capacity is calculated and thickness of copper foil is designed to meet thermal requirements of the whole system. Also dielectric layer of substrate must be a wise selection so that dielectric's performance along with the base metal has a short thermal path and meets the requirements in all terms of mechanical, electrical and structural. Figure A-2 shows a single-layer and double-layer technology of board and Figure A-3 shows the way the board technology works.

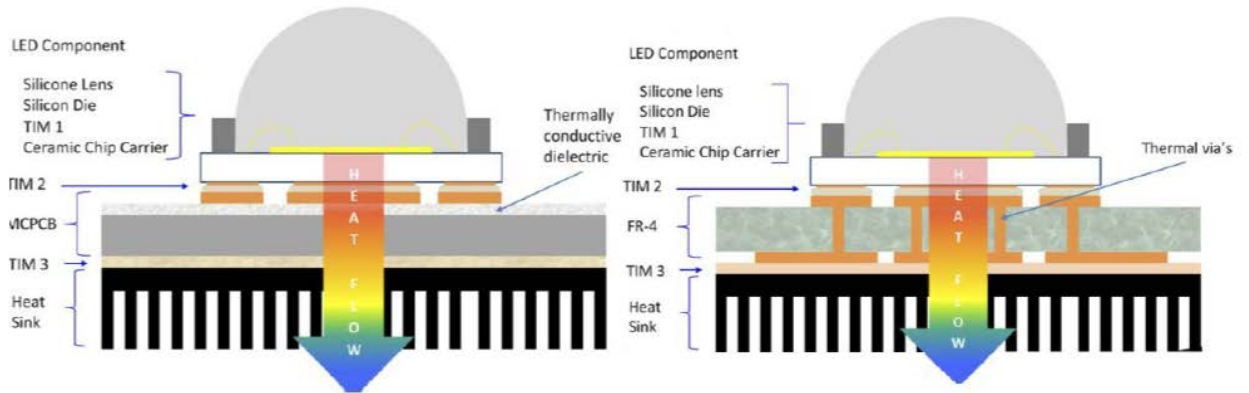


Figure A-3. Board technology efficiency in terms of heat transfer [Bergquist]

APPENDIX B

HEAT PIPE DETAILS

A heat pipe consists of an evaporator, an adiabatic and a condenser region. The heat collected by the evaporator of a heat pipe constantly sinks at the condenser section and there is only a little volume of fluid which is thermally in equilibrium with the vapor. Heat loss in the adiabatic region is mainly ignored when adequate insulation is used. As seen in Figure B-1, an operation principle of a conventional heat pipe is based the working fluid and the fact that it circulates inside the heat pipe.

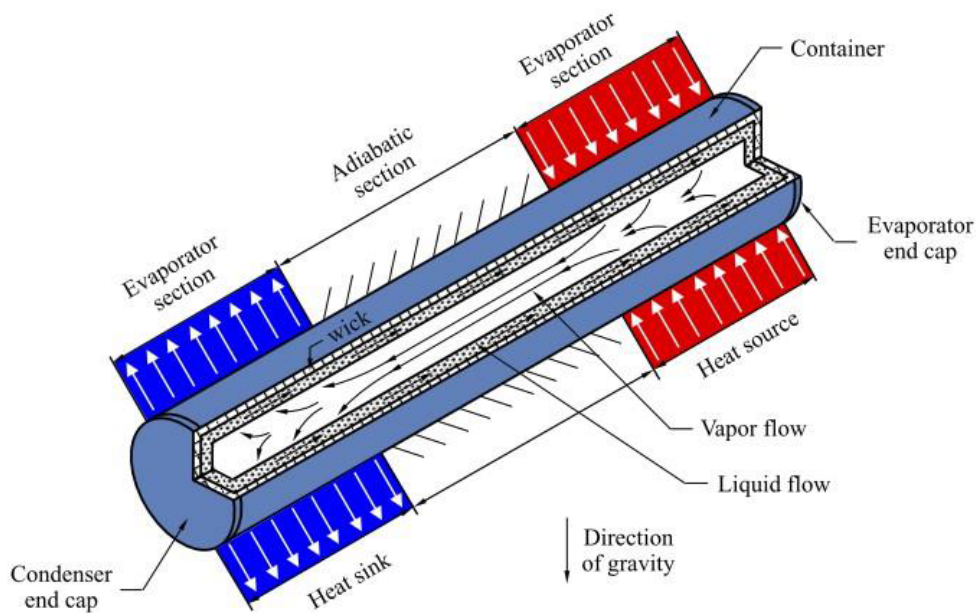


Figure B-1. A heat pipe [22]

In this study, experiments are designed and performed based on a standard commercial heat pipe. Heat pipe test setup was based on measuring its performance according to power input and orientations. A typical heat pipe schematic is shown in Figure B-2 in order to understand the way it works.

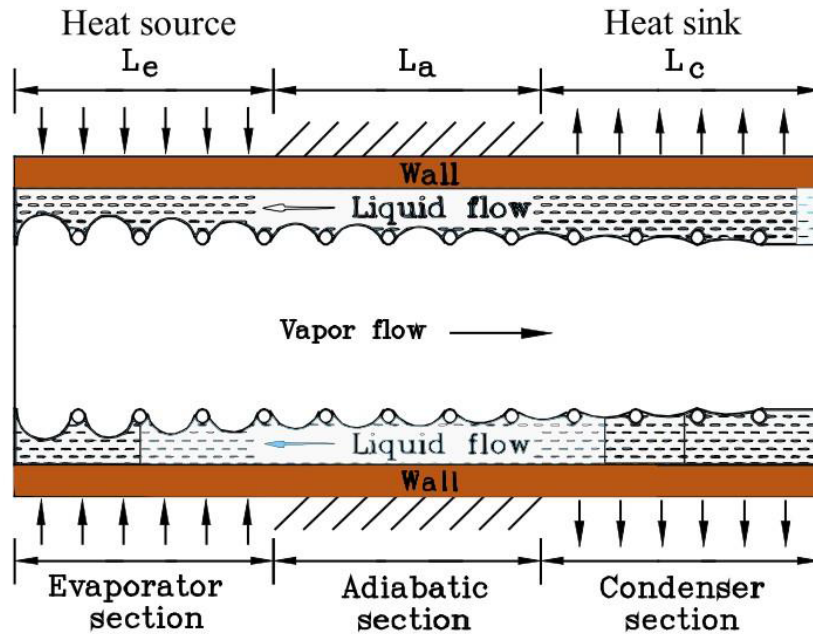


Figure B-2. Shape of the liquid-vapor interface [22]

REFERENCES

- [1] G. Elger, H. Willwohl, and J. Schug, "Thermal analysis of high power LED subassemblies for automotive front light application," in Electronic System- Integration Technology Conference (ESTC), 2012 4th, pp. 1-8, IEEE, 2012.
- [2] "Inside an LED lamp," 2014. <http://electricheatingcosts.com/inside-an-LED-lamp-bulb/>.
- [3] F. Chen, K. Wang, Z. Mao, X. Fu, C. Li, M. Zhao, and S. Liu, "Application specific LED packaging for automotive forward-lighting application and design of whole lamp module," in Electronic Components and Technology Conference (ECTC), 2012 IEEE 62nd, pp. 182-186, IEEE, 2012.
- [4] Q. Lin, W. Chunqing, and T. Yanhong, "Thermal design of a LED multi-chip module for automotive headlights," in Electronic Packaging Technology and High Density Packaging (ICEPT-HDP), 2012 13th International Conference, pp. 1435-1438, IEEE, 2012.
- [5] S. Jang and M. W. Shin, "Thermal analysis of LED arrays for automotive head-lamp with a novel cooling system," Device and Materials Reliability, IEEE Transactions, vol. 8, no. 3, pp. 561-564, 2008.
- [6] Y. Lai, N. Cordero, F. Barthel, F. Tebbe, J. Kuhn, R. Apfelbeck, and D. Würtenberger, "Liquid cooling of bright LEDs for automotive applications," Applied Thermal Engineering, vol. 29, no. 5, pp. 1239-1244, 2009.
- [7] B. Guenin, "Thermal vias- a packaging engineers best friend," Electronics Cooling, 2004.
- [8] "Fuel economy," 2014. <http://www.fueleconomy.gov>.

- [9] M. Palocz-Andresen, *Decreasing Fuel Consumption and Exhaust Gas Emissions in Transportation: Sensing, Control and Reduction of Emissions*. Springer Science & Business Media, 2012.
- [10] “Greenhouse gas equivalencies calculator,” 2014. <http://www.epa.gov/cleanenergy/energy-resources/calculator.html>.
- [11] “Car headlights from candles torches to LED xenon,” 2014. <http://findautomotiveschools.com/car-headlights-from-candles-torches-to-led-xenon>.
- [12] “Led in headlamps,” 2014. <http://www.al-lighting.com/lighting/headlamps/led/>.
- [13] “The feds don’t know what to make of Audis new LED headlamps,” 2014. <http://www.extremetech.com/extreme/148601-the-feds-dont-know-what-to-make-of-audis-new-headlamps>.
- [14] J. Bielecki, A. S. Jwania, F. El Khatib, and T. Poorman, “Thermal considerations for LED components in an automotive lamp,” in *Semiconductor Thermal Measurement and Management Symposium, 2007. SEMI-THERM 2007. Twenty Third Annual IEEE*, pp. 37-43, IEEE, 2007.
- [15] M. Arik, C. A. Becker, S. E. Weaver, and J. Petroski, “Thermal management of LEDs: package to system,” in *Optical Science and Technology, SPIE’s 48th Annual Meeting*, pp. 64-75, International Society for Optics and Photonics, 2004.
- [16] D. Sabatino and K. Yoder, “Pyrolytic graphite heat sinks: A study of circuit board applications,” 2014.
- [17] “How to repair broken LED tail lights,” 2014. <http://www.carsdirect.com/aftermarket-parts/how-to-repair-broken-led-tail-lights>.
- [18] F. P. Incropera, *Fundamentals of heat and mass transfer*. John Wiley & Sons, 2011.
- [19] K. Kwok, B. Divakar, and K. Cheng, “Design of an LED thermal system for automotive systems,” in *Power Electronics Systems and Applications, 2009. PESA 2009. 3rd International Conference*, pp. 1-4, IEEE, 2009.
- [20] A. E. Bergles, “Evolution of cooling technology for electrical, electronic, and microelectronic equipment,” *Components and Packaging Technologies, IEEE Transactions on*, vol. 26, no. 1, pp. 6-15, 2003.
- [21] *Advanced Materials for Thermal Management of Electronic Packaging* By Xingcun Colin Tong Ph.D

- [22] A. Faghri, Heat pipe science and technology. Global Digital Press, 1995.
- [23] A. Faghri, “Heat pipes: Review, opportunities and challenges,” *Frontiers in Heat Pipes (FHP)*, vol. 5, no. 1, 2014.
- [24] “Heat pipe integration strategies for LED applications,” 2014. <http://www.electronics-cooling.com/2013/09/heat-pipe-integration-strategies-for-LED-applications/>.
- [25] “Conventional printed circuit board technologies,” 2014. <http://www.globalspec.com/reference/70670/203279/html-head-chapter-2-conventional-printed-circuit-board-technologies>.
- [26] D. Pounds and R. W. Bonner, “High heat flux heat pipes embedded in metal core printed circuit boards for LED thermal management,” in *Thermal and Thermo-mechanical Phenomena in Electronic Systems (ITherm)*, 2014 IEEE Intersociety Conference on, pp. 267-271, IEEE, 2014.
- [27] M. Arik, A. Setlur, S. Weaver, D. Haitko, and J. Petroski, “Chip to system levels thermal needs and alternative thermal technologies for high brightness LEDs,” *Journal of Electronic Packaging*, vol. 129, no. 3, pp. 328-338, 2007.
- [28] Icepak, A. N. S. Y. S. (2012). 14.0 Documentation. ANSYS Inc.
- [29] Loh, C.K., Enisa Harris, and Chou, D.J., “Comparative Study of Heat Pipes Performances in Different Orientations”, 21st IEEE Semi-Therm Symposium
- [30] “LED LIGHTING” 2014. <http://www.fancygens.com/led-lighting/>
- [31] Bottoms, B. ; Tsuruya, M. ; Richardson, C., iNEMI packaging technology roadmap highlights, IEEE 2014 International Conference on Electronics Packaging (ICEP).

VITA

Ferina Saati Khosroshahi was born in Tabriz, Iran. While completing her work at NODET High School in Tabriz, she was chosen as a candidate for National Physics Olympiad in Summer 2005 and was awarded a Bronze medal. In 2007, she entered University of Tehran, receiving full-scholarship. She obtained the degree of Bachelor of Science in mechanical engineering in July 2012. In January, 2013, she entered the Graduate School at Ozyegin University in Istanbul. During the following years, she was a teacher assistant and a research assistant.

Permanent Address: 51-35 Johann-Wilhelm-Klein-Strasse Linz, Austria 4040

E-mail address: ferina.saati@gmail.com

This thesis was typed by the author herself.